

Fall 12-18-2015

Interaction between Angiotensin II and BDNF in Modulating Sympathetic Nerve Activity

Bryan K. Becker
University of Nebraska Medical Center

Tell us how you used this information in this [short survey](#).

Follow this and additional works at: <https://digitalcommons.unmc.edu/etd>



Part of the [Cellular and Molecular Physiology Commons](#), [Medical Physiology Commons](#), and the [Systems and Integrative Physiology Commons](#)

Recommended Citation

Becker, Bryan K., "Interaction between Angiotensin II and BDNF in Modulating Sympathetic Nerve Activity" (2015). *Theses & Dissertations*. 51.

<https://digitalcommons.unmc.edu/etd/51>

This Dissertation is brought to you for free and open access by the Graduate Studies at DigitalCommons@UNMC. It has been accepted for inclusion in Theses & Dissertations by an authorized administrator of DigitalCommons@UNMC. For more information, please contact digitalcommons@unmc.edu.

INTERACTION BETWEEN ANGIOTENSIN II AND BDNF IN MODULATING SYMPATHETIC NERVE ACTIVITY

by

Bryan Becker

A DISSERTATION

Presented to the Faculty of
the University of Nebraska Graduate College
in Partial Fulfillment of the Requirements
for the Degree of Doctor of Philosophy

Cellular & Integrative Physiology
Graduate Program

Under the Supervision of Professor Irving H. Zucker

University of Nebraska Medical Center

Omaha, Nebraska

December, 2015

Supervisory Committee:

Steven Sansom, Ph.D.

Lie Gao, Ph.D.

Matthew Zimmerman, Ph.D.

Wallace Thoreson, Ph.D.

ACKNOWLEDGEMENTS

“NON HÆC SINE NVMINE DIVVM EVENIVNT”

&

“HÆC OLIM MEMINISSE IVVABIT”

- Virgil, Aeneid

“Who we are cannot be separated from where we’re from.”

– Malcom Gladwell, *Outliers: The Story of Success*

There are more people to whom I owe an immense debt of gratitude than space and time permits. The pursuit of a doctorate is one which is not possible without the support and assistance of a great number of people, and here, with great trepidation knowing I am unable to adequately express my gratitude to everyone involved, I seek to acknowledge those who have greatly contributed to the successful completion of my doctoral work. I am not a self-made man; rather, I am the result of the hard work and care of those who preceded me both in science and life.

“If I have seen further, it is by standing on the shoulders of giants” – Isaac Newton.

nanos gigantum humeris insidentes

The support and guidance of my mentor, Dr. Irving Zucker, has been invaluable to the completion of my doctoral degree. He has provided incalculable amounts of time and energy into my training throughout the past few years, and his continual excitement and wonder in the work of science has been a contagious fire toward the fostering of new ideas and hypotheses. The culture of his lab is one in which new ideas thrive and challenging experimental approaches are taken head on. His patience with trainees is remarkable, and I have been undeniably blessed by his willingness to allow me to undertake time-consuming projects with steep experimental learning curves. Dr. Zucker’s accessibility is unparalleled; never was I made to feel as though I were encroaching on his time, as he was always willing to discuss new data or work through problems as they arose.

Within the Zucker lab, there are also many people without whom this dissertation would not have been possible. Dr. Hanjun Wang was a second mentor of sorts to me during my predoctoral

training. Sharing lab and desk space with Dr. Wang may have been the single greatest factor in promoting my success. From the many conversations about the philosophy of science and experimental design, to his seemingly limitless technical and surgical abilities, Dr. Wang was daily a compatriot and guide in the trenches of science. My fellow graduate students, particularly Dr. Alicia Schiller and Peter Pellegrino, have also been a daily source of support and guidance as was the influence and guidance of post-doctoral members such as Dr. Karla Haack. Technical assistance from Johnnie Hackley, Kay Talbitzer, and Pam Curry was also instrumental in completion of this work. The faculty, fellow graduate students, and office staff of the department of Cellular and Integrative Physiology also deserve a great amount of gratitude. Pearl Sorenson, Kim Kavan, and Cindy Norton were invaluable in keeping me organized, sane, and able to complete grant submissions and meetings on time.

My thesis committee has also been tireless in their support and encouragement in my completion of this work. Drs. Steven Sansom, Matthew Zimmerman, Lie Gao, and Wallace Thoreson have been a regular source of advice and guidance. They have each shaped the completion of this dissertation in innumerable ways.

There are many great teachers in my past that are deserving of recognition. I grew up in a small town in rural South Dakota and was blessed with an embarrassment of riches when it came to knowledgeable and dedicated teachers. In particular, my love of science was greatly influenced by my junior high and high school science teacher Mr. Steve Konda. Relentless in his pursuit to provide us with a quality science education, we had access to incredible equipment and tools for such a small school. His creative laboratory demonstrations continue to stick with me. In college, the influence of Dr. David Woodman further honed a desire to pursue physiology as an area of study, and equipped me with many communication and teaching skills.

I know I would not be the person I am today, nor could I have accomplished this work without the influence and support of my family, especially my parents and grandparents. My father and grandfather instilled in me the value and honor of working hard as they each tended the same

soil handed down to them by their fathers. Each insatiably curious, meticulous, and brilliant – they taught me the joy of an inquisitive mind as we tore apart machinery to repair and restore it, as we built and fixed structures on the farm, and as we tended to the health of crops and livestock. I am convinced that the skills and attitudes I learned growing up with these two great men on the farm have shaped me into the scientist I am now becoming. My mother gave me a love for science as her nursing career allowed her to teach me about health and disease, about caring for those around us, and about the pursuit to make the world a little better place than how we found it. It was only through the sacrifice and hard work of my parents that I was able to succeed in school, attend college, and continue on toward my doctorate. I owe all I am today to my parents and grandparents.

My daughters, Sarachaia and Mariana, have been a fountain of joy and encouragement. Chaia, born at the start of my graduate training, has grown alongside this dissertation and has loved me throughout. Both my daughters give me the drive to continue to do better science, and to try and give them a better world to inherit. My wife, Rena, has been a bedrock of strength and support throughout my graduate career and is deserving of much more gratitude than I am able to provide here. She has been a constant source of encouragement and love. Throughout the many long workdays, late nights, and weekends in the lab, she has never wavered in her support. She is the hardest working person I know. She always listened and supported my crazy ideas, such as deciding to pursue a Ph.D., and has steeled my resolve whenever I questioned my own capabilities. She is the strongest and most beautiful person I know. I love you Rena.

SDG

INTERACTION BETWEEN ANGIOTENSIN II AND BDNF IN MODULATING SYMPATHETIC NERVE ACTIVITY:

Bryan K. Becker, Ph.D.

University of Nebraska Medical Center, 2015

Supervisor: Irving H. Zucker, Ph.D.

Over activation of the sympathetic nervous system is prevalent in many forms of cardiovascular disease such as chronic heart failure (CHF) and hypertension. Although increased neuronal renin-angiotensin system activity in presympathetic neurons has been well implicated in mediating this sympatho-excitation, many of the neuronal effects of angiotensin II (Ang II) signaling remain poorly understood. One particular mechanism of Ang II-mediated increases in presympathetic neuronal activity is through reductions in voltage-gated K^+ currents. Another pathway that has profound effects on neuronal K^+ currents and that has been previously implicated in Ang II-signaling is brain-derived neurotrophic factor (BDNF) activity through its receptor tyrosine kinase B (TrkB). Therefore, we hypothesized that BDNF/TrkB signaling is an important mediator of the neuronal effects of Ang II in modulating voltage-gated K^+ currents and autonomic dysfunction in cardiovascular disease states such as CHF and hypertension. We employed cell culture and whole-animal models to explore this hypothesis and utilized electrophysiological, molecular, and *in vivo* physiological techniques. Patch-clamp studies demonstrated that BDNF is involved in Ang II-induced reductions to K^+ currents. Further *in-vivo* experiments found that overexpression of Kv4.3 into the rostral ventrolateral medulla attenuates the increase in sympathetic nerve activity of rats post-myocardial infarction. Baroreflex dysfunction is common in CHF, and desensitization of central neuronal areas such as the nucleus tractus solitarius (NTS) can mediate this dysfunction. We therefore hypothesized that changes in BDNF/TrkB signaling in the NTS mediated baroreflex dysfunction in CHF. Blocking TrkB with ANA-12 in the NTS blunted baroreflex sensitivity in sham rats but had little effect on the already blunted baroreflex sensitivity of CHF rats. TrkB expression was reduced in CHF rats, implicating reduced BDNF/TrkB signaling

in the NTS as a mechanism for reduced baroreflex sensitivity during CHF. In a final set of experiments we explored the connection between Ang II and BDNF *in vivo*. Central administration of Ang II increased mean arterial pressure and induced sympatho-excitation, both of which were attenuated by coinfusion of ANA-12. Overall, these data implicate BDNF as an important factor in mediating the neuronal effects of Ang II on K⁺ currents, hemodynamics, baroreflex sensitivity, and sympathetic nerve activity.

TABLE OF CONTENTS

ACKNOWLEDGEMENTS.....	ii
ABSTRACT.....	v
TABLE OF CONTENTS.....	vii
LIST OF FIGURES	xi
LIST OF TABLES.....	xiii
LIST OF ABBREVIATIONS	xiv
INTRODUCTION	1
Cardiovascular Disease.....	2
Chronic Heart Failure	3
Hypertension.....	6
Renin-Angiotensin System	7
Sympatho-excitation	9
Central Autonomic Control Centers	10
Potassium Currents and Neuronal Activity.....	13
Neurotrophic Factors and Neuronal Activity.....	15
Objectives of the Dissertation.....	18
CHAPTER I: OVEREXPRESSION OF Kv4.3 IN RVLM OF RATS POST-MYOCARDIAL INFARCTION REDUCES SYMPATHETIC TONE.....	20
INTRODUCTION	21
METHODS	22
Animal Preparation	22
Model of CHF.....	22
Telemetry Implantation.....	22

Conscious Telemetry Recordings	24
Bilateral RVLM Injections of Adenoviral Particles	24
Acute Experimental Set-up and RSNA Recording	25
Construction of Arterial Baroreflex Curves.....	26
Western Blotting and Immunofluorescence.....	26
Statistics.....	27
RESULTS	28
Model of CHF.....	28
Kv4.3 Levels in the RVLM of Rats Post-MI.....	30
Hemodynamic Parameters of Rats Post-MI Improved by adKv4.3.....	32
adKv4.3 Improves Baroreflex Parameters of Rats Post-MI	37
adKv4.3 Attenuates the Increased RSNA Post-MI.....	39
DISCUSSION.....	42
Major Findings of Current Study.....	42
Conscious Parameters Following adKv4.3	42
Anesthetized Parameters Following adKv4.3.....	43
Limitations and Perspectives of Current Study	43
CHAPTER II: BDNF CONTRIBUTES TO ANGIOTENSIN II-MEDIATED REDUCTIONS IN PEAK VOLTAGE-GATED K ⁺ CURRENTS IN CULTURED CATH.A CELLS*	45
INTRODUCTION	46
METHODS	48
Chemicals	48
Cell Culture.....	48
Electrophysiology	48
Western Blotting	49

Statistics	50
RESULTS	51
Ang II Increases BDNF Expression.....	51
BDNF Reduces I _A	53
BDNF is Involved in the Ang II-Induced Reduction of I _A	56
Involvement of p38 MAPK in the BDNF-Induced Reduction of I _A	59
DISCUSSION	62
CHAPTER III: INFLUENCE OF BDNF/TRKB SIGNALING IN THE NTS ON BAROREFLEX SENSITIVITY IN RATS WITH CHRONIC HEART FAILURE	66
INTRODUCTION	67
METHODS	69
Animal Preparation	69
Microinjections into the NTS	69
Western Blotting	70
Statistics	71
RESULTS	72
Body Weight, Organ Weight, and Baseline Hemodynamics.....	72
Functional and Histological Identification of the dmNTS.....	74
Response to BDNF in the dmNTS in Sham and CHF Rats	76
Responses to ANA 12 into the dmNTS in Sham and CHF Rats	77
Effect of ANA 12 in the dmNTS on Baroreflex Sensitivity	80
Expression of BDNF and TrkB in the dmNTS in Sham and CHF Rats	85
DISCUSSION	87
Limitations	91

CHAPTER IV: CONTRIBUTION OF BDNF/TRKB SIGNALING TO SYMPATHO-EXCITATION FOLLOWING ICV ANGTIOTENSIN II.....	93
INTRODUCTION	94
METHODS	96
Animal Model.....	96
Animal Preparation and ICV Infusions.....	96
Conscious Parameters	97
Acute Animal Preparation	97
Statistics.....	97
RESULTS	99
Hemodynamic Responses to ICV Ang II.....	99
ICV Ang II and ANA-12 Alter Metabolic Balance	105
Acute Experiments Following ICV Ang II.....	108
Body and Organ Weights Following ICV Ang II.....	115
DISCUSSION.....	117
DISCUSSION.....	122
Major Findings of the Dissertation	123
Objectives 1-2: BDNF and Potassium Currents	125
Objective 3: BDNF in Baroreflex Control.....	127
Objective 4: Central Ang II-induced Sympatho-excitation and BDNF	128
Conclusions and Perspectives	129
REFERENCES	132
APPENDIX.....	148

LIST OF FIGURES

Figure 1– The vicious cycle of chronic heart failure.	5
Figure 2 - Simplified schematic of the central cardiovascular control centers of the rat brain.....	12
Figure 3 - Schematic diagram of the objectives of the dissertation.	19
Figure 4 – Experimental schematic of timeline for adKv4.3 overexpression.	23
Figure 5 – Adenoviral overexpression of Kv4.3 restores Kv4.3 in RVLN of rats post-MI.....	31
Figure 6 - adKv4.3 improves conscious hemodynamic parameters in rats post-MI.....	33
Figure 7 - Representative HRV plots from one rat before and after adKv4.3	34
Figure 8 - Mean SDNN data from adGFP and adKv4.3 rats.	35
Figure 9 - RMSSD and LF/HF ratios are unchanged between groups.	36
Figure 10 - Baroreflex function is improved in rats post-MI with adKv4.3	38
Figure 11 - Representative traces of RSNA from rats post-MI	40
Figure 12 - Mean data of RSNA from sham and post-MI rats with adGFP or adKv4.3	41
Figure 13 - Expression of BDNF, pro-BDNF, and TrkB following Ang II treatment.....	52
Figure 14 - BDNF decreases peak K ⁺ current in CATH.a cells.....	54
Figure 15 - Acute BDNF treatment has no effect on K ⁺ currents.	55
Figure 16 - Inhibiting BDNF/TrkB attenuates Ang II-mediated suppression of peak K ⁺ current .	57
Figure 17 - AT1R is not involved in BDNF-mediated suppression of K ⁺ currents.	58
Figure 18 - p38 MAPK is involved in BDNF-mediated suppression of K ⁺ currents.....	60
Figure 19. Histological analysis and functional identification of microinjection sites in the dorsal medial nucleus tractus solitarius (dmNTS)	75
Figure 20 - Representative figures showing the effects of microinjection into the dmNTS.....	78
Figure 21 - Dose-dependent effects of microinjection of BDNF.....	79
Figure 22 - Representative figures showing the effects of bilateral microinjection of ANA12 on BRS	81

Figure 23 – Effects of ANA-12 on baroreflex control of HR.....	82
Figure 24 - Effects of ANA-12 on baroreflex control of sympathetic nerve activity	83
Figure 25 - Protein expression of BDNF and TrkB in dmNTS of sham and CHF rats	86
Figure 26 - Experimental timeline and schematic for ICV infusion of Ang II \pm ANA-12	98
Figure 27 - Effect of ICV Ang II with or without ANA-12 on MAP	100
Figure 28 – Effect of ICV Ang II with or without ANA-12 on HR.....	101
Figure 29 - Heart rate variability parameters following ICV Ang II	102
Figure 30 - Frequency domain analysis following IVC Ang II	103
Figure 31 - Spontaneous baroreflex sensitivity following ICV Ang II.....	104
Figure 32 - Water balance following ICV Ang II.....	106
Figure 33 - Daily food balance following ICV Ang II.	107
Figure 34 - Ang II blunts the HR baroreflex.....	110
Figure 35 - Renal sympathetic nerve activity baroreflex following ICV Ang II	111
Figure 36 – Representative tracings of renal sympathetic nerve activity following Ang II or Ang II + ANA-12.....	113
Figure 37 - Baseline renal sympathetic nerve activity following ICV Ang II	114
Figure 38 - Representative Diagram of the Major Findings of the Dissertation.....	124

APPENDIX FIGURES

Figure A1 – Representative confocal image of labeled RVLM neurons following IML injection of rhodamine beads.....	149
Figure A2 – Increased expression of BDNF in whole brainstem of mice following Ang II and PVN of rats with CHF.....	150
Figure A3 – Preliminary results exploring dose-response of ICV Ang II	151

LIST OF TABLES

Table 1 – Hemodynamic, echocardiographic, and weight parameters	29
Table 2 - Effects of BDNF with or without p38 MAPK inhibition on kinetic parameters of I _A ...	61
Table 3 - Hemodynamic and echocardiographic data in sham and CHF rats	73
Table 4 - Summary data for baroreflex function before and after microinjection of chemicals into the dmNTS in sham and CHF rats.....	84
Table 5 - Left Ventricular Hemodynamic Parameters	109
Table 6 - Baroreflex parameters following ICV Ang ± ANA-12	112
Table 7 - Final body and organ weights following ICV treatment	116

LIST OF ABBREVIATIONS

ACE	angiotensin converting enzyme
aCSF	artificial cerebrospinal fluid
adGFP	adenoviral green florescent protein
adKv4.3	adenoviral Kv4.3
AHP	after hyperpolarizing potential
Ang II	angiotensin II
AP	action potential
AT1R	angiotensin type-1 receptor
AT2R	angiotensin type-2 receptor
BDNF	brain-derived neurotrophic factor
BP50	blood pressure at midpoint of baroreflex range
BRS	baroreflex sensitivity
BW	body weight
CaMK	calcium/calmodulin kinase
CHF	chronic heart failure
CREB	cyclic adenosyl monophosphate-responsive element-binding protein
CVLM	caudal ventrolateral medulla
DBP	diastolic blood pressure
dmNTS	dorsal medial nucleus tractus solitarius
EF	ejection fraction
ERK	extracellular signal-regulated kinase
FS	fractional shortening
GABA	gamma-aminobutyric acid
Gmax	max gain of baroreflex

HF	heart failure
HR	heart rate
HRV	heart rate variability
HW	heart weight
I _A	A-type potassium current
ICV	intracerebroventricular
IML	intermediolateral column of the spinal cord
IPSP	inhibitory post-synaptic potential
IRP	isovolumetric relaxation point
I-V	current-voltage
K _v	voltage-gated potassium channel/current
LF	low frequency
LTP	long-term potentiation
LV	left ventricle/ventricular
LVEDP	left ventricular end diastolic pressure
MAP	mean arterial pressure
MAPK	mitogen-activated protein kinase
mnPO	median preoptic nucleus
NGF	nerve growth factor
NMDA	N-methyl-D-aspartate
NT-3	neurotrophin-3
NT-4	neurotrophin-4
NTS	nucleus tractus solitarius
NYHA	New York Heart Association
post-MI	post-myocardial infarction
PVN	paraventricular nucleus

RAS	renin-angiotensin system
RMSSD	root mean squared of successive differences
RSNA	renal sympathetic nerve activity
RVLM	rostral ventrolateral medulla
SBP	systolic blood pressure
sBRS	spontaneous baroreflex sensitivity
SDNN	standard deviation of N-N intervals
SFO	subfornical organ
SHR	spontaneous hypertensive rate
TL	tibia length
TrkB	receptor tyrosine kinase B
WLW	wet lung weight

INTRODUCTION

Cardiovascular Disease

Cardiovascular diseases are the leading cause of mortality and morbidity worldwide and as such pose a large health and economic burden (Kearney *et al.*, 2005). Although death rates from all cardiovascular disease fell by 31% from 2000 to 2010, cardiovascular disease is still responsible for approximately 1 in every 3 deaths in the United States (Go *et al.*, 2013). This equates to over 2150 deaths per day. As cardiovascular diseases are diverse and stem from a large number of etiologies, treatment options are likewise widely diverse, often with limited effectiveness. Many current treatment options address secondary symptoms in hopes of ameliorating the end-organ damage associated with declining cardiovascular function. Therefore both basic and clinical research endeavors target the underlying causative and translational factors in cardiovascular disease in the hopes of better understanding the mechanisms involved in the pathophysiology of cardiovascular disease.

Although the entire class of cardiovascular diseases comprises a large number of differing pathologies including genetic cardiomyopathies, vascular dysfunction, stroke, and arrhythmias to name only a few, chronic heart failure (CHF) and hypertension are the two most common forms of cardiovascular disease. Heart failure and hypertension share a number of similar pathophysiological mechanisms. Patients with hypertension are at a much higher risk for developing heart failure or stroke, and the growing incidence of hypertension predicts a future with a growing number of patients with heart failure and cardiovascular comorbidities.

Chronic Heart Failure

Chronic heart failure is the leading cause of mortality in the United States and many developed nations (Go *et al.*, 2013). Simply stated, CHF is a decrease in the pumping efficiency of the heart resulting from a variety of etiologies be it by dilation due to pressure overload in hypertension, myocardial infarction caused by atherosclerotic blockage of a coronary artery, or diabetic cardiomyopathy. The decrease in pumping efficiency leads to reduced cardiac output and initiates a series of compensatory mechanisms with the intent of preserving arterial pressure and tissue perfusion. These compensatory mechanisms involve increased renin-angiotensin system (RAS) activity, changes to the autonomic nervous system, and cardiomyocyte remodeling (Zucker *et al.*, 2012). Although often successful in preserving cardiac function in the short term, as the underlying causes are not addressed (e.g. myocardial infarction), over time these compensatory mechanisms themselves can result in further damage to cardiomyocytes. This further damage begets more compensatory action and a vicious, positive-feedback cycle of heart failure emerges (Figure 1). As this detrimental cycle continues, the compensatory ability, or reserve capacity, of the heart diminishes. Often a reduced cardiac reserve is only noticed during exercise, when the heart is put under acute stress that causes it to reach the limits of its compensated reserve capacity. This decreased exercise capacity is generally referred to as exercise intolerance and exercise is often used in the clinic to diagnose CHF. When damage and remodeling exceed the reserve capacity of the heart, decompensated CHF emerges (Hall, 2011).

A number of clinically useful categories for classifying CHF have been developed, and the most common is the New York Heart Association (NYHA) classification system, which ranges from class I (least severe/symptomatic) to class IV (most severe with significant symptomatic presentation, i.e. decompensated). Treatment options vary for each classification and range from recommended exercise and dietary changes to high dose diuretics, RAS inhibitors and sympatholytics, or in severe cases require the need for cardiac transplantation. Some of these

treatment strategies will be discussed below as they relate to targeting the compensatory components of the vicious cycle of CHF. However, as many treatment options target the end-organ effects and symptoms of this progressive cycle, investigation into the initiating causative factors is needed in order to elucidate important pathways for future therapeutic targets.

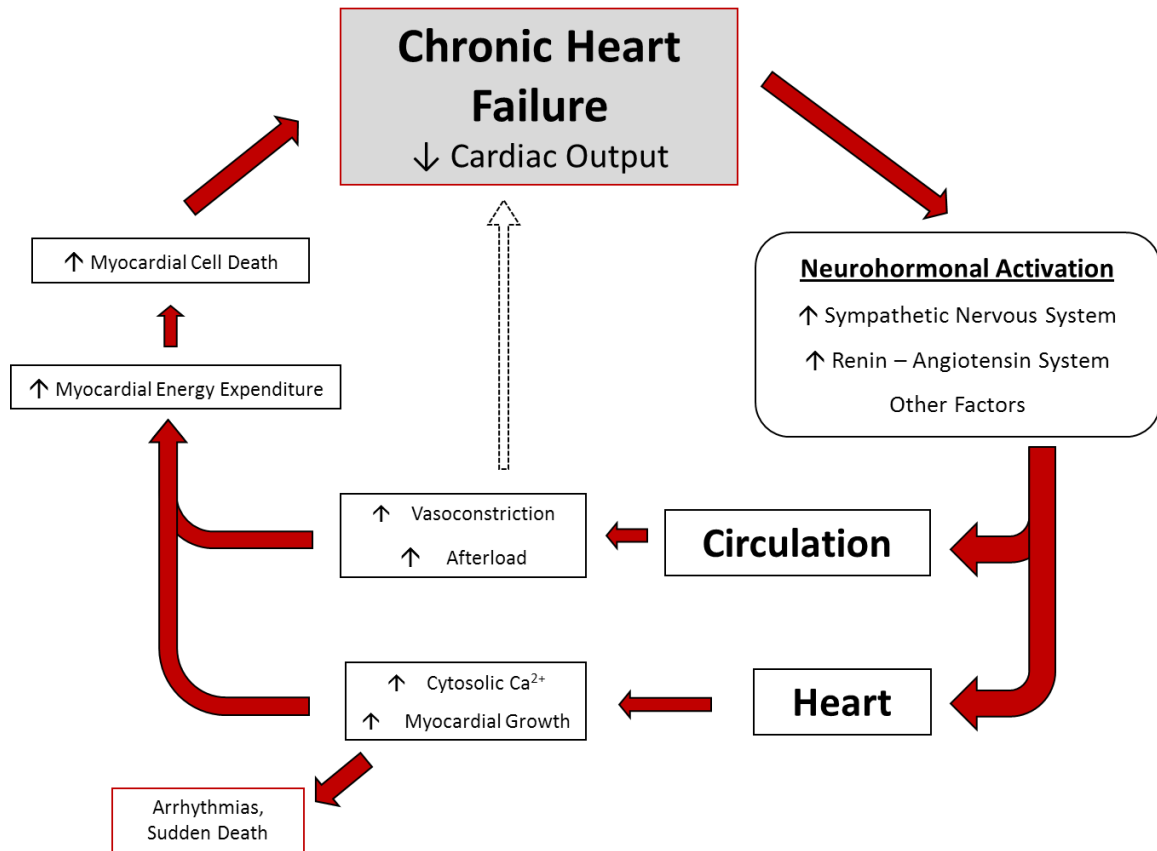


Figure 1– The vicious cycle of chronic heart failure.

Schematic representation of the progression of chronic heart failure. Decreases in cardiac output evoke neurohumoral compensatory mechanisms including increased sympathetic nervous system activity and renin-angiotensin system activation. This places further strain on the myocardium leading to further declines in function and a perpetuation of the cycle.

Hypertension

One of the most significant risk factors for the development of CHF or other causes of death is hypertension (Stevens, 2009). In the United States, one out of every three adults has hypertension (Go *et al.*, 2013). Hypertension is currently defined as systolic blood pressure (SBP) ≥ 140 mmHg or diastolic blood pressure (DBP) ≥ 90 mmHg and prehypertension as SBP of 120-139 mmHg or DBP of 80-89 mmHg (Rosendorff *et al.*, 2015). Hypertension can contribute to the development of coronary artery disease; a major initiating cause for the development of CHF. Each 20 mmHg increase in SBP doubles the risk for fatal coronary events. Age has also been demonstrated to increase the risk for developing both hypertension, associated acute coronary events, and CHF. As of 2004, 73% of patients presenting with acute decompensated CHF exhibited hypertension, making it the most common comorbidity associated with CHF (Adams Kirkwood F *et al.*, 2005).

Although there are many causes of secondary hypertension such as renal artery stenosis, diabetes, and obesity, a well-defined etiology for primary or essential hypertension remains elusive. A number of experimental models and indications within the hypertensive population suggest that there is a neurological component to the development of many forms of hypertension through increased activity of the sympathetic nervous system. The RAS has also been demonstrated to be critical in mediating hypertension with experimental evidence indicating an important role for the central nervous system RAS in promoting sympatho-excitation (Young & Davisson, 2015).

Renin-Angiotensin System

Common in many forms of hypertension and CHF are activation of the RAS. For the purposes of this dissertation, the brain RAS is of primary importance. The primary effector peptide of the RAS is angiotensin II (Ang II) which is cleaved from angiotensin I by angiotensin converting enzyme (ACE). Ang II is known to mediate cellular effects through binding to its G-protein coupled, angiotensin type 1 receptor (AT1R) and the angiotensin type 2 receptor (AT2R). Metabolites of Ang II, such as Ang 1-7, have been shown to bind to other receptors such as the Mas receptor (Young *et al.*, 1986; Xiao *et al.*, 2011, 2013). AT1R is generally thought to mediate the central processes leading to sympatho-excitation (Zimmerman, 2002; Zimmerman *et al.*, 2004; Gao *et al.*, 2004, 2008; Yin *et al.*, 2010; Haack *et al.*, 2012) and baroreflex dysfunction (Gao *et al.*, 2005b; Wang *et al.*, 2007). The AT2R and the Mas receptor comprise the so-called protective arm of central RAS signaling (Gao *et al.*, 2008, 2014; Yang *et al.*, 2011; Xiao *et al.*, 2011; Zucker *et al.*, 2012; Unger *et al.*, 2015). Pharmacological inhibitors of RAS are often used in treating CHF and hypertension. ACE-inhibitors such as captopril (Franzosi & Santoro, 1998) and angiotensin receptor blockers such losartan (Farsang, 2011) have been indicated for the treatment of hypertension and CHF.

It has generally been thought that elevated levels of circulating Ang II in CHF and hypertension do not have direct access to central areas of cardiovascular control as the peptide is too large to adequately pass the blood brain barrier. Recent evidence has questioned this assumption by demonstrating both increased blood brain barrier permeability due to Ang II (Faraco & Iadecola, 2013) and by observing labeled Ang II extravasation into many areas of the hypothalamus and brainstem that are involved in cardiovascular control previously thought to be inaccessible to circulating Ang II (Biancardi *et al.*, 2013). Along with increased blood brain permeability, areas of the central nervous system lacking a robust blood brain barrier, such as the circumventricular organs, pose particular interest in central Ang II regulation due to their ability to detect circulating

factors (Mangiapane & Simpson, 1980; Zimmerman *et al.*, 2004; Latchford *et al.*, 2005; Ferguson, 2009).

In addition to the role of circulating Ang II influencing central neuronal network activity, the brain itself has been demonstrated to fully express its own endogenous RAS (Grobe *et al.*, 2008). This neuronal-derived RAS suggests that the RAS is acting in a different physiological manner than its traditional actions in the periphery and implicates RAS activity, particularly Ang II signaling, in altering neuronal activity as a neurotransmitter, neuromodulator, or some combination thereof. To this end, much of the work by us and others has focused on the neuronal actions of the central RAS and its role in mediating sympatho-excitation.

Sympatho-excitation

Chronic heart failure and many forms of hypertension are characterized by excessive sympathetic nerve activity (Guyenet, 2006; Zucker *et al.*, 2012). This increase in sympathetic outflow has multiple effects on innervated visceral organs. Cardiac sympathetic nerves releasing norepinephrine and acting on adrenergic receptors in the myocardium increase Ca^{2+} signaling and thus increase inotropic parameters of the heart along with an increase in heart rate thus increasing myocardial oxygen demand. The use of β_1 -adrenergic blockers such as metoprolol is often used to decrease cardiac sympathetic tone reducing heart rate and metabolic demand. Renal sympathetic nerve activity results in afferent arteriolar constriction decreasing glomerular filtration rate, induces sodium and water reabsorption, and stimulates renin release thus increasing RAS activity (Hall, 2011). Vascular sympathetic tone induces vasoconstriction, resulting in a robust increase in vascular resistance and increased blood pressure.

Increased sympathetic tone is correlated with increasing NYHA CHF class as there is increased bursting of muscle sympathetic nerves with increasing severity of CHF (Ferguson *et al.*, 1990). Sympatho-excitation is also a negative predictor of survival in that patients with an elevated plasma norepinephrine concentration experienced greater mortality rates compared to those with lower plasma norepinephrine concentrations (Davies *et al.*, 2000). Understanding the central mechanisms underlying this increase in sympathetic tone is an important goal for the future management of cardiovascular diseases.

Central Autonomic Control Centers

The central neuronal populations that contribute to cardiovascular and sympathetic control are distributed throughout the brain in the forebrain, hypothalamus, and brainstem. In brief, the network can be summarized into a number of circuits one of which incorporates the baroreflex arc in which peripheral baroreceptor afferent neurons terminate in the nucleus tractus solitarius (NTS). Excitatory projections (e.g. glutamatergic) extend to the caudal ventrolateral medulla (CVLM) in which a mode switch occurs and inhibitory neurons (e.g. GABAergic) project to the rostral ventrolateral medulla (RVLM). The RVLM has direct projections to the intermediolateral (IML) column of the spinal cord (Oshima *et al.*, 2006; Yue *et al.*, 2014) connecting it to sympathetic preganglionic neurons and ultimately end organ sympathetic nerves (Figure A1). The RVLM is therefore under robust baroreflex control and is also an important mediator of total vasomotor tone. Ablation or pharmacological inhibition of the RVLM removes nearly all vasomotor tone (Schreihofer *et al.*, 2000).

As mentioned above, circumventricular organs such as the subfornical organ (SFO) and osmosensitive neurons in areas like the median preoptic nucleus (mnPO) can sense circulating factors. These centers have projections to nuclei in the hypothalamus such as the paraventricular nucleus (PVN). Paraventricular neurons also have direct projections to sympathetic preganglionic neurons and to the RVLM. Neurons in the NTS responding to atrial volume receptors suppress PVN activity through GABAergic interneurons. This provides a negative feedback loop for the osmosensitive pathway as an increased dipsogenic response to high osmolarity is limited by atrial stretch from the increase in volume following the increased thirst. The PVN therefore plays a key role in mediating forebrain osmosensitive and circulating Ang II sensitive areas of the SFO with input from the NTS. Activity of the PVN can either directly influence vasomotor tone through connections with sympathetic preganglionic neurons or through the RVLM (Guyenet, 2006).

These and other important autonomic centers have been well studied in the area of autonomic control of blood pressure and sympathetic nerve activity in the settings of CHF and hypertension and will be discussed further in the subsequent chapters of this dissertation. A simplified schematic of these central areas of cardiovascular control is provided in Figure 2.

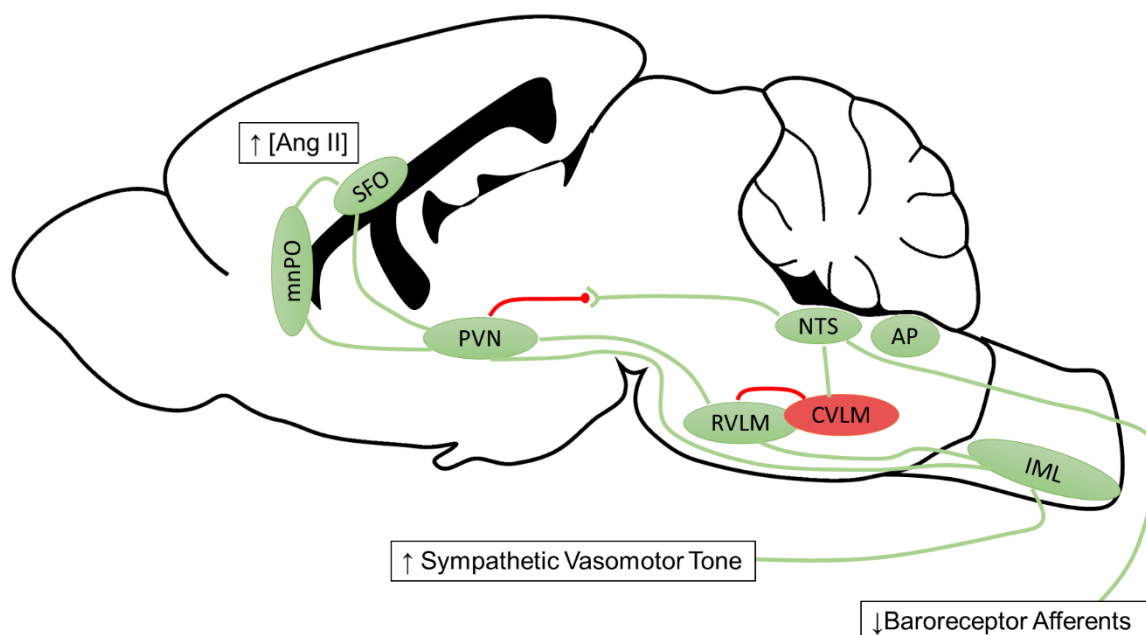


Figure 2 - Simplified schematic of the central cardiovascular control centers of the rat brain.

In the setting of chronic heart failure or hypertension baroreceptor dysfunction leads to decreased afferent activity to the NTS. This removes the tonic suppression of RVLM activity from the CVLM and results in increased sympathetic outflow to end organs. Furthermore, central angiotensin II signaling throughout the control centers, and particularly in the SFO and other circumventricular organs increases sympathetic outflow through the PVN and RVLM.

AP = area postrema; NTS = nucleus tractus solitarius; CVLM = caudal ventrolateral medulla; RVLM = rostral ventrolateral medulla; PVN = paraventricular nucleus; SFO = subfornical organ; mnPO = median preoptic nucleus; IML = intermediolateral column of the spinal cord.

Potassium Currents and Neuronal Activity

Changes in potassium currents are integral to the mechanism by which Ang II alters neuronal activity, and of particular interest are voltage-gated K⁺ (K_v) currents. Peak, transient inactivating currents (I_A) in neurons are conducted by K_v channel proteins Kv1.4, Kv3.3-4, and Kv4.1-4 (Kim & Hoffman, 2007). I_A was first observed and described by Hagiwara et al. (1961) and was given the name I_A by Connor and Stevens (1971). I_A is present in many tissues such as myocardium, smooth muscle, lung, and neurons (Birnbaum *et al.*, 2004). In the central nervous system, Kv4.x isoforms tend to be the predominately expressed channel proteins responsible for conduction of I_A. Kv4.2 and Kv4.3 are highly expressed throughout the brain and Kv4.1 is more limited to granule cells of the olfactory bulb (Serôdio & Rudy, 1998). In hippocampal CA1 neurons, I_A (mainly conducted by Kv4.2) is an important regulator of neuronal excitability and synaptic plasticity involved in long-term potentiation (LTP) (Birnbaum *et al.*, 2004) through its regulation of action potential (AP) threshold, initiation, repolarization, and AP width (Kim *et al.*, 2005; Chen *et al.*, 2006; Nerbonne *et al.*, 2008; Carrasquillo *et al.*, 2012; Kim & Hoffman, 2012). In fact, much of the work on I_A has been investigated in CA1 neurons of the hippocampus and has greatly enhanced our understanding of the physiological mechanisms by which I_A alters neuronal activity and synaptic plasticity. Overexpression of Kv4.2, which increases I_A, reduced the synaptic expression of NMDA receptors and prevented LTP. Conversely, reducing I_A increases NMDA receptor synaptic availability and increased LTP (Kim *et al.*, 2007; Jung *et al.*, 2008) demonstrating I_A to be a negative regulator of neuronal excitability by altering glutamatergic neurotransmission and LTP synaptic plasticity. Beyond the subthreshold, AP limiting actions of I_A, suprathreshold activity reshapes the AP causing it to be narrower and more robust with longer duration after-hyperpolarization potentials (AHPs), which together reduce AP frequency (Kim *et al.*, 2005). In summary, studies, particularly on Kv4.2 in CA1 neurons, of the hippocampus suggest a role for I_A in reducing neuronal excitability and LTP-driven synaptic plasticity.

The distribution of Kv4.x protein expression in autonomic centers of the medulla and brain stem appears to be mixed between Kv4.2 and Kv4.3 depending on the particular nucleus in question (Serôdio & Rudy, 1998). Paraventricular neurons appear to have a predominance of Kv1.4 and Kv4.3 with little to no Kv4.2 (Sonner & Stern, 2007), and the RVLM has been shown to express Kv4.3 (Gao *et al.*, 2010; Wu *et al.*, 2012). In PVN projecting neurons, I_A exhibits remarkably similar electrophysiological characteristics to the hippocampus in that inhibition of I_A alters AHPs and AP width to increase AP frequency although it has no effect on AP threshold (Sonner & Stern, 2007).

As I_A comprises a critical component in regulating neuronal activity and electrophysiological characteristics, it stands to reason that alterations to I_A may contribute to the pathology of various neurological disease states. In fact, I_A has been implicated in various forms of epilepsy (Fransén & Tigerholm, 2010; Lerche *et al.*, 2013) and pain hypersensitivity (Chien *et al.*, 2007; Cao *et al.*, 2010). Recent attention has been given to I_A in mediating the sympatho-excitation associated with CHF and hypertension. In RVLM projecting PVN neurons, neuronal activity is increased from a reduction in I_A (Sonner *et al.*, 2008), and a decreased expression of Kv4.3 along with reduced I_A was observed in the RVLM of rats with CHF (Gao *et al.*, 2010). Contributing to I_A dysfunction in these disease states is the involvement of the RAS. Ang II signaling through AT1R reduces Kv4.3 expression and I_A *in vitro* (Gao *et al.*, 2010), reduces I_A in neonatal rat hypothalamic and brain stem neurons (Wang *et al.*, 1997), and reduces I_A and steady state K^+ currents *in vitro* via mitochondria-produced superoxide. Conversely, the protective arm of the RAS, AT2R and Mas receptor signaling, increase I_A and total K^+ current densities (Kang *et al.*, 1992, 1993; Yang *et al.*, 2011). Although the involvement of the RAS in modulating I_A is becoming more established, the particular signaling mechanisms and mediators of long-term changes are not well defined.

Neurotrophic Factors and Neuronal Activity

Classically, the role of neurotrophic factors has been understood to aid neuronal development and dendritic sprouting (Levi-Montalcini *et al.*, 1954; Cohen & Levi-Montalcini, 1960; Levi-Montalcini & Calissano, 1979); however, recent attention has been focused on elucidating the role of neurotrophic factors in neuronal network patterning and neuronal sensitivity by facilitating actions such as LTP and altering ion channel function (Rose *et al.*, 2004; Blum & Konnerth, 2005; Minichiello, 2009; Park *et al.*, 2014). Due to the ability of neurotrophins to modulate neuronal synaptic plasticity, LTP, and ion channel function, they offer a potential mechanism for the modulation of autonomic neuronal pathways in promoting sympatho-excitation in CHF and hypertension.

Neurotrophins consist of a small family of secreted peptides including nerve growth factor (NGF), brain-derived neurotrophic factor (BDNF), neurotrophin 3 (NT-3), and neurotrophin 4 (NT-4). Central nervous system distribution of these factors is varied. NGF is primarily localized in areas of the hippocampus, olfactory bulb, and cortex (Shelton & Reichardt, 1986) and expression can be induced in the hypothalamus and brainstem by the antimetabolic drug colchicine (Ceccatelli *et al.*, 1991). Neurotrophin-3 expression is limited to hippocampal neurons and cerebellar granule cells (Maisonpierre *et al.*, 1990; Ceccatelli *et al.*, 1991). Neurotrophin-4 appears to be expressed throughout the rat brain (Timmusk *et al.*, 1993). The central nervous system expresses high levels of BDNF. Conner *et al.* (1997) characterized the expression level of BDNF protein throughout the rat brain. They found high expression levels in the SFO, parvocellular hypothalamic PVN neurons, NTS, and area postrema. RVLM expression was not reported. The high expression levels of BDNF in these autonomic control centers suggests that it may play an important role in modulation of autonomic neuronal activity and synaptic plasticity. Importantly, BDNF has been previously implicated in autonomic pathway dysfunction (Mattson & Wan, 2008; Martin *et al.*, 2009).

BDNF signaling through receptor tyrosine kinase B (TrkB) can function as both a neurotransmitter and neuromodulator and can thus act both acutely and chronically to alter neuronal firing and neuronal sensitivity to synaptic input (Rose *et al.*, 2004). BDNF/TrkB signaling ability to potentiate synapses and increase glutamatergic signaling and excitatory ion channel activity has been well investigated in the hippocampus (Minichiello, 2009). BDNF/TrkB signaling elicits several long-term neuromodulatory actions as well as immediate, rapid signaling that affects neuronal activity. BDNF rapidly enhances vesicular neurotransmitter release from excitatory neurons (Shinoda *et al.*, 2014) in the hippocampus. TrkB phosphorylation of NMDA receptors increases their open probability (Levine *et al.*, 1998), and BDNF/TrkB signaling results in rapid opening of TrpC channels (Li *et al.*, 1999), Nav1.9 channels (Blum *et al.*, 2002), and Ca²⁺ influx (Rose *et al.*, 2003). In peripheral dorsal root ganglion neurons involved in diabetic neuropathy, endogenous BDNF signaling was found to mediate increased neuronal sensitivity through reductions in I_A and total K⁺ currents (Cao *et al.*, 2010). Preliminary observations from our laboratory have observed increased firing rate and decreased AP threshold in dorsal root ganglion neurons following incubation with BDNF (Wang HJ, unpublished observations).

The RAS may also play a role in mediating the expression levels of BDNF and contribute to BDNF/TrkB signaling. In rat and human adrenocortical cells Ang II induces BDNF expression via an AT1R mechanism (Szekeres *et al.*, 2010) and intracisternal Ang II induces robust BDNF expression in RVLM neurons (Chan *et al.*, 2010). Our preliminary experiments also suggested an increase in BDNF in the brainstem of mice following subcutaneous Ang II (Figure A2A) and increased BDNF in the PVN of rats with CHF (Figure A2B). Paradoxically, one report found that in SHR rats whole brain expression of BDNF increased after AT1R antagonism. The authors also reported increased BDNF expression in human cerebrovascular endothelial cells after treatment with Ang II and AT1R blockade with candesartan, implicating AT2R in the mechanism of BDNF expression (Alhusban *et al.*, 2013). These reports all implicate a connection between the

RAS and BDNF expression; however, the precise mechanisms and receptors involved remain poorly defined.

Furthermore, BDNF/TrkB signaling and AT1R signaling share a number of commonalities (Salim *et al.*, 2011). Both involve activation of the same kinases such as mitogen-activated protein kinase/extracellular signal-regulated kinase (MAPK/ERK) (York *et al.*, 1998; Chan *et al.*, 2005, 2007; Park & Poo, 2012; Xiao *et al.*, 2013) and Ca²⁺/calmodulin kinase (CaMK) (Sun *et al.*, 2003; Caldeira *et al.*, 2007; Minichiello, 2009). Interestingly, Kv4.2 has been demonstrated to be a substrate for MAPK/ERK (Adams *et al.*, 2000), and CamKII-MAPK pathway destabilizes Kv4.3 mRNA (Zhou *et al.*, 2012) further supporting the ability of downstream signaling pathways of BDNF/TrkB and AT1R to modulate I_A. Both AT1R and BDNF/TrkB pathways also utilize cyclic adenosyl monophosphate-responsive element-binding protein (CREB) transcriptional control (Ginty *et al.*, 1994; Gaiddon *et al.*, 1996; Mitra *et al.*, 2010; Chan *et al.*, 2010). These commonalities in signaling and the increased expression of BDNF following Ang II, point toward an exciting and novel area of research for investigating the role BDNF and the RAS play in mediating neuronal sensitivity and potentiation of sympatho-excitation during cardiovascular disease states.

Objectives of the Dissertation

The mechanisms and factors involved in the Ang II-mediated reduction in neuronal K⁺ currents leading to the development of sympatho-excitation in cardiovascular diseases such as CHF and hypertension are not fully known. BDNF/TrkB signaling poses a potential mechanism for potentiation of presympathetic neuronal activity in the central nervous system. Therefore, we **hypothesized that BDNF/TrkB signaling is an important mediator of the neuronal effects of Ang II in modulating voltage-gated K⁺ currents and autonomic dysfunction in cardiovascular disease states such as CHF and hypertension.**

Specifically, the objectives set forth in this dissertation are as follows:

1. To evaluate the *in vivo* contribution of Kv4.3 in the RVLM to sympathetic nervous system activity.
2. To determine if BDNF/TrkB signaling is involved in Ang II-mediated reductions of K⁺ currents.
3. To investigate the potential contribution of BDNF/TrkB signaling to autonomic dysfunction in a rat model of CHF.
4. To investigate the involvement of BDNF/TrkB in mediating sympatho-excitation caused by central Ang II signaling.

Each objective will be presented in the following chapters with each study containing a brief introduction, detailed methods, results and brief discussion of major findings. A final comprehensive discussion will follow providing a cohesive overview of the major findings and implications of the dissertation. A schematic of the objectives is presented in Figure 3.

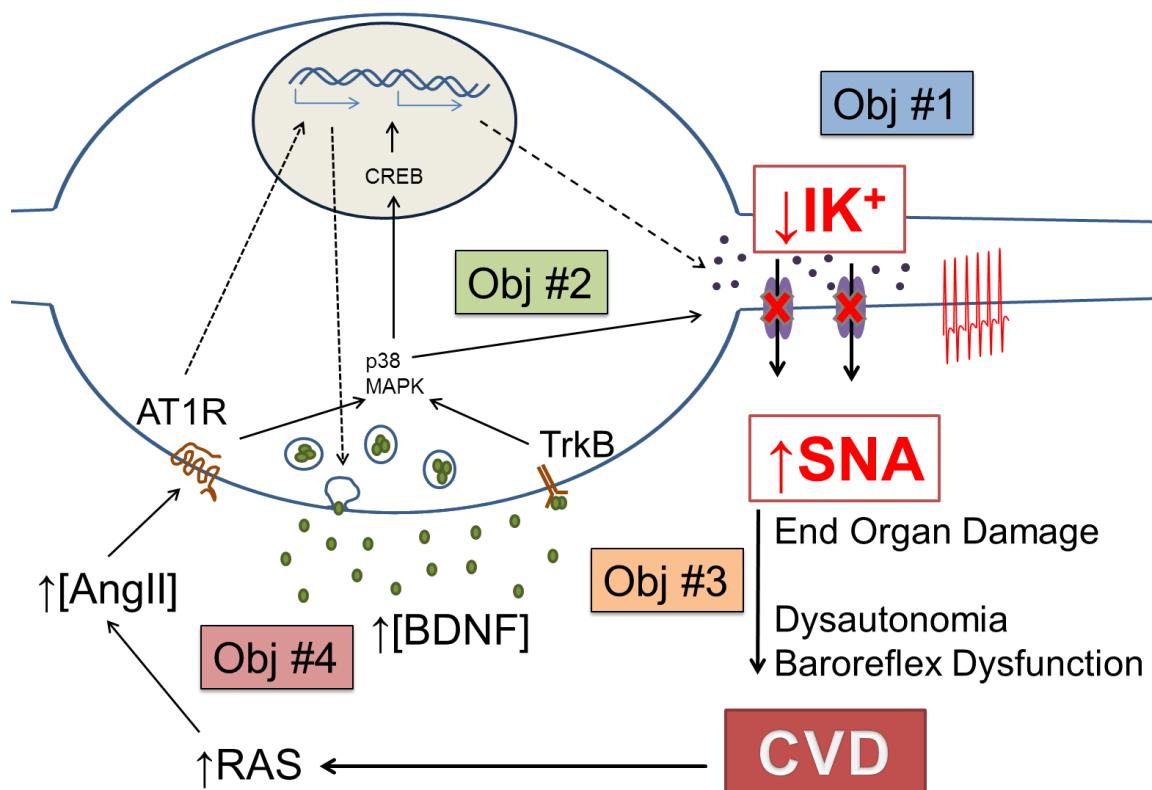


Figure 3 - Schematic diagram of the objectives of the dissertation.

Objective (Obj) #1 will evaluate the *in vivo* contribution of Kv4.3 in the RVLM to sympathetic nervous system activity.

Obj #2 will determine if BDNF/TrkB signaling is involved in Ang II-mediated reductions of K⁺ currents.

Obj #3 will investigate the potential contribution of BDNF/TrkB signaling to autonomic dysfunction in a rat model of CHF.

Obj #4 will investigate the involvement of BDNF/TrkB in mediating sympatho-excitation caused by central Ang II signaling.

**CHAPTER I: OVEREXPRESSION OF Kv4.3 IN
RVLM OF RATS POST-MYOCARDIAL
INFARCTION REDUCES SYMPATHETIC TONE**

INTRODUCTION

As mentioned in the preceding section, the expression and activity of the voltage-gated K⁺ channel, Kv4.3, is decreased in the RVLM of rats with CHF (Gao *et al.*, 2010). Because a suppression of these I_A-type channels results in a sensitized and more excitable neuronal state (Sonner & Stern, 2007; Sonner *et al.*, 2008), the decreased availability and function of this channel indicates a potential mechanism by which increased sympathetic activity may occur. However, it remains to be seen what role these channels play in the RVLM of the intact, conscious rat in the CHF state, or if the availability of these channels in RVLM neurons directly mediates sympathetic tone.

In a recent study, Gerald *et al.* (2014) overexpressed the potassium channel Kir2.1 in the RVLM of spontaneously hypertensive rats (SHR). This channel was selected by the authors due to its ability to decrease neuronal activity and was thus used to demonstrate the importance of tonic RVLM neuronal tone in maintenance of the hypertensive state of the SHR. Overexpression of Kir2.1 reduced MAP and the low frequency component of systolic pressure in SHRs, indicating a reduction in sympathetic tone following depression of RVLM neuronal activity. This study provides further rationale for investigations into potassium channel activity in the RVLM during sympatho-excitatory disease states such as hypertension and CHF. Although, because of the selection of the Kir2.1 channel simply due to its ability to suppress neuronal activity, and the lack of evidence implicating the channel in the RVLM during cardiovascular diseases, the basic research implications of the study are limited.

We therefore aimed to investigate the role of Kv4.3 in RVLM neurons during disease states such as CHF based, in part, on our previous evidence. **We hypothesized that overexpression of Kv4.3 in the RVLM of rats with CHF attenuates the increased sympathetic tone associated with CHF.**

METHODS

Animal Preparation

For these experiments a total of 19 male Sprague-Dawley rats of approximately 200 g were used. These experiments were approved by the Institutional Animal Care and Use Committee of the University of Nebraska Medical Center and were carried out under the guidelines of the National Institutes of Health *Guide for the Care and Use of Laboratory Animals*. An overview of the experimental paradigm and timeline is provided in Figure 4.

Model of CHF

CHF was produced by left coronary artery ligation as described in previous studies (Fishbein *et al.*, 1978; Pfeffer *et al.*, 1979; Wang *et al.*, 2008, 2010*b*, 2010*a*). Briefly, the rat was ventilated at a rate of 60 breaths/min with 3% isoflurane as a left thoracotomy was performed through the fifth intercostal space, the pericardium was opened, the heart was exteriorized, and the left anterior descending coronary artery was ligated with 6-0 prolene suture. Successful infarction of the left ventricle (LV) was confirmed by blanching of the myocardium at the time of ligation. Sham animals were subjected to thoracotomy but the coronary artery was not ligated.

In all animals 4 weeks post-myocardial infarction (post-MI) or sham surgery cardiac function was measured by echocardiography (VEVO 770, Visual Sonics, Inc.) as previously described. Animals with an ejection fraction (EF) of less than 45% were included into the post-MI group while those possessing EF greater than 60% were considered sham.

Telemetry Implantation

Following echocardiography and group designation, rats were implanted with telemetry units for recording of conscious, freely moving blood pressure as described previously (Gao *et al.*, 2014). In brief, animals were anesthetized with 2-4% isoflurane via inhalation. The left femoral artery was dissected and a DSI telemetry unit (TA11PA-40) catheter was inserted and advanced

into the abdominal aorta. The telemetry unit was placed in a pocket formed under the abdominal skin and tied in place. Rats were allowed to recover for 7 days before the initiation of any further experiments.

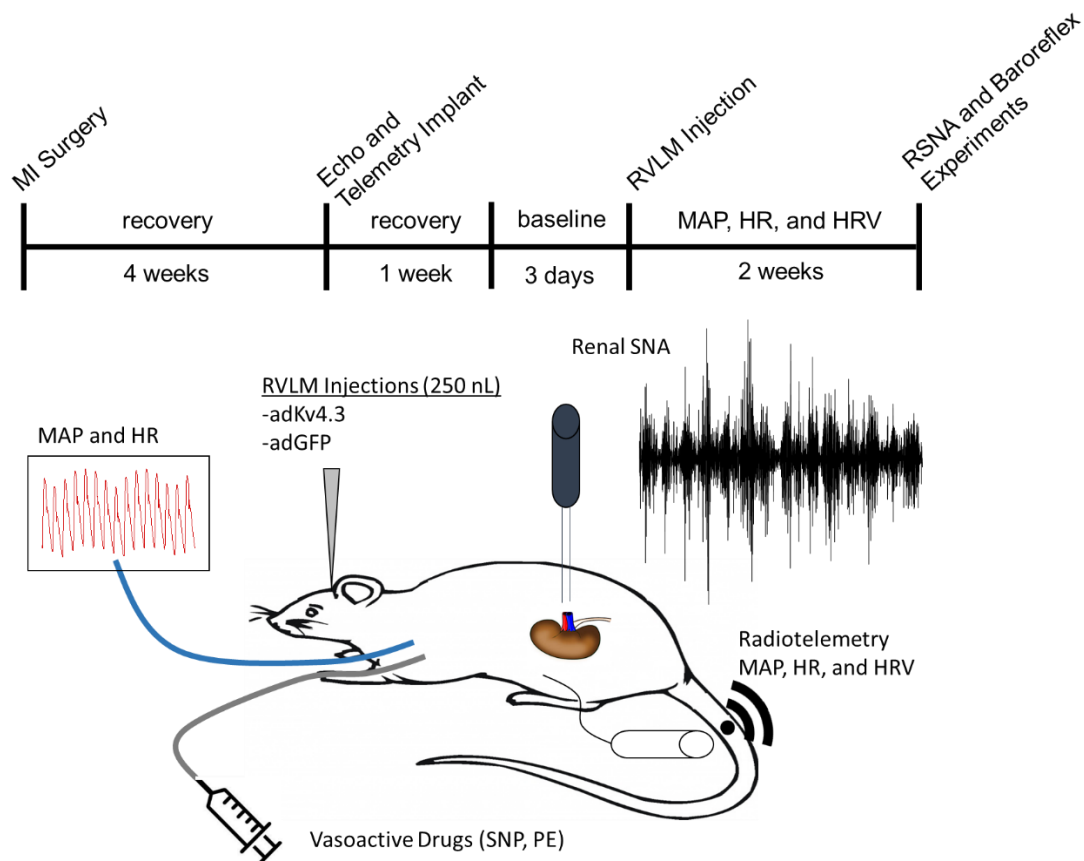


Figure 4 – Experimental schematic of timeline for adKv4.3 overexpression.

Conscious Telemetry Recordings

Following one week recovery from telemetry implantation, freely-moving blood pressure traces were recorded between the hours of 11 am to 3 pm using AD Instruments LabChart (v. 7) software with a sampling rate of 1 kHz (Bhatia *et al.*, 2010). Quiet periods of 1.5 hr duration without excessive movement artifacts were extracted from the total recordings and used for analysis. Mean arterial pressure (MAP) and heart rate (HR) were extracted from the telemetry pulse wave. Heart rate variability (HRV) measurements were analyzed by the HRV plugin in LabChart extracted from the pulse wave after passing through a 45 Hz low-pass filter. Normal to normal intervals were triggered by the maximal derivative of the pulse wave as this best correlates the pulse wave variability to HRV analysis (Pellegrino *et al.*, 2014). Standard deviation of normal to normal (SDNN), root mean squared of the successive differences (RMSSD), normalized low frequency (LF) (0.07 – 0.6 Hz), normalized high frequency (HF) (0.6-3.0 Hz), and the LF/HF ratio were calculated using LabChart software.

Bilateral RVLM Injections of Adenoviral Particles

Following baseline hemodynamic measurements, rats were placed into a stereotaxic apparatus and the dorsal surface of the skull was exposed. Bregma and Lambda were identified and the skull was positioned so that it was in the same horizontal plane. Small holes were formed through the skull using an 18 gauge needle bilaterally at 3.0 mm posterior to lambda and 2.3 mm lateral to the midline. The tip of a 500 nL Hamilton syringe was inserted 10.0 mm below the surface of the skull. 250 nL/side of adenovirus 5 containing Kv4.3 driven by a synapsin-1 promoter (adKv4.3) of 4×10^{10} pfu/ml or eGFP driven by a synapsin-1 promoter (adGFP) of 3×10^{10} pfu/ml was injected over the course of 5 min per side after which the syringe was withdrawn. The skin was sutured and the animal was recovered. Both viral constructs were made by the University of Iowa Gene Transfer Vector Core.

Acute Experimental Set-up and RSNA Recording

For the acute, terminal experiments, rats were anesthetized with urethane (800 mg/kg ip) and α -chloralose (40 mg/kg ip). The trachea was cannulated, and the rat was paralyzed with pancuronium bromide (1 mg/kg iv, 0.1 mg/kg thereafter as needed) and ventilated artificially with room air supplemented with 100% oxygen. A Millar catheter (SPR 524; size, 3.5-Fr; Millar Instruments, Houston, TX) was advanced through the right carotid artery into the LV to determine LV end-diastolic pressure (LVEDP). The transducer was then pulled back into the aorta and left in place to record arterial pressure. HR was derived from the arterial pressure pulse with a PowerLab model 16S (ADInstruments, Colorado Springs, CO) using LabChart software. The right jugular vein was cannulated for intravenous injections. Supplemental doses of α -chloralose (20 mg/kg, iv) were administered to maintain an appropriate level of anesthesia. Body temperature was maintained at $\sim 37^{\circ}\text{C}$ with an animal temperature controller (ATC1000; World Precision Instruments).

Renal sympathetic nerve activity (RSNA) was recorded as previously described (Wang *et al.*, 2014). Generally, the left kidney, renal artery, and nerves were exposed through a left retroperitoneal flank incision. Sympathetic nerves running on or beside the renal artery were identified. The renal nerve was cut distally to avoid recording afferent activity. The renal sympathetic nerves were placed on a pair of platinum-iridium recording electrodes and then were covered with a fast-setting silicone (Kwik-Sil; World Precision Instruments). Nerve activity was amplified ($\times 10000$) and filtered (bandwidth: 100 to 3000 Hz) using a Grass P55C preamplifier. The nerve signal was monitored on an oscilloscope (model 121 N; Tektronix, Beaverton, OR). The signal from the oscilloscope was displayed on a computer where it was rectified, integrated, sampled (1 kHz), and converted to a digital signal by the PowerLab data acquisition system. Maximal nerve activity was observed shortly after euthanasia, and the background noise for sympathetic nerve activity was recorded 15-20 min after the rat was euthanized. Respective noise levels were subtracted from the nerve recording data before percentage changes from baseline were

calculated. Integrated RSNA was normalized as 100% baseline during the control period (Wang *et al.*, 2007, 2014). Nerve activity was normalized for each individual rat by setting the maximal activity to 100% and subtracting out the noise floor from the integrated signal. Resting/control activity was then described as a % of max as described previously (Wang *et al.*, 2010b).

Construction of Arterial Baroreflex Curves

Baroreflex curves were generated by measuring the HR and RSNA responses to decreases and increases in arterial pressure by intravenous administration of sodium nitroprusside (25 µg) followed by phenylephrine (10 µg) as previously described (Wang *et al.*, 2014). The RSNA response was normalized as a percent of baseline. A sigmoid logistic function was fit to the data using a nonlinear regression program (SigmaPlot version 8.0). Four parameters were derived from the following equation: %RSNA or HR = $A / (1 + \exp[B(\text{MAP} - C)]) + D$, where A is the RSNA or HR range, B is the slope coefficient, C is the pressure at the midpoint of the range (BP50), and D is minimum RSNA or HR. The peak slope [or maximum gain (Gainmax)] was determined by taking the first derivative of the baroreflex curve described by the equation (Kent *et al.*, 1972).

Western Blotting and Immunofluorescence

Brains were rapidly dissected from animals following euthanasia, quickly frozen on dry ice, and stored in -80 °C. Brains were sectioned by cryostat and RVLM containing punches were taken bilaterally at coordinates 2.5-3.0 rostral to the area postrema, 1.8-2.0 lateral to the midline, and 3.0-3.4 dorsal to the ventral surface of the brainstem according to the Palkovits technique (Palkovits M, 1983) as described previously (Haack *et al.*, 2012). Punches were homogenized by sonication in RIPA buffer supplemented with protease inhibitor cocktail (P8340, Sigma-Aldrich), centrifuged at 250,000 rpm for 30 min, and supernatants collected. Total protein was estimated by a Pierce BCA protein assay kit (Rockford, IL). A total of 25 µg (approximately 25 µl) of protein was boiled for 5 min in an equal volume of 4% SDS sample buffer and was loaded into a 10% SDS-PAGE gel, and ran at 100 V for approximately 1 h on a Bio-Rad mini-gel electrophoresis apparatus

(Hercules, CA). The protein was then transferred to a nitrocellulose membrane (Li-Cor, Lincoln, NE) at 50 V for 90 min. Membranes were then blocked in Li-Cor blocking solution (Lincoln, NE) for 1 h. Membranes were incubated overnight at 4 °C in PBS with primary antibodies to Kv4.3 (1:2000; ab123347) (AbCam, Cambridge, MA) and alpha-tubulin (1:5000; sc-10D8) (SantaCruz Biotechnologies, CA), and incubated with Li-Cor secondary infrared-labeled antibodies (IRDye 680LT 926-68022 at 1:10000 and IRDye 800CW 926-32214 at 1:5000) for 1 h at room temperature in PBS with 1% SDS. Bands were visualized using a Li-Cor Odyssey system and analyzed using Li-Cor Image Studio software.

In a subset of animals from both adGFP and adKv4.3 groups, rats were fixed by transcardial perfusion of ice-cold PBS followed by ice-cold 4% paraformaldehyde (PFA). Brains were post-fixed in 4% PFA for 48 h and dehydrated in 30% sucrose. Coronal sections were made through the RVLM by cryostat and mounted on slides. Sections were incubated with primary antibody to Kv4.3 (1:200) overnight, washed, and incubated with secondary antibody (1:200) (AlexaFluor 568; A11036) for 2 h before coverslips were mounted with FluoroMount mounting solution, and slices were visualized under a florescent microscope.

Statistics

All parameters were analyzed via a one-way ANOVA followed by a Tukey's post-hoc test. A $P < 0.05$ was considered statistically significant. Statistical analysis was done using SigmaPlot 11.0 (Systat Software) or SPSS (IBM).

RESULTS

Model of CHF

In the current study, rats were grouped into post-MI or sham by means of echocardiographic measurements, and hemodynamic parameters characteristic of post-MI were evaluated at the time of the acute, terminal experiments followed by confirmation of the presence of an infarcted heart. These parameters are contained in Table 1. Although all parameters associated with CHF (cardiac hypertrophy, wet lung weight, LVEDP) were elevated in the post-MI vs Sham group, many of these parameters did not reach statistical significance nor did they reach levels characteristic of our previous studies involving infarcted CHF rats. As we therefore cannot classify the post-MI rats as CHF, we refer to the grouping as post-MI based upon echocardiographic parameters and the presence of infarct.

Table 1 – Hemodynamic, echocardiographic, and weight parameters

	post-MI + adGFP	post-MI + adKv4.3	Sham + adGFP	Sham + adKv4.3
n	5	6	4	4
Body weight (g)	389 ± 24.5	420 ± 19.4	405 ± 24.9	400 ± 9.4
Heart weight (g)	1.54 ± 0.11	1.63 ± 0.12	1.27 ± 0.06	1.36 ± 0.05
H/BW (g/kg)	4.10 ± 0.52	3.86 ± 0.16	3.17 ± 0.20	3.39 ± 0.10
H/TL (g/cm)	0.31 ± 0.03	0.28 ± 0.02	0.29 ± 0.01	0.23 ± 0.01
WL (g)	2.42 ± 0.31	2.07 ± 0.20	1.76 ± 0.09	1.81 ± 0.11
EF (%)	40 ± 7.2*	37 ± 4.2*	69 ± 8.2	64 ± 7.3
LVEDP (mmHg)	7.04 ± 1.88	6.38 ± 0.86	3.89 ± 0.61	3.29 ± 0.62
Max dP/dT (mmHg/s)	6411 ± 671	5967 ± 665	4810 ± 626	5068 ± 561
Min dP/dT (mmHg/s)	-5832 ± 948	-4813 ± 326	-5013 ± 555	-4936 ± 978
Tau (ms)	15.6 ± 1.4	21.8 ± 1.6	17.9 ± 2.1	17.8 ± 2.8
Contractility Index (1/s)	77.7 ± 6.3	77.7 ± 2.7	88.6 ± 8.9	93.1 ± 11.0
IRP Average dP/dT (mmHg/s)	-3130 ± 239	-2817 ± 175	-2656 ± 391	-2500 ± 453
Pressure Time Index (mmHg.s)	8.2 ± 0.5	8.6 ± 0.7	6.2 ± 0.6	5.8 ± 1.2

H/BW = heart weight/body weight; H/TL = heart weight/tibia length; WL = wet lung weight; EF = ejection fraction; LVEDP = Left ventricular end diastolic pressure; IRP = isovolumetric relaxation period; *P < 0.05 vs. Sham+GFP

Kv4.3 Levels in the RVLM of Rats Post-MI

In RVLM containing punches of post-MI animals, Kv4.3 expression appeared to be reduced compared to sham controls. Through adenoviral transfection of synapsin-driven Kv4.3, the expression levels of Kv4.3 protein was restored to sham levels. Immunofluorescence staining demonstrated expression of GFP in adGFP transfected neurons and Kv4.3 in adKv4.3 transfected neurons of the RVLM (Figure 5).

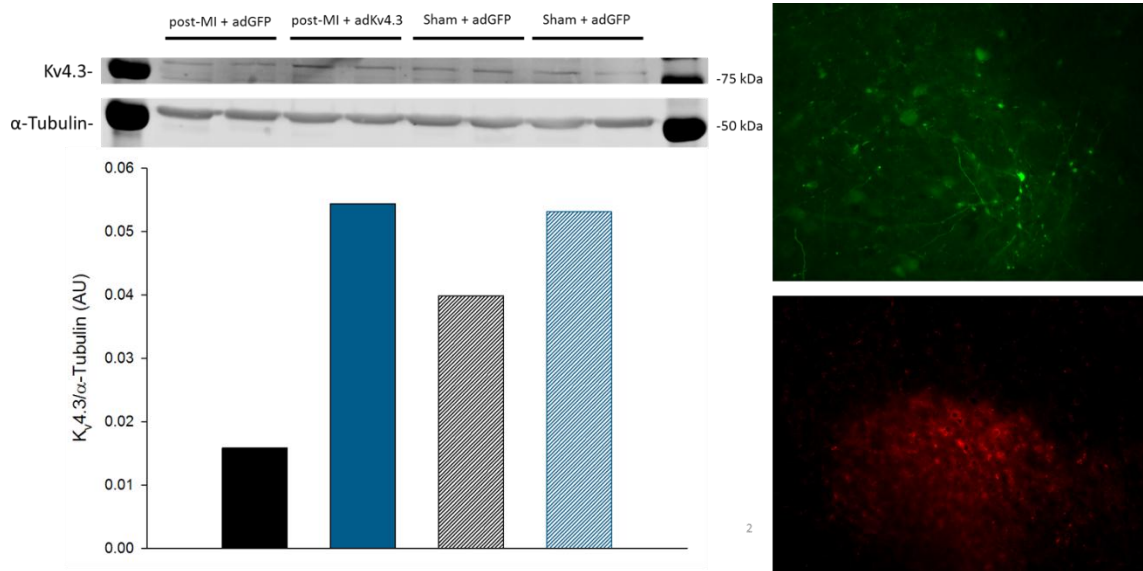


Figure 5 – Adenoviral overexpression of Kv4.3 restores Kv4.3 in RVL of rats post-MI

Representative Western blot of Kv4.3 protein expression in RVL punches and mean data quantifying expression level (n = 2/group). Representative immunofluorescence images of adGFP (top) and adKv4.3 (bottom) demonstrating neuronal transfection of target protein.

Hemodynamic Parameters of Rats Post-MI Improved by adKv4.3

Following adKv4.3, rats with post-MI exhibited lower MAP as measured by telemetry (Figure 6A). Rats post-MI displayed elevated HR as compared to sham controls (Figure 6B), and this elevation was attenuated by overexpression of Kv4.3 in the RVLM. SDNN was also improved following adKv4.3 as seen in the representative plots from one post-MI + adKv4.3 rat in Figure 7 and mean group data in Figure 8. No significant differences were observed between groups in RMSSD or LF/HF ratio (Figure 9).

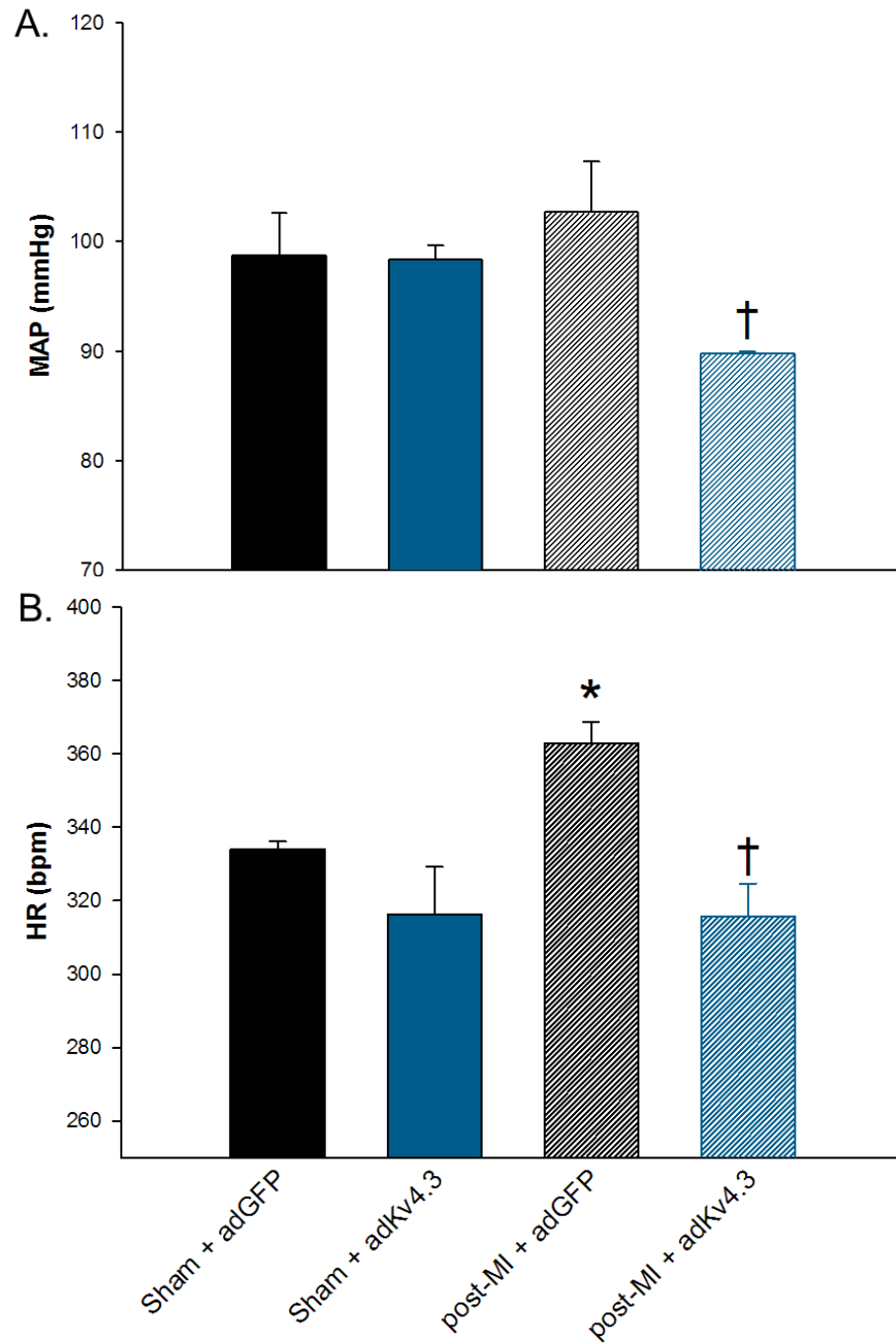


Figure 6 - adKv4.3 improves conscious hemodynamic parameters in rats post-MI

MAP and HR are reduced in CHF animals transfected with adKv4.3 as measured via telemetry. One-way ANOVA; *, $P < 0.05$ vs. Sham+adGFP; †, $P < 0.05$ vs. CHF+adGFP; n = 4-6/group.

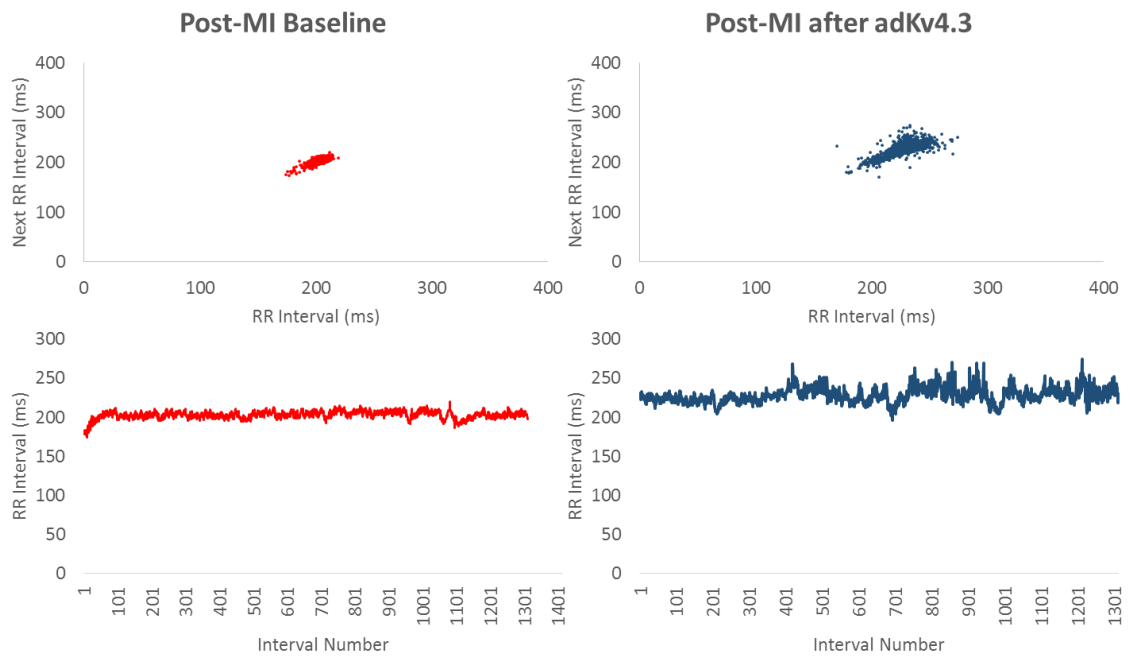


Figure 7 - Representative HRV plots from one rat before and after adKv4.3

Representative Poincaré plot (top) and tachogram (bottom) for the same rat subject before (left) and after (right) RVLM injection of adKv4.3. HRV is improved as seen by the increased distribution of RR (NN) and RR+1 (Next RR) in the Poincaré plot and increased variability demonstrated in the tachogram.

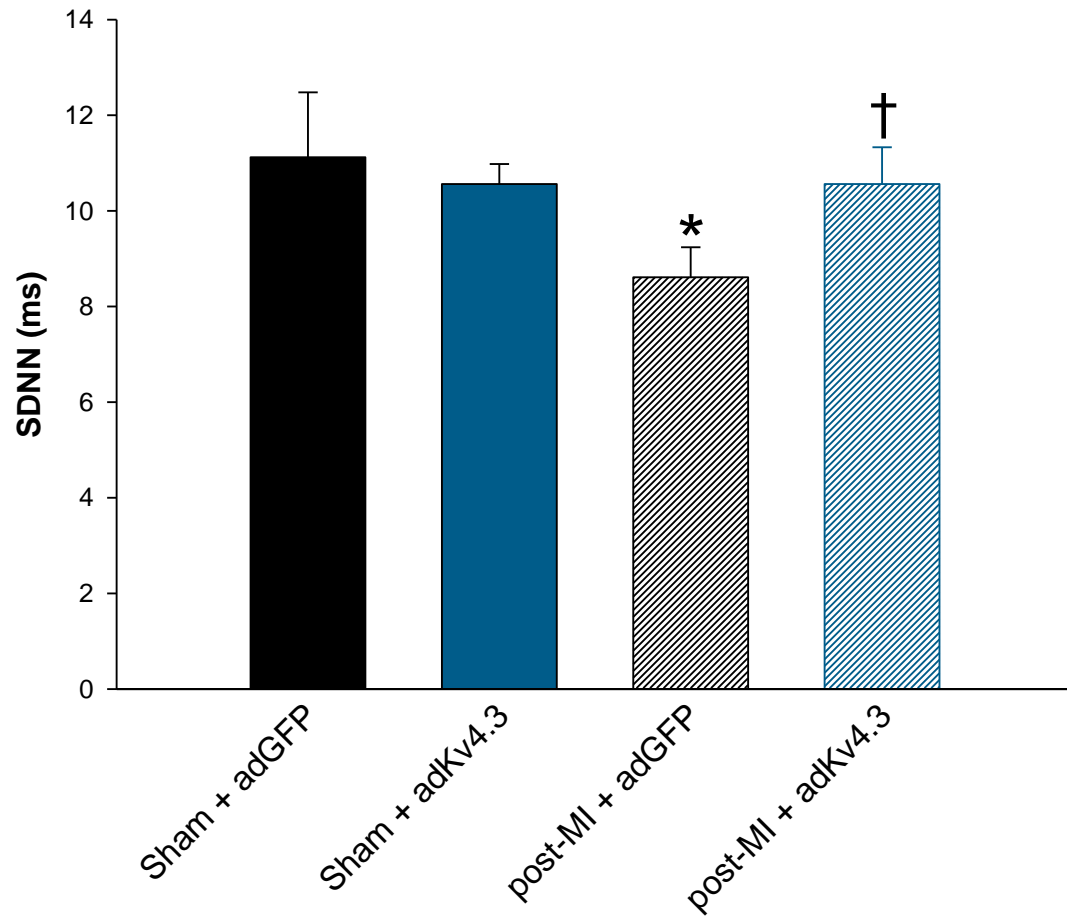


Figure 8 - Mean SDNN data from adGFP and adKv4.3 rats.

SDNN measured via telemetry in conscious rats. *, $P < 0.05$ vs. Sham+adGFP; †, $P < 0.05$ vs. CHF+adGFP; $n = 4-6$ /group.

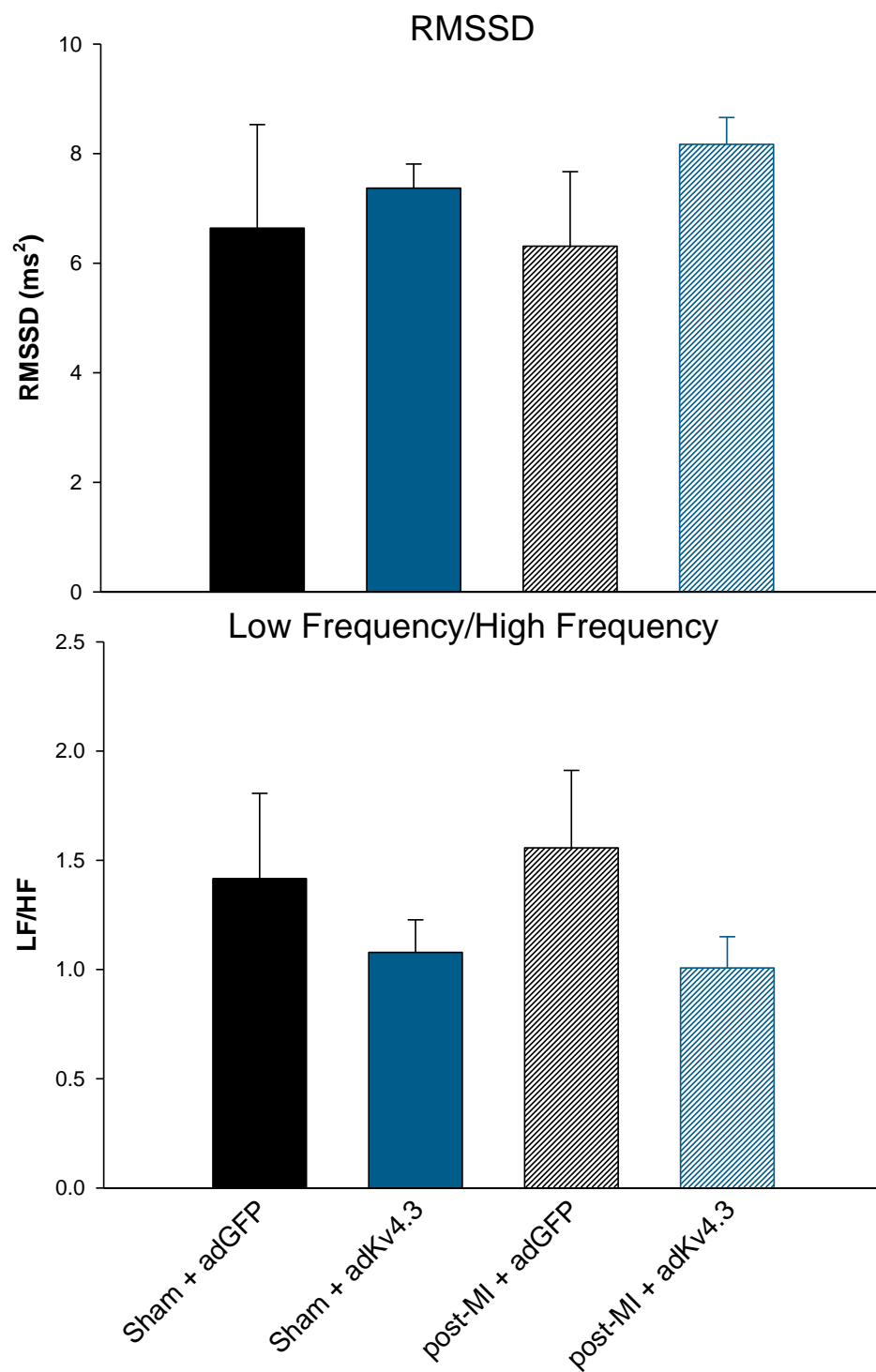


Figure 9 - RMSSD and LF/HF ratios are unchanged between groups.

RMSSD (top) and LF/HF (bottom) as recorded via telemetry in conscious rats. $n = 4-6/\text{group}$.

adKv4.3 Improves Baroreflex Parameters of Rats Post-MI

In the acute anesthetized preparation, adKv4.3 tended to increase baroreflex range and significantly increased max gain in post-MI rats injected with adKv4.3 vs. adGFP in regards to both the HR and RSNA responses to changes in MAP (Figure 10).

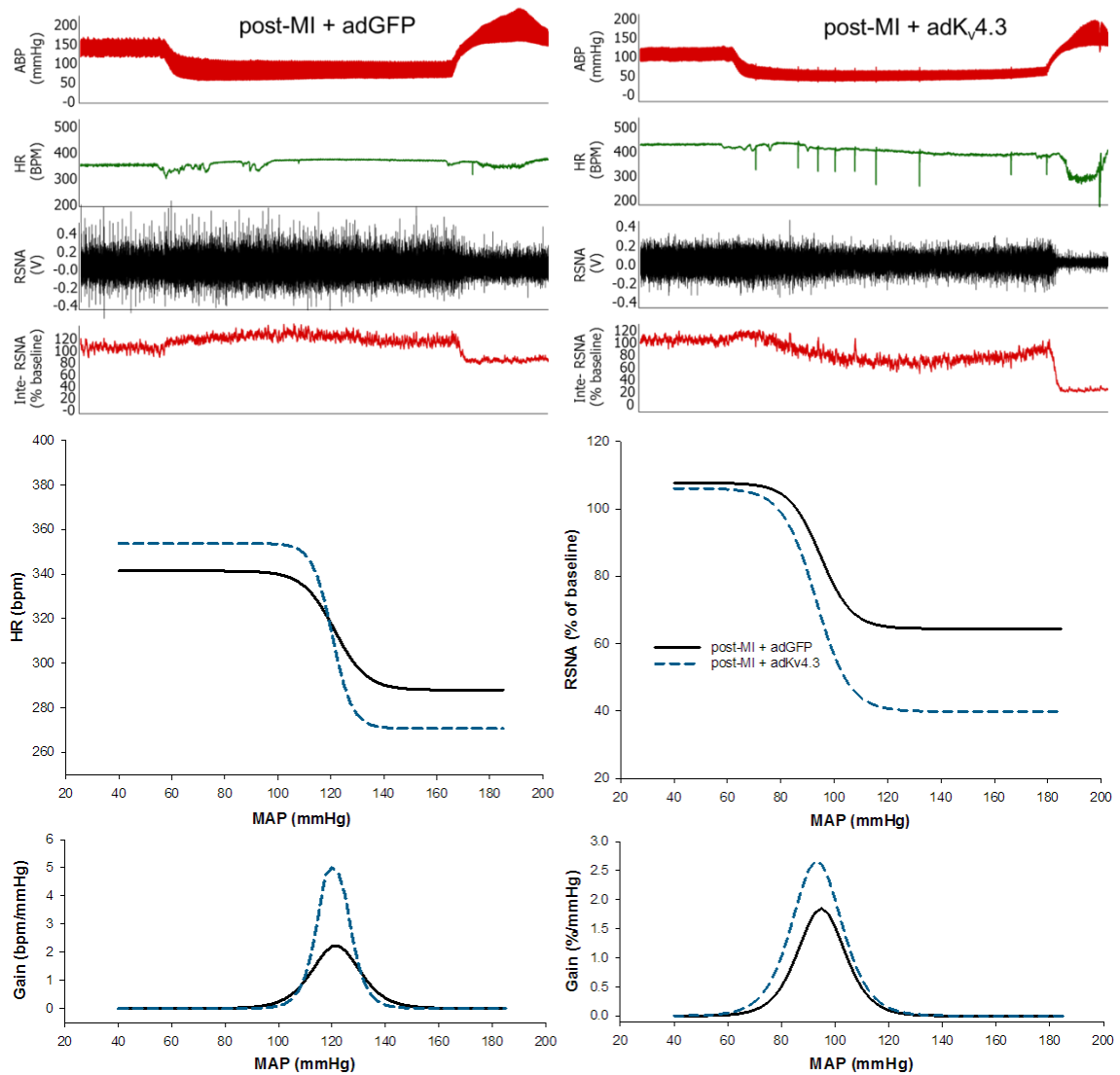


Figure 10 - Baroreflex function is improved in rats post-MI with adKv4.3

Representative tracings (top) and composite baroreflex curves (bottom) demonstrating improved HR and RSNA baroreflex responses in rats post-MI with adKv4.3 in RVLM.

adKv4.3 Attenuates the Increased RSNA Post-MI

Post-MI rats displayed an elevated RSNA expressed as a % of maximum activity relative to sham controls (Figure 12), and overexpression of Kv4.3 in the RVLM resulted in an attenuated RSNA in post-MI rats relative to adGFP controls (Figure 11 and Figure 12).

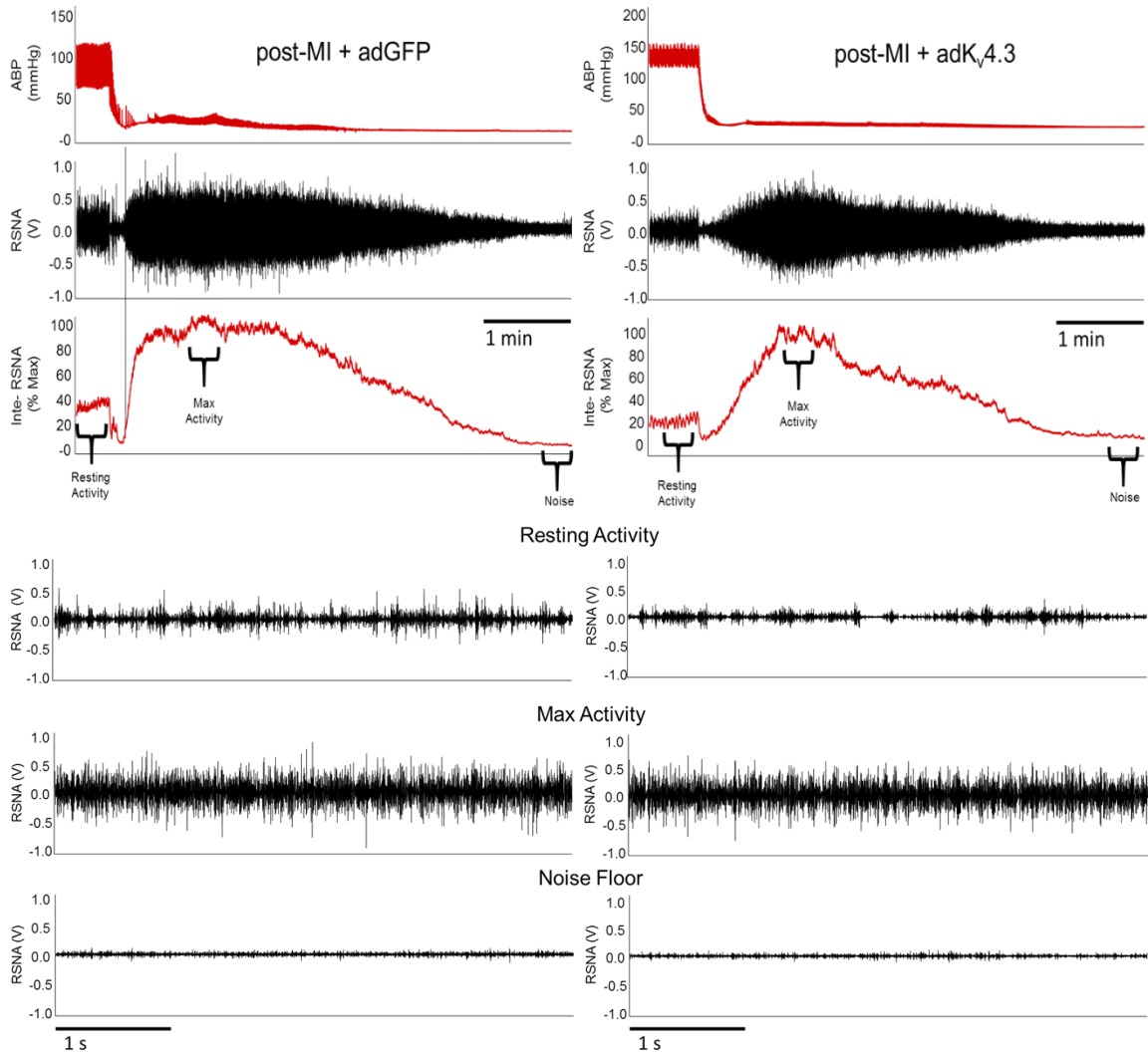


Figure 11 - Representative traces of RSNA from rats post-MI

Demonstration of calculation of baseline RSNA as expressed as a % of max activity elicited following euthanasia and subtraction of noise floor. Faster traces are provided in lower panels. RSNA from rats post-MI transfected with either adGFP (left) or adKv4.3 (right).

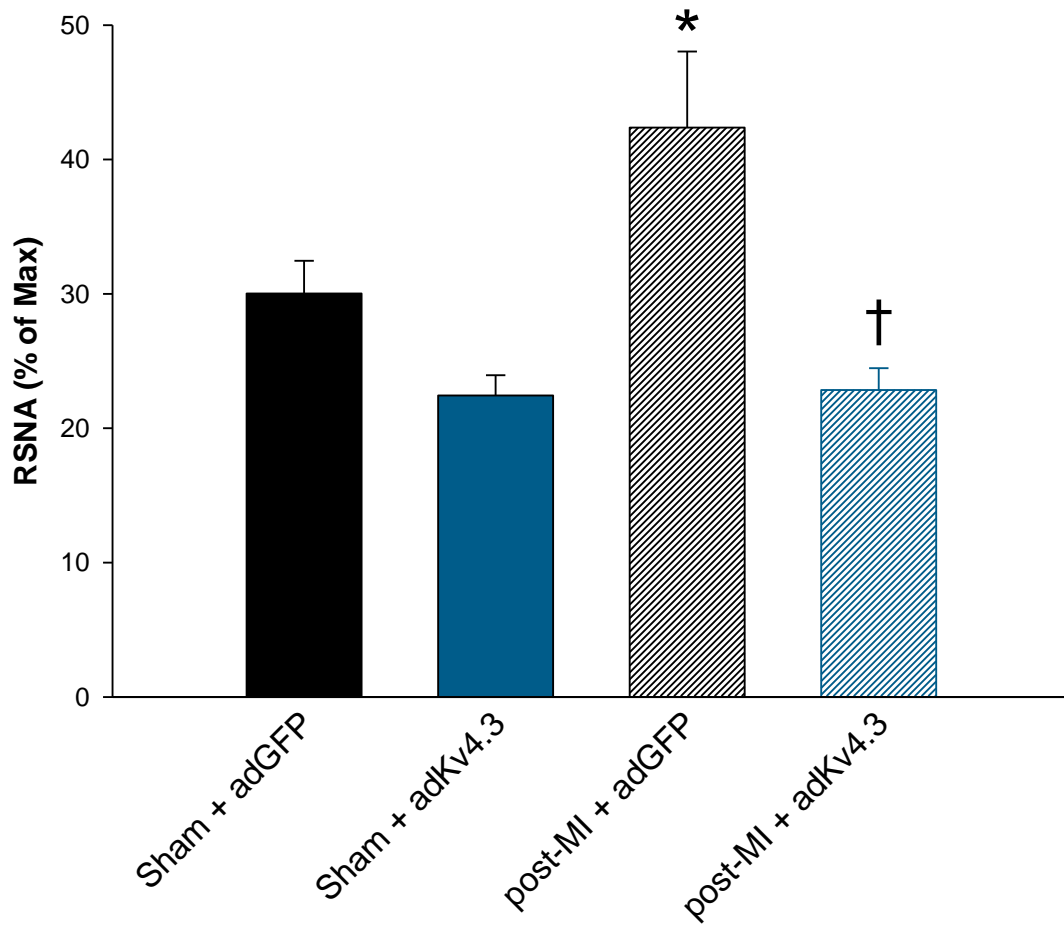


Figure 12 - Mean data of RSNA from sham and post-MI rats with adGFP or adKv4.3

One-way ANOVA; * $P < 0.05$ vs. Sham+adGFP; † $P < 0.05$ vs. CHF+adGFP; $n = 4-6$ /group.

DISCUSSION

Major Findings of Current Study

The current study provides further evidence in favor of reduced Kv4.3 expression in the RVLM of rats post-MI (Figure 5) (Gao et al., 2010) and extends those findings to demonstrate the physiological importance of these channels in reducing sympathetic tone. A decrease in the availability and activity of these channels could promote a sympatho-excitatory state as observed during post-MI, and overexpression of the channels in the RVLM attenuates this sympatho-excitation.

Conscious Parameters Following adKv4.3

The findings that overexpression of Kv4.3 reduced MAP are interesting in that MAP was not increased in post-MI rats in this current study. Furthermore, adKv4.3 did not reduce MAP in sham groups relative to adGFP. As CHF is inherently a disease characterized by a reduction in cardiac output and associated with increases in sympathetic tone, MAP may not be a relevant marker for pathological progression post-MI, particularly at the 4-6 week post-MI period evaluated in the current study. Because LVEDP also trended toward an increase, but did not reach significance, the animals studied herein may have been progressing toward congestive heart failure but were likely still able to remain compensated. Thus, MAP was maintained and unaltered in this group of animals. However, as we withdrew the excess sympathetic tone by overexpression of Kv4.3, MAP fell because of the likely reduction in vasomotor sympathetic tone.

HR was reduced following adKv4.3 (Figure 6), and along with this reduction, markers of HRV were also improved relative to post-MI + adGFP (Figure 8). In the time domain analysis of HRV, SDNN was increased following adKv4.3 in post-MI rats (Figure 8) indicating either a withdrawal of sympathetic tone or an increase in vagal tone. As RMSSD is reflective of rapid, vagal-mediated variations in R-R interval (Stein *et al.*, 1994; DeGiorgio *et al.*, 2011) and remains

unchanged across our experimental groups, we conclude that the improved HRV following adKv4.3 is due to a direct decrease in sympathetic tone and not an improvement in vagal tone.

Anesthetized Parameters Following adKv4.3

In the anesthetized preparation, observations further demonstrated the ability of adKv4.3 in the RVLM to attenuate sympathetic tone. First, through direct measurements of sympathetic tone by recording RSNA, we observed attenuated sympathetic activity following adKv4.3 in post-MI rats. This further strengthens the observations from conscious rats indicating sympathetic withdrawal following restoration of Kv4.3 expression in the RVLM.

Second, we observed a trend toward improved baroreflex function in post-MI rats treated with adKv4.3. Baroreflex sensitivity is decreased in CHF (Goldstein *et al.*, 1975; Wang *et al.*, 2004; Zucker *et al.*, 2009; Kar *et al.*, 2011) and correlates with increased rates of mortality (Schwartz *et al.*, 1988; La Rovere *et al.*, 1998). The progression of baroreflex desensitization is complex and consists of both peripheral alterations to baroreceptor afferent input and central neuronal network dysregulation (Gnecchi Ruscone *et al.*, 1987; Gao *et al.*, 2005a; Wang *et al.*, 2008). Many of the central mechanisms for baroreceptor desensitization remain unknown although evidence indicates a role for the renin-angiotensin system in mediating this dysfunction through increases in sympathetic outflow (Gao *et al.*, 2005a; Wang *et al.*, 2008; Zucker *et al.*, 2009). As the RVLM is one of the final presympathetic integration centers of the brainstem and directly projects to the outflow tract of the spinal cord, elevated RVLM neuronal tone will suppress baroreflex function independent of input from higher order baroreflex centers such as the NTS. Decreasing the neuronal activity of the RVLM by restoring levels of Kv4.3 can improve the baroreflex by directly reducing sympathetic outflow.

Limitations and Perspectives of Current Study

The major limitation of the current study is the use of moderately infarcted, less severe CHF rats. This major limitation impacts our ability to make any strong conclusions regarding the

expression levels of Kv4.3 and the sympatho-excitatory effects post-MI and adenoviral transfection. As Table 1 shows, the rats used in the current study, although possessing a significantly reduced EF, do not have significantly elevated heart mass, lung edema, or LVEDP. Failing to have significant differences between groups outside of echocardiographic parameters may severely underestimate the pathophysiological mechanisms at play in these groups of experiments. Nonetheless, these moderate CHF rats appear to have reduced Kv4.3 expression levels in RVLM and display elevated RSNA which are both improved by adKv4.3. Complication may arise from these moderately infarcted rats as we are likely to be underestimating the effect of adKv4.3. Future work in confirmed instances of CHF or following central Ang II manipulation will be invaluable to further elucidate the contribution of decreased Kv4.3 expression in the RVLM to increased sympathetic tone.

Although interesting for understanding the basic mechanisms of the development of sympatho-excitation during CHF, adenoviral transfection may not be a viable therapeutic approach for treatment of patients with CHF or associated dysautonomia. The current study lends further credence to the observation of the importance in Kv4.3 channels in the RVLM in suppressing sympathetic tone and provides rationale for exploration of treatment options aimed at maintaining or restoring levels of voltage-gated K^+ channels in areas such as the RVLM. Further work is needed to investigate the molecular mechanisms at play in initiating the reduced levels of Kv4.3, and such is presented in the subsequent chapters of this dissertation.

**CHAPTER II: BDNF CONTRIBUTES TO
ANGIOTENSIN II-MEDIATED REDUCTIONS IN
PEAK VOLTAGE-GATED K⁺ CURRENTS IN
CULTURED CATH.A CELLS***

*The material presented in this chapter was previously published: Becker BK, Wang H, Tian C, Zucker IH. BDNF contributes to angiotensin II-mediated reductions in peak voltage-gated K⁺ current in cultured CATH.a cells. *Physiol. Rep.* 3: 1–8, 2015.

INTRODUCTION

As discussed earlier in this dissertation, increased circulating levels of angiotensin II (Ang II) during the progression of CHF have been shown to contribute to sympatho-excitation (Guyenet, 2006; Zucker *et al.*, 2009). Elevated circulating Ang II may activate brainstem neurons in pre-sympathetic control areas, such as the RVLM, by initiating disruption of the blood brain barrier (Biancardi *et al.*, 2013) or stimulating circumventricular neurons such as in the SFO (Zimmerman, 2002; Zimmerman *et al.*, 2004). Furthermore, increased activity of a local brain RAS in areas such as the RVLM may promote the development of increased sympathetic outflow. For instance, Gao *et al.* (2008) have shown an increase in AT1R expression in the RVLM of animals with experimental CHF. Therefore, therapies that interrupt sympathetic nervous system activity or inhibit Ang II signaling have been widely utilized to slow the development of CHF. However, it is not completely clear how Ang II increases neuronal activity.

One way in which Ang II may increase sympathetic outflow is by increasing the sensitivity and excitability of pre-sympathetic neurons through suppression of voltage-gated K⁺ channels that conduct the voltage-sensitive, rapidly inactivating current, I_A. Acutely, Ang II inhibits I_A by increasing cellular levels of superoxide anion (Yin *et al.*, 2010). As discussed more fully above, in the RVLM of experimental models of CHF, there is reduced expression of the channel Kv4.3, that has been demonstrated in the RVLM of experimental models of CHF (Gao *et al.*, 2010). This protein contributes to the generation of I_A (Sonner & Stern, 2007; Carrasquillo *et al.*, 2012) and work in the preceding chapter indicates that restoring levels of Kv4.3 in the RVLM mitigate the increased sympatho-excitation during CHF.

How Ang II elicits long-term reductions in Kv channel expression and I_A amplitude is not well understood, and whether other factors are involved has been incompletely investigated. In this regard, BDNF signaling has been shown to modulate I_A in a manner similar to that of Ang II (Youssoufian & Walmsley, 2007; Cao *et al.*, 2010), and BDNF-induced increases in neuronal

excitability have been extensively investigated (Huang & Reichardt, 2003; Minichiello, 2009). Furthermore, Ang II has been demonstrated to increase the expression of BDNF in neurons and other tissues (Szekeres *et al.*, 2010; Chan *et al.*, 2010). To our knowledge, no studies have investigated the interaction of Ang II and BDNF in modulating I_A and neuronal excitability. Therefore, **we hypothesized that the Ang II-mediated reduction in voltage-gated K^+ currents is due, in part, to BDNF signaling.** To test this hypothesis, we measured I_A in CATH.a cells treated with Ang II or BDNF. We also investigated the contribution of Ang II and BDNF on the p38 MAPK axis, which is an important component of both Ang II and BDNF signaling (Katoh-Semba *et al.*, 2009; Xiao *et al.*, 2013).

METHODS

Chemicals

Ang II, losartan, and SB-203580 (a MAPK inhibitor) were purchased from Sigma-Aldrich (St. Louis, MO). Human recombinant BDNF, rabbit polyclonal antibody for BDNF (H-117), and mouse monoclonal alpha-tubulin antibody (10D8) were purchased from Santa Cruz Biotechnology Inc. (Santa Cruz, CA). All chemicals and compounds for electrophysiological solutions were purchased from Sigma-Aldrich unless otherwise stated.

Cell Culture

CATH.a cells were purchased from American Type Culture Collection (Manassas, VA), grown in RPMI 1640 medium supplemented with 8% horse serum, 4% fetal bovine serum, and 1% penicillin/streptomycin obtained from Gibco (Life Technologies, Grand Island, NY), and maintained in a humidified incubator at 37 °C with 5% CO₂. Cells were differentiated by incubating them in serum-free RPMI medium for 48-72 h as has been described previously (Qi *et al.*, 1997; Mitra *et al.*, 2010). Differentiated CATH.a cells were then treated with the designated agent dissolved in PBS and incubated in serum-free medium for the specified time period after which they were collected for Western blot analysis or electrophysiology. CATH.a cells are a central nervous system catecholaminergic cell line derived from a tumor in the locus coeruleus of a transgenic SV40 T antigen mouse (Suri *et al.*, 1993; Qi *et al.*, 1997). The line expresses many ion channels similarly to neurons, synaptophysin, tyrosine hydroxylase/norepinephrine, and components of the RAS (Yin *et al.*, 2010; Mitra *et al.*, 2010; Yang *et al.*, 2011; Xiao *et al.*, 2013) making them a suitable model for the study of ion channel dysfunction following Ang II treatment.

Electrophysiology

Electrophysiological recordings were conducted similar to those previously reported from our laboratory and others (Gao *et al.*, 2010; Yin *et al.*, 2010). In brief, medium from the polystyrene

dish with differentiated CATH.a cells was aspirated, the cells were washed with PBS, and extracellular electrophysiology solution was added to the dish. The extracellular solution contained (in mM): 140 NaCl, 5.4 KCl, 0.5 MgCl₂, 5.5 HEPES, 11 glucose, and 10 sucrose. It was buffered to pH of 7.4 with NaOH and 0.5 μM tetrodotoxin was added in order to block TTX-sensitive, voltage-gated Na⁺ channels. Patch pipettes were pulled using a P-97 Flaming/Brown micropipette puller (Sutter Instruments, Novato, CA), fire polished to a final resistance of 2-4 MΩ, and filled with solution containing (in mM): 105 potassium-aspartate, 20 KCl, 10 EGTA, 5 Mg-ATP, 10 HEPES, and 25 glucose, adjusted to pH 7.2 with KOH. K⁺ currents were recorded by an Axopatch 200B amplifier and digitized using a Digidata 1440A interface (Molecular Devices, Sunnydale, CA). Data collection and analysis were done using pCLAMP 10 software (Molecular Devices). Whole-cell membrane capacitance was determined by canceling the capacitive current evoked by a 10-mV voltage step. Currents were not leak subtracted, and signals were filtered at 5 kHz and sampled at 10 kHz. Cells were held at -60 mV or -80 mV and 400-ms duration voltage steps were applied in 10-mV increments to +80 or +110 mV.

Peak current amplitude (pA) representing I_A, time to peak current (ms), time of activation (τ_{act}; ms) or decay (τ_{decay}; ms), and the maximum slope during activation or decay were measured at each voltage-step after the total trace had been normalized by the whole-cell membrane capacitance using analysis functions in pCLAMP software.

Western Blotting

After treatment, CATH.a cells were scraped from polystyrene culture dishes and immediately placed in ice-cold RIPA buffer supplemented with protease inhibitor cocktail (P8340, Sigma-Aldrich) and phosphatase inhibitor cocktail (P5726, Sigma-Aldrich). Cells were homogenized by sonication and total protein concentration was estimated by a Pierce BCA protein assay kit (Rockford, IL). A total of 20 μg (approximately 20 μl) of protein was boiled for 5 min in an equal volume of 4% SDS sample buffer and was loaded into a 7.5 or 12% SDS-PAGE gel, and

ran at 100 V for approximately 1 h on a Bio-Rad mini-gel electrophoresis apparatus (Hercules, CA). The protein was then transferred to a nitrocellulose membrane (Li-Cor, Lincoln, NE) at 50 V for 90 min. Membranes were then blocked in a 1:1 solution of Li-Cor blocking solution (Lincoln, NE) and PBS for 1 h. Membranes were then incubated overnight at 4 °C in PBS with primary antibodies to BDNF (1:2000) and alpha-tubulin (1:5000), and incubated with Li-Cor secondary infrared-labeled antibodies (IRDye 680LT 926-68022 at 1:10000 and IRDye 800CW 926-32214 at 1:5000) for 1 h at room temperature in PBS with 1% SDS. Bands were visualized using a Li-Cor Odyssey system and analyzed using Li-Cor Odyssey software.

Statistics

All data are expressed as mean \pm SEM. One-way analysis of variance was used to compare group differences between Western blot data with Tukey's post-hoc analysis. A repeated measures one-way analysis of variance was used to determine treatment interactions in electrophysiological I-V measurements. SigmaPlot 11.0 (Systat Software Inc., San Jose, CA) and SPSS (IBM, Armonk, NY) were used to complete statistical analysis. A *p* value of $< .05$ was used to determine statistical significance.

RESULTS

Ang II Increases BDNF Expression

Following treatment of CATH.a cells with 100 nM Ang II for 2 or 6 h, both pro-BDNF and BDNF expression increased relative to non-treated controls as measured by Western blot. We failed to observe an increase in the relative expression levels of TrkB following Ang II treatment at either 2 or 6 h (Figure 13D).

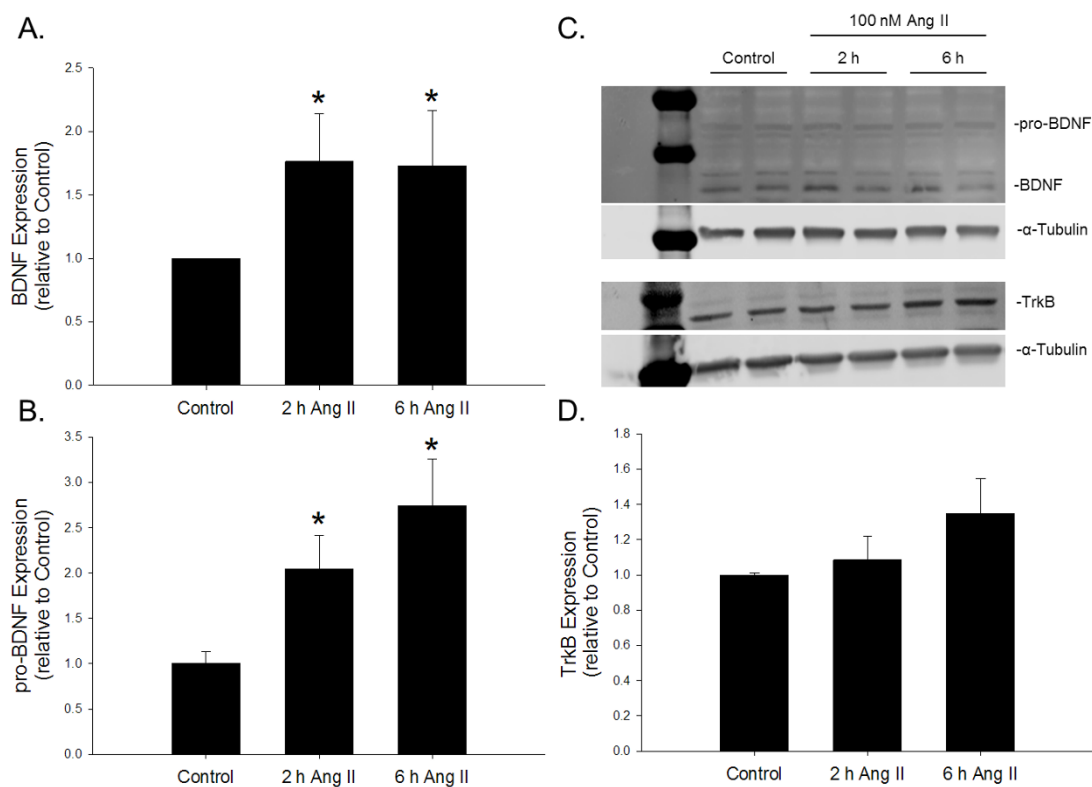


Figure 13 - Expression of BDNF, pro-BDNF, and TrkB following Ang II treatment

Representative blots (C) and relative expression levels of BDNF (A), pro-BDNF (B), and TrkB (D) following treatment of CATH.a cells with 100 nM Ang II for 2 or 6 h. *, $P < 0.05$ vs. Control treatment, $n = 5-8$ /group.

BDNF Reduces I_A

To investigate whether BDNF affects I_A in CATH.a cells, patch-clamp experiments were performed. Previous reports have demonstrated reductions in voltage-gated K^+ currents following 50 ng/ml of BDNF after 2-4 h (Cao *et al.*, 2010, 2012). Treatment of neurons with 50 ng/ml of BDNF for 2 h reduced mean I_A by 65% during a voltage-step to +70 mV (Figure 14). Because this effect was similar to the previously reported reduction of I_A due to Ang II treatment (Gao *et al.*, 2010), and because Ang II has also been shown to rapidly suppress voltage-gated K^+ current (Yin *et al.*, 2010), we explored whether an acute treatment with BDNF would produce a similar effect to that of acute application of Ang II. However, peak current was not altered after superfusion of CATH.a cells with 50 ng/ml BDNF for 10 min (Figure 15).

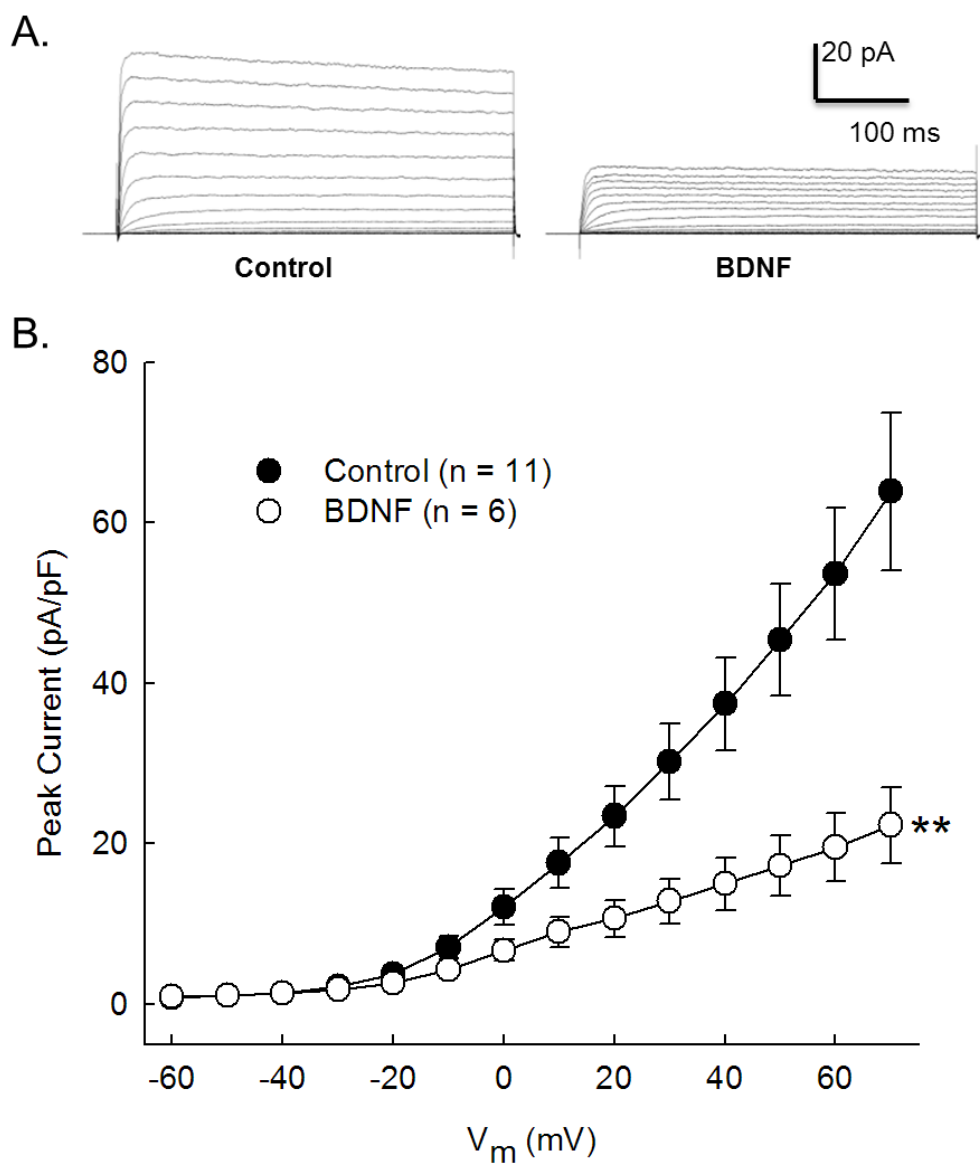


Figure 14 - BDNF decreases peak K⁺ current in CATH.a cells

Representative traces (A) and mean I-V plots of peak K⁺ current density (B) in CATH.a cells treated with 50 ng/ml BDNF for 2 h. **, P < 0.01 interaction between groups as measured by RM-ANOVA.

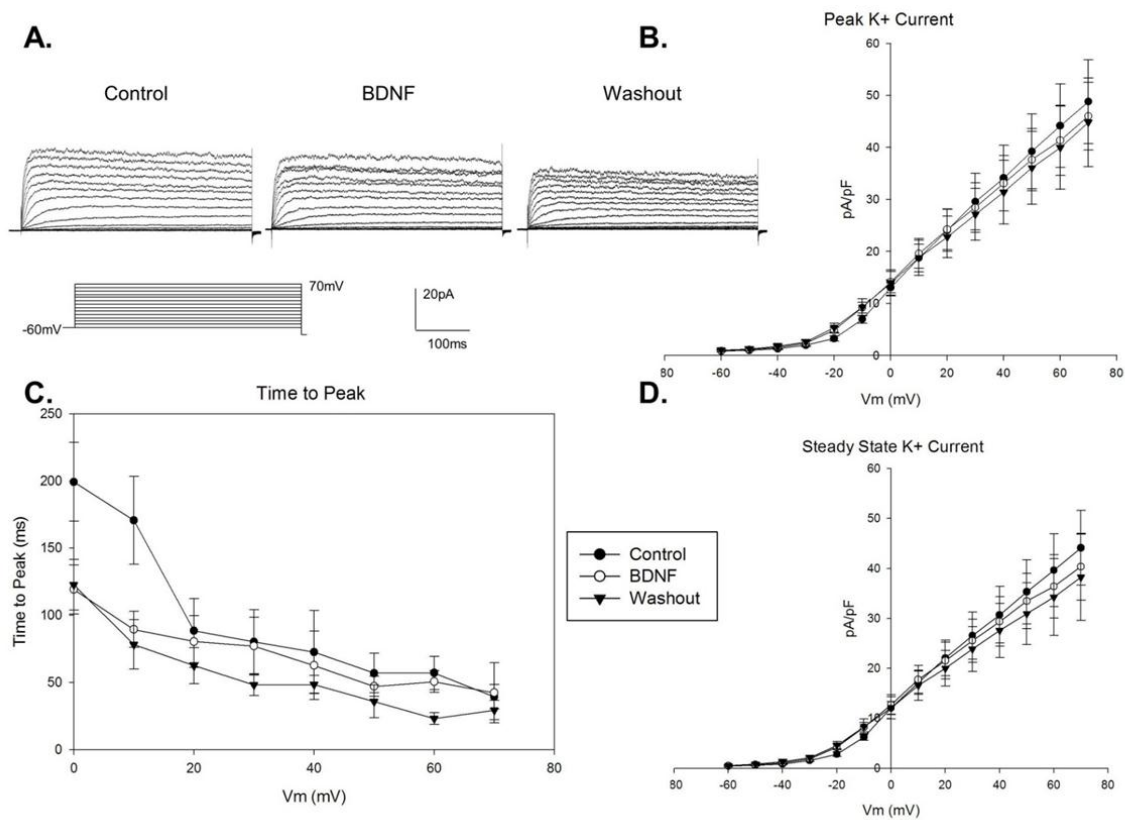


Figure 15 - Acute BDNF treatment has no effect on K⁺ currents.

Representative traces (A) and mean I-V plots of peak K⁺ current density (B) and steady-state K⁺ current density (D) in CATH.a cells following 10 minutes superfusion of 50 ng/mL BDNF and washout. Time to peak current displayed in (C). n = 6

BDNF is Involved in the Ang II-Induced Reduction of I_A

Based upon the ability of BDNF to reduce I_A , we investigated the involvement of BDNF in the Ang II-induced reduction of I_A . Inhibition of endogenous BDNF signaling by pretreatment with an anti-BDNF antibody attenuated the reduction in peak current following incubation with Ang II (Figure 16). In order to determine if anti-BDNF antibody had any independent effects on K^+ current, CATH.a cells were incubated with anti-BDNF antibody alone. Peak current was not altered by incubation of neurons with anti-BDNF antibody alone relative to control (116.0 ± 10.7 pA/pF at +80 mV voltage step., $n = 7$, $P = .74$ between groups).

Because BDNF or Ang II can independently reduce I_A , and because BDNF signaling is involved in the mediation of the Ang II-induced reduction in I_A , we investigated whether Ang II signaling is involved in the BDNF-induced suppression of I_A . Cells were pretreated with 100 nM losartan, an AT1R blocker, for 30 min prior to 50 ng/ml BDNF incubation for 2 h. I_A was not altered in losartan-treated neurons (Figure 17).

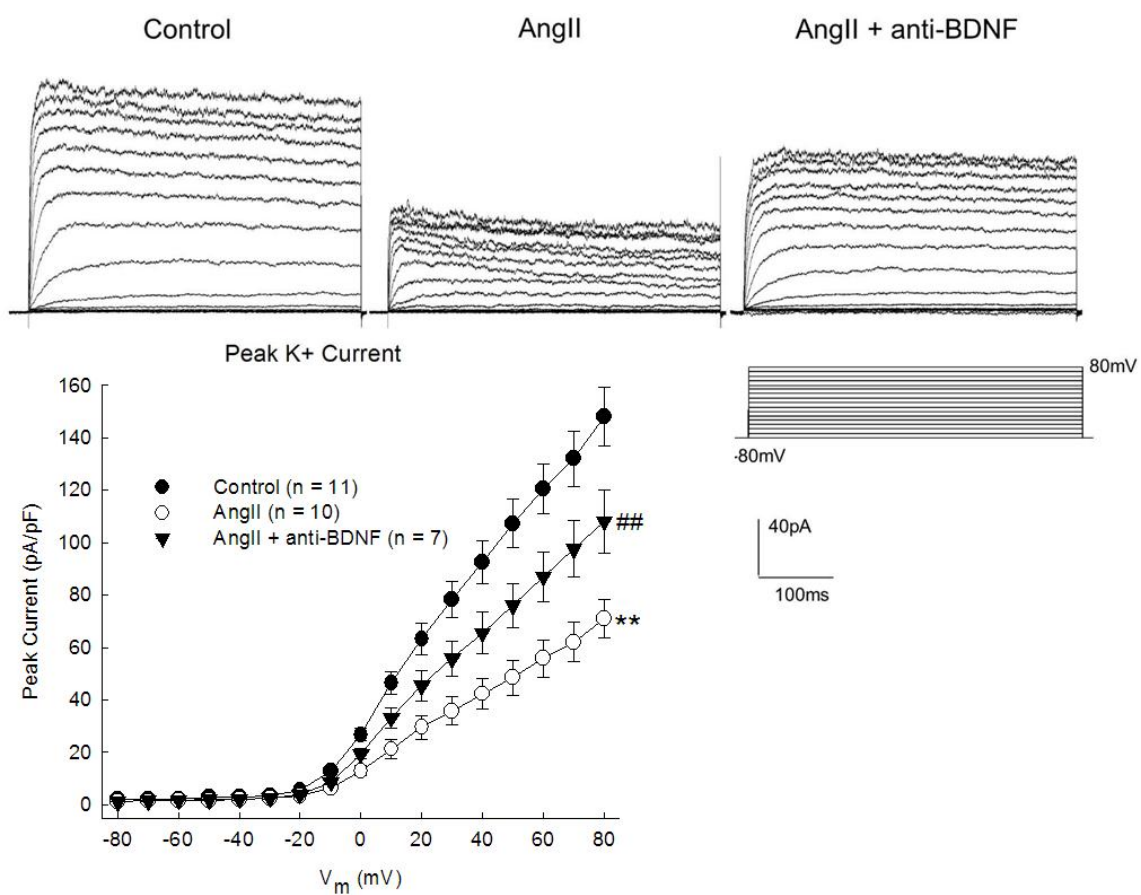


Figure 16 - Inhibiting BDNF/TrkB attenuates Ang II-mediated suppression of peak K⁺ current

Representative traces and mean I-V plots of peak K⁺ current density of CATH.a cells incubated with 100 nM Ang II for 6 h or pretreated with 50 ng/ml anti-BDNF antibody for 30 min prior to Ang II. **, P < 0.01 group interaction vs. Control and ##, P < .01 vs. Ang II group interaction as measured by RM-ANOVA.

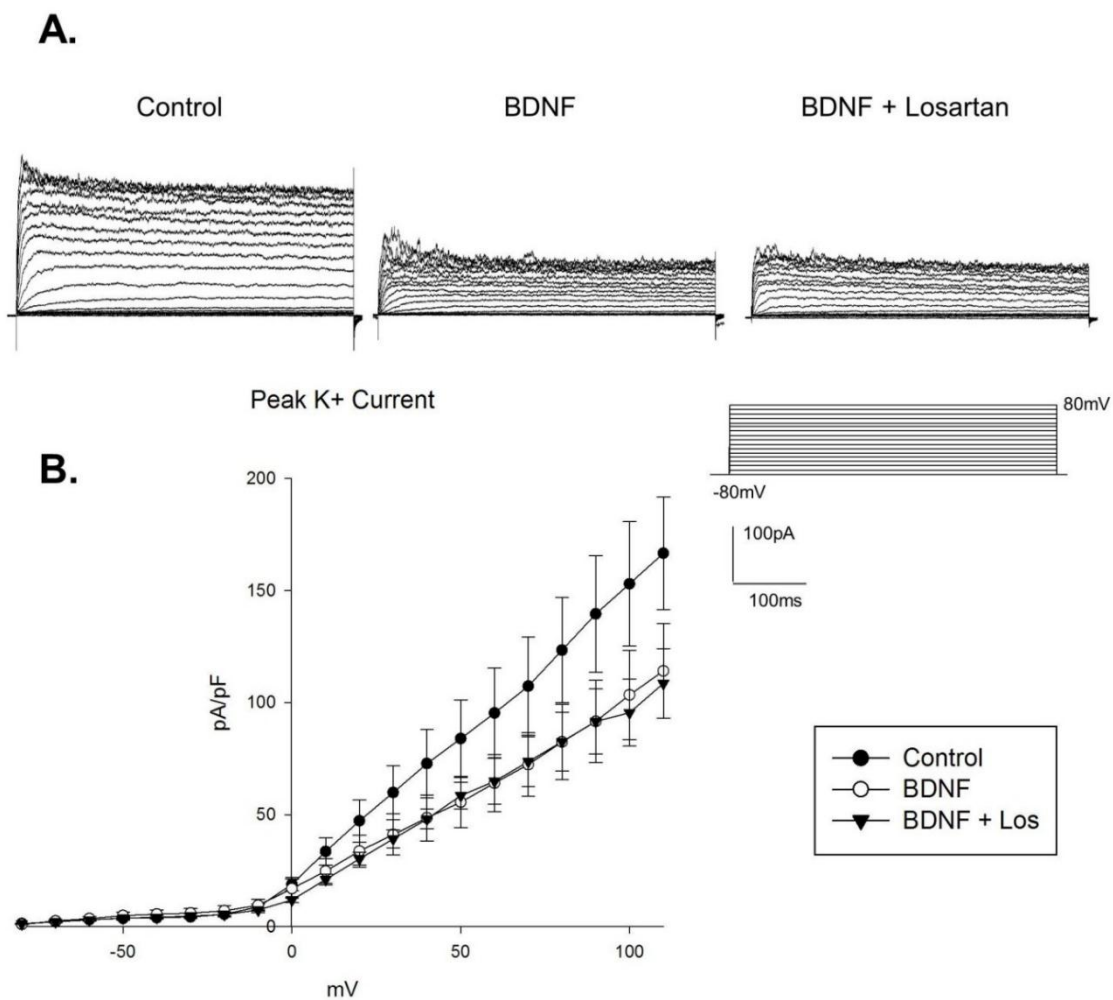


Figure 17 - AT1R is not involved in BDNF-mediated suppression of K⁺ currents.

Representative traces (A) and mean I-V plot of peak K⁺ current (B) in CATH.a cells treated with 50 ng/mL BDNF with or without pretreatment with 100 nM losartan (Los). n = 5/group

Involvement of p38 MAPK in the BDNF-Induced Reduction of I_A

Previous results have demonstrated the involvement of p38 MAPK in Ang II-mediated reductions in I_A and downregulation of Kv4.3 protein (Gao *et al.*, 2010). To determine if p38 MAPK is involved in the BDNF-induced reduction of I_A , patch-clamp experiments were performed after treating CATH.a cells for 2 h with 50 ng/ml with or without pretreatment of the p38 MAPK inhibitor SB-203580 (100 nM) for 30 min. Inhibiting p38 MAPK completely prevented the reduction in I_A following BDNF (Figure 18).

Time to peak current was measured following 50 ng/ml BDNF treatment for 2 h with or without 30-min pretreatment with 100 nM SB-203580. Time to peak current during the voltage-step to +80 mV was not changed following BDNF treatment (66.8 ± 21.9 ms, $P = 0.4$, $n = 8$) relative to control (46.9 ± 17.4 ms, $n = 8$). Likewise, time to peak current was not changed by BDNF after cells were pretreated with SB-203580 (41.4 ± 9.0 ms, $P = 0.79$, $n = 10$) relative to BDNF.

Next, to evaluate whether BDNF affects kinetic properties of I_A , various time-related parameters were calculated following incubation of CATH.a cells with 50 ng/ml BDNF for 2 h with or without 30-min pretreatment of 100nM SB-203580. BDNF treatment increased mean τ_{act} by 52 ms relative to control (Table 2). The τ_{act} was not attenuated by pretreatment with SB-203580 ($P = .97$ relative to BDNF alone). The other kinetic parameters measured (τ_{decay} , maximum rise slope, and maximum decay slope) were not affected by BDNF or SB-203580 (Table 2).

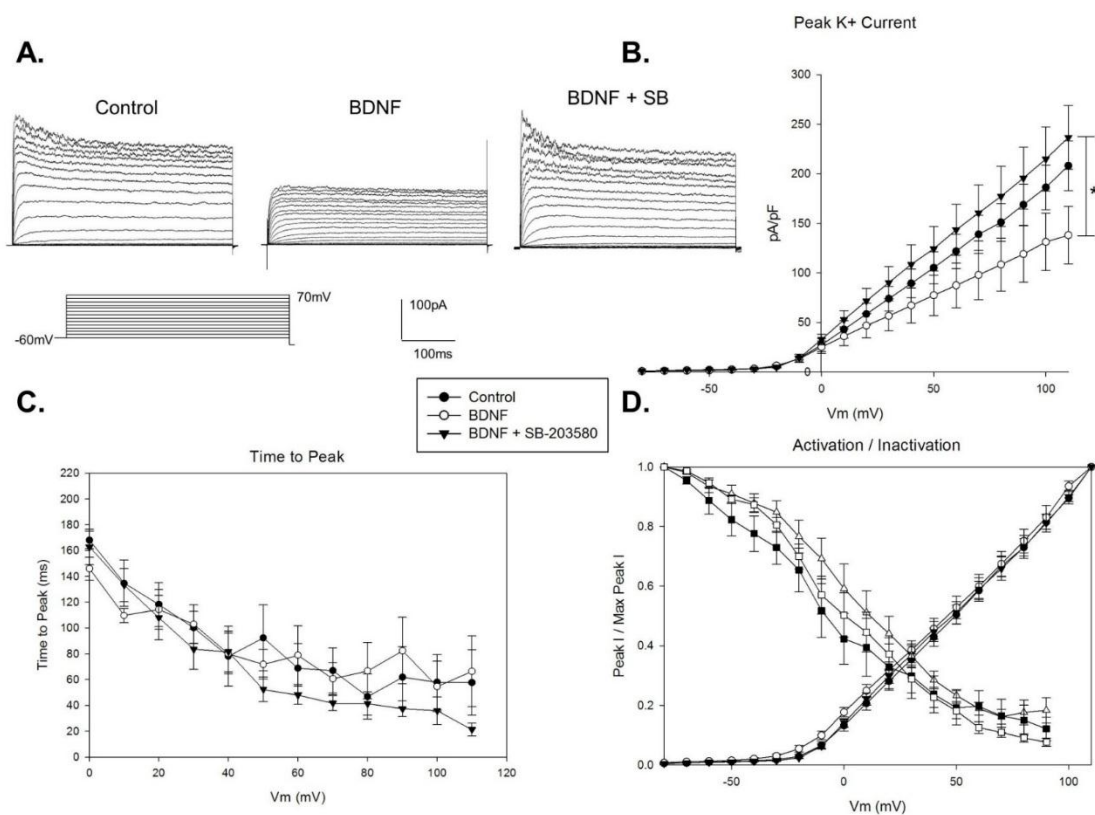


Figure 18 - p38 MAPK is involved in BDNF-mediated suppression of K⁺ currents.

Representative traces (A), mean I-V plots of peak K⁺ current density (B), time to peak current (C) and Activation/Inactivation plot (D) in CATH.a cells incubated with 50 ng/ml BDNF for 2 h or pretreated with 100 nM SB-203580 (SB) for 30 min prior to BDNF. *, $P < 0.05$ group interaction between BDNF and SB+BDNF as measured by RM-ANOVA. $n = 8-10$ /group

Table 2 - Effects of BDNF with or without p38 MAPK inhibition on kinetic parameters of I_A

Treatment	τ_{act} (ms)	<i>P</i>	τ_{decay} (ms)	<i>P</i>	Max Rise Slope (pA/ms)	<i>P</i>	Max Decay Slope (pA/ms)	<i>P</i>	<i>N</i>
Control	5.5 ± 4.2		48.5 ± 16.3		31.9 ± 7.1		-31.0 ± 6.3		8
BDNF	58.0 ± 15.3	0.00 1	17.0 ± 5.0	0.1 6	25.8 ± 3.9	0.96	-23.3 ± 3.5	0.33	8
SB + BDNF	55.3 ± 18.0	0.04	32.4 ± 9.6	0.6 5	39.6 ± 3.6	0.09	-35.6 ± 3.5	0.53	10

Note: P values are relative to Control group. τ = time of activation (act) or decay.

DISCUSSION

The major findings of this study are that BDNF reduces peak I_A and that the Ang II-induced decrease in I_A in CATH.a cells is attenuated by inhibiting the action of BDNF (Figure 16) and that p38 MAPK is involved in the signaling of BDNF-induced reductions in I_A (Figure 18). These results suggest that BDNF and p38 MAPK may be key mediators involved in the reduction of I_A due to Ang II. Previous reports have demonstrated reduction in I_A following 100 nM Ang II treatment for 6 h (Gao *et al.*, 2010), similar to our present findings (Figure 16). However, little is known about the signaling cascades involved in this Ang II-mediated change in electrophysiological phenotype. Here we demonstrate the upregulation of BDNF protein following Ang II treatment (Figure 13) and the involvement of BDNF in the Ang II-induced reduction of I_A (Figure 16).

Ang II is known to have immediate effects on K^+ currents and neuronal firing through signaling by reactive oxygen species. Specifically, Ang II elicits an increase in intracellular superoxide anion that inhibits peak and steady state K^+ currents within 10 minutes (Yin *et al.*, 2010). Our results suggest that BDNF may not be involved in acute modulation of K^+ currents, because no changes to peak K^+ current were observed following 10 min superfusion of BDNF (Figure 15). Thus, Ang II may have multiple modes of modulating K^+ currents: acutely, by generation of reactive oxygen species; and long-term, through BDNF signaling. Furthermore, these results suggest that the reduction of I_A following treatment with Ang II or BDNF for several hours is likely due to a decrease in the expression of channels responsible for I_A such as Kv4.2 or Kv4.3 and not due to direct inhibition of K^+ channel activity. Although BDNF increased τ_{act} , other kinetic parameters of peak K^+ current remained unchanged, indicating that the main action of BDNF on suppressing I_A are likely through reducing the total expression of Kv4.3, which correlates well with our previous results demonstrating reductions in Kv4.3 expression following Ang II treatment (Gao *et al.*, 2010).

Ang II has been shown to act as a neurotransmitter that depolarizes neurons and increases excitability (Oz & Renaud, 2002; Latchford *et al.*, 2005; Zaika *et al.*, 2006), and BDNF is released in response to neuronal activity to facilitate the development of LTP (Huang & Reichardt, 2003; Nagappan & Lu, 2005; Minichiello, 2009). These events raise the possibility that the development of sympatho-excitation in CHF or some forms of hypertension could be due to the interplay between Ang II-elicited increases in neuronal activity in brainstem nuclei, such as the RVLM, and aberrant development of long-term potentiation through BDNF. Further investigation is needed to determine if Ang II causes an increase in BDNF activity through signaling cascades or if BDNF activity is increased due to increased neuronal activity stimulated by Ang II.

A recent study by Erdos *et al.* (2015) demonstrated that overexpression of BDNF in neurons of the PVN was sufficient to raise blood pressure, HR, and markers of sympathetic tone, implicating the ability of BDNF to modulate presympathetic neuronal pathways and increase sympatho-excitation. Interestingly, these effects were attenuated by intracerebroventricular (ICV) administration of the AT1R blocker losartan suggesting the critical role of the Ang II signaling in the mechanism of BDNF signaling. This study along with the data presented here suggest a possible convergent signaling and bidirectional interaction of the Ang II and BDNF pathways. It remains to be seen if the convergence of these signaling pathways is involved in mediating the sympatho-excitatory conditions seen during disease states such as heart failure and hypertension.

It has been shown that inhibition of p38 MAPK with SB-203580 can attenuate the reduction in Kv4.3 mRNA following Ang II treatment (Gao *et al.*, 2010). Here, we demonstrate that SB-203580 can prevent the reduction in I_A following treatment with BDNF. These observations, along with the involvement of BDNF in Ang II-induced reductions in I_A , suggest that p38 MAPK plays a role in the convergence of BDNF and Ang II signaling.

A potential limitation of the current study is the use of an anti-BDNF antibody to inhibit BDNF signaling through its receptor tyrosine kinase (TrkB). Other potential methods to block BDNF signaling through TrkB include pharmacological inhibition using drugs such as K252a.

Although often cited as a specific inhibitor of TrkB, K252a can also inhibit the action of a number of tyrosine kinases including p38 MAPK (Martin *et al.*, n.d.). As we were interested in the activity of p38 MAPK in this study, this precluded the use of K252a. Use of anti-BDNF antibody to prevent BDNF/TrkB interaction has demonstrated to be an effective inhibitor of BDNF/TrkB signaling (Cao *et al.*, 2012).

The CATH.a cell model has been extensively used in investigations of Ang II signaling and K⁺ current modulation (Gao *et al.*, 2010; Yin *et al.*, 2010; Yang *et al.*, 2011; Haack *et al.*, 2012; Xiao *et al.*, 2013). This cell line fully expresses the necessary proteins for Ang II signaling and expresses a number of K⁺ channels including Kv4.3. Therefore, it is appropriate for investigation of the effects of Ang II on K⁺ currents. In our hands, we are unable to elicit action potentials from CATH.a cells, which limits the direct application of these results to sympatho-excitation in that we were unable to observe changes in neuronal sensitivity and action potential frequency. However, previous studies using acutely dissociated neonatal neurons have demonstrated similar effects of Ang II on K⁺ currents (Kang *et al.*, 1992, 1993). More robust electrophysiological experimentation such as brain slice measurements or acutely dissociated neurons from animal models of CHF is needed to confirm these current findings and previous studies in integrative physiological systems. Moreover, although our data demonstrate important molecular and signaling interactions in modulating K⁺ currents *in vitro*, further investigations are needed to observe the impact of these findings to whole-animal physiology, which will be presented in the following chapters of the current dissertation.

These findings indicate the involvement of BDNF signaling in Ang II-mediated reductions of I_A and suggest the convergence of BDNF and Ang II signaling on p38 MAPK. These data provide new insight into the mechanisms responsible for altered intrinsic neuronal excitability in diseases characterized by sympatho-excitation such as CHF and hypertension. Further investigation into the specific channels and neuronal populations affected by BDNF and Ang II in the intact

animal will be beneficial in further understanding the basic physiology and treatment possibilities for these prevalent diseases.

**CHAPTER III: INFLUENCE OF BDNF/TRKB
SIGNALING IN THE NTS ON BAROREFLEX
SENSITIVITY IN RATS WITH CHRONIC HEART
FAILURE**

INTRODUCTION

CHF is a prevalent disease characterized by numerous humoral and autonomic alterations such as increased sympathetic nervous system tone and a desensitization of baroreflex control (Zucker *et al.*, 2012). Baroreflex control of HR and sympathetic nerve activity provides an important short-term feedback loop that buffers changes to MAP and controls cardiac output. Alterations in baroreflex sensitivity (BRS) are indicative of dysautonomia and altered feedback control of the cardiovascular system in the CHF state (Goldstein *et al.*, 1975; Zucker *et al.*, 2009). Baroreflex desensitization is prognostic for negative outcomes in patients with CHF (Schwartz *et al.*, 1988; La Rovere *et al.*, 1998). A reduction in BRS may result from numerous peripheral and central alterations (Gnecchi Ruscone *et al.*, 1987; Gao *et al.*, 2005a; Wang *et al.*, 2008), many of which are still unknown. The dorsal medial NTS (dmNTS) comprises the primary central termination of baroreceptor afferents and serves as the initiating central site of the baroreflex arc (Seller & Illert, 1969; Jordan & Spyer, 1977; Tang & Dworkin, 2007a, 2009). Although previous studies have reported a role for glutamatergic signaling in the dmNTS (Dietrich *et al.*, 1982; Andresen & Yang, 1995), the involvement of other neurotransmitters and neuromodulators in the baroreflex control at the level of dmNTS, especially in the CHF state are largely unknown. In addition, there is a lack of understanding of the role played by neurotrophic factors that may influence central desensitization of the baroreflex in CHF.

The family of neurotrophic factors comprises one such class of potential factors that may influence autonomic neuronal activity. BDNF has been implicated in autonomic pathway dysfunction (Mattson & Wan, 2008; Martin *et al.*, 2009). BDNF can function as both a neurotransmitter and neuromodulator and can thus act both acutely and chronically to alter neuronal firing and neuronal sensitivity to synaptic input (Rose *et al.*, 2004). Signaling by BDNF and its receptor, TrkB has long been understood to potentiate synapses and increase glutamatergic signaling and excitatory ion channel activity in a large number of neuronal pathways such as the

hippocampus (Minichiello, 2009). However, whether BDNF/TrkB signaling in NTS is involved in autonomic regulation in both normal and CHF states is unknown. Therefore, the overall objective of the current study was **to investigate the potential contribution of BDNF/TrkB signaling to autonomic dysfunction in a rat model of CHF**. The specific aims were twofold:

1. to identify a role for BDNF/TrkB signaling at the level of dmNTS in modulating baroreflex function in the normal state and
2. to explore the potential contribution of abnormal BDNF/TrkB signaling to the central desensitization of baroreflex function in animals with CHF.

METHODS

Experiments were performed on male Sprague-Dawley rats weighing approximately 200 g at the time of the myocardial infarction and approximately 400 to 520 g at the time of the acute experiment. These experiments were approved by the Institutional Animal Care and Use Committee of the University of Nebraska Medical Center and were carried out under the guidelines of the National Institutes of Health *Guide for the Care and Use of Laboratory Animals*.

Animal Preparation

CHF was produced by left coronary artery ligation as described in Chapter II and as in previous studies (Wang *et al.*, 2010b, 2010a, 2014). In the present study, all rats (n=24) survived from the sham surgery. However, approximately 74% (26 out of 35) survived coronary artery ligation surgery. Three infarcted rats were excluded due to a small infarct size (<15%) measured at the time of the terminal, acute experiment.

Acute experiments were conducted as described in detail in Chapter I including hemodynamic measurements via Millar catheter, RSNA recording, and baroreflex experiments.

Microinjections into the NTS

NTS microinjection was performed as previously described (Wang *et al.*, 2007). Generally, microinjections were made from four- or five-barrel micropipettes with total tip diameters of 20–30 μm and performed using a four-channel pressure injector (PM2000B; World Precision Instruments). The injections were made over a 10 s period, and a 50 nl injection volume was measured by observing the movement of the fluid meniscus along a reticule in a microscope. The dmNTS (coordinates in mm with respect to calamus scriptorius: 0.5 rostral, 0.5–0.6 lateral, and 0.4–0.5 deep) (Paxinos & Watson, 1998) was identified by injecting L-glutamate (10 mM, 50 nl) and observing a depressor response of at least 15 mmHg. In order to examine the potential effects of microinjection of exogenous BDNF into dmNTS on MAP, HR and RSNA in normal and CHF

states, unilateral microinjection of different doses of BDNF (10 and 100 pg, Santa-Cruz Biotechnologies, Santa Cruz, CA) or artificial cerebrospinal fluid (aCSF, vehicle) into dmNTS was performed in sham and CHF rats. The time interval for each dose of BDNF or vehicle injection was at least 15 minutes. At the end of the experiments, 50 nl of 2% Pontamine sky blue were injected for marking the injection sites.

In separate groups of rats, in order to evaluate the role of endogenous BDNF/TrkB signaling in modulating baroreflex function in normal and CHF states, baroreflex function was examined before and 10 min after bilateral microinjection of the TrkB antagonist, ANA12 (Sigma-Aldrich, St. Louis, MO) or DMSO (vehicle) into dmNTS in sham and CHF rats. The effects of bilateral microinjection of different doses of ANA12 (62.5 and 125 μ M) into dmNTS on basal MAP, HR and RSNA were also observed. The time interval between bilateral ANA12 microinjections was within a 2 min period. At the end of the experiments, 50 nl of 2% Pontamine sky blue were injected for marking the injection sites.

Western Blotting

Five sham-operated and five CHF rats were anesthetized, and cardiac function measured within 30 min. Rats were euthanized with an overdose of pentobarbital sodium (150 mg/kg, IV), brains were quickly extracted, frozen on dry ice and stored at -80 °C. At the same time, the hearts and lungs were rapidly removed, placed on dry ice and infarct size was quickly measured. Brainstems were sliced using a cryostat and the dmNTS was punched bilaterally from CHF and sham rats using a tissue biopsy needle of 1.0 mm inner diameter 0.4-1.0 mm posterior to Obex, 0.5-0.6 mm lateral to the midline, and 0.4-0.5 mm from the dorsal surface of the brainstem. Tissue punches were homogenized in RIPA buffer (Sigma Aldrich, St. Louis, MO) containing protease and phosphatase inhibitors (Sigma Aldrich, St. Louis, MO) via sonication. Homogenates were centrifuged, and the supernatant was collected. Total protein was estimated via a Pierce BSA assay (Thermo Scientific, Rockford, IL) and boiled in equal volume of 4% SDS sample buffer. Protein

was loaded in equal amounts of 15 µg total protein into each well of 7% (for TrkB analysis) or 12% (for BDNF analysis) SDS-PAGE gels. Gels were electrophoresed, and transferred onto nitrocellulose membranes (Millipore, Billerica, MA) at 50 V for 90 min. Membranes were blocked in Li-Cor blocking solution (Lincoln, NE) for one hour and incubated overnight in 4 °C with primary antibodies to TrkB (1:2,000; ab33655 Abcam, Cambridge, MA), or BDNF (1:2,000; ab46176 Abcam) with α -Tubulin (1:5,000; sc-53646 SantaCruz Biotechnology, Santa Cruz, CA) as a loading control. Blots were washed and incubated with Li-Cor secondary infrared-labeled antibodies (IRDye 680LT 926-68022 at 1:5000 and IRDye 800CW 926-32214 at 1:2000) for 1 h at room temperature in PBS with 1% SDS. Blots were washed and visualized using Li-Cor Odyssey system and bands quantified via Li-Cor Image Studio software.

Statistics

All data are expressed as mean \pm standard error of the mean. Differences between groups were determined by a one or two-way ANOVA followed by a Tukey *post hoc* test. Changes in baroreflex function before and after NTS microinjection of ANA12 were determined by paired t test. A p value <0.05 was considered statistically significant.

RESULTS

Body Weight, Organ Weight, and Baseline Hemodynamics

Echocardiographic and hemodynamic measurements of sham-operated and CHF rats are summarized in Table 1. MI-induced cardiac dilation in CHF rats was indicated by increased LV systolic and diastolic diameters and volumes measured by echocardiography at the 6th week post MI. Furthermore, these 6-week MI rats exhibited reduced ejection fraction and fractional shortening compared with sham rats, indicating decreased cardiac systolic function. Hemodynamic data collected at the time of the terminal experiments (~14 weeks) further demonstrated that there was a significant increase in LVEDP in CHF rats compared to sham rats. Left ventricular dp/dtmax and min were also significantly lower in CHF rats. The heart weight and lung weight to-body weight ratios were significantly higher in CHF rats than in sham-operated rats, suggesting cardiac hypertrophy and substantial pulmonary congestion in the CHF state. Moreover, in rats with CHF, a gross examination revealed a dense scar in the anterior ventricular wall. The mean infarct area was $43.3 \pm 1.1\%$ of the LV area. No infarcts were identified in sham-operated rats. Pleural fluid and ascites were also found in some of CHF rats but none in the sham-operated rats. Compared to sham rats, there was a slight but significant decrease in baseline MAP in CHF rats.

Table 3 - Hemodynamic and echocardiographic data in sham and CHF rats

	Sham (n=24)	CHF (n=23)
Body weight (g)	426 ± 7	450±7
Heart weight (mg)	1271 ± 26	2170 ± 67*
HW/BW (mg/g)	2.99 ± 0.06	4.83 ± 0.13 *
WLW/BW (mg/g)	4.33 ± 0.08	8.97 ± 0.25 *
MAP (mmHg)	105.5 ± 2.4	90.2 ± 1.9*
LVEDP (mmHg)	4.1 ± 0.4	21.0 ± 1.0*
HR (bpm)	368.9 ± 6.0	355.4 ± 6.0
LVEDD (mm)	6.91 ± 0.1	10.77 ± 0.1*
LVESD (mm)	3.99 ± 0.1	8.92 ± 0.1*
LVEDV (μl)	69 ± 8	427 ± 26*
LVESV (μl)	255 ± 11	649 ± 30*
EF (%)	72.9 ± 0.7	34.2 ± 1.3*
FS (%)	42.0 ± 0.6	17.2 ± 0.7*
dP/dT _{max}	8765 ± 410	4634 ± 204*
dP/dT _{min}	-8145 ± 291	-3272 ± 123*
Infarct size (%)	0	43.3± 1.1 *

Values are mean ± SE. BW, body weight; HW, heart weight; WLW, wet lung weight; MAP, mean arterial pressure; LVEDP, left ventricle end-diastolic pressure; HR, heart rate. LVEDD, left ventricle end-diastolic diameter; LVESD, left ventricle end-systolic diameter; LVESV, left ventricle end- systolic volume; LVEDV, left ventricle end-diastolic volume; EF, ejection fraction; FS, fractional shortening. *P < 0.05 vs. CHF.

Functional and Histological Identification of the dmNTS

To define the role of BDNF/TrkB signaling in modulating baroreflex function in sham and CHF rats, we focused on the dmNTS, a region that primarily receives and integrates sensory input from peripheral baroreceptors and is critical for baroreflex control of the sympathetic nervous system. In all microinjection experiments the location of the pipette in the dmNTS was confirmed by bradycardia, depressor and sympatho-inhibitory responses to microinjection of glutamate (10 mM; 50 nl). Figure 19 illustrates the reduction in MAP, HR and RSNA in response to microinjection of glutamate in the dmNTS from one representative sham rat. Histological analysis of the injection sites stained with 2% Pontamine sky blue is also shown in Figure 19.

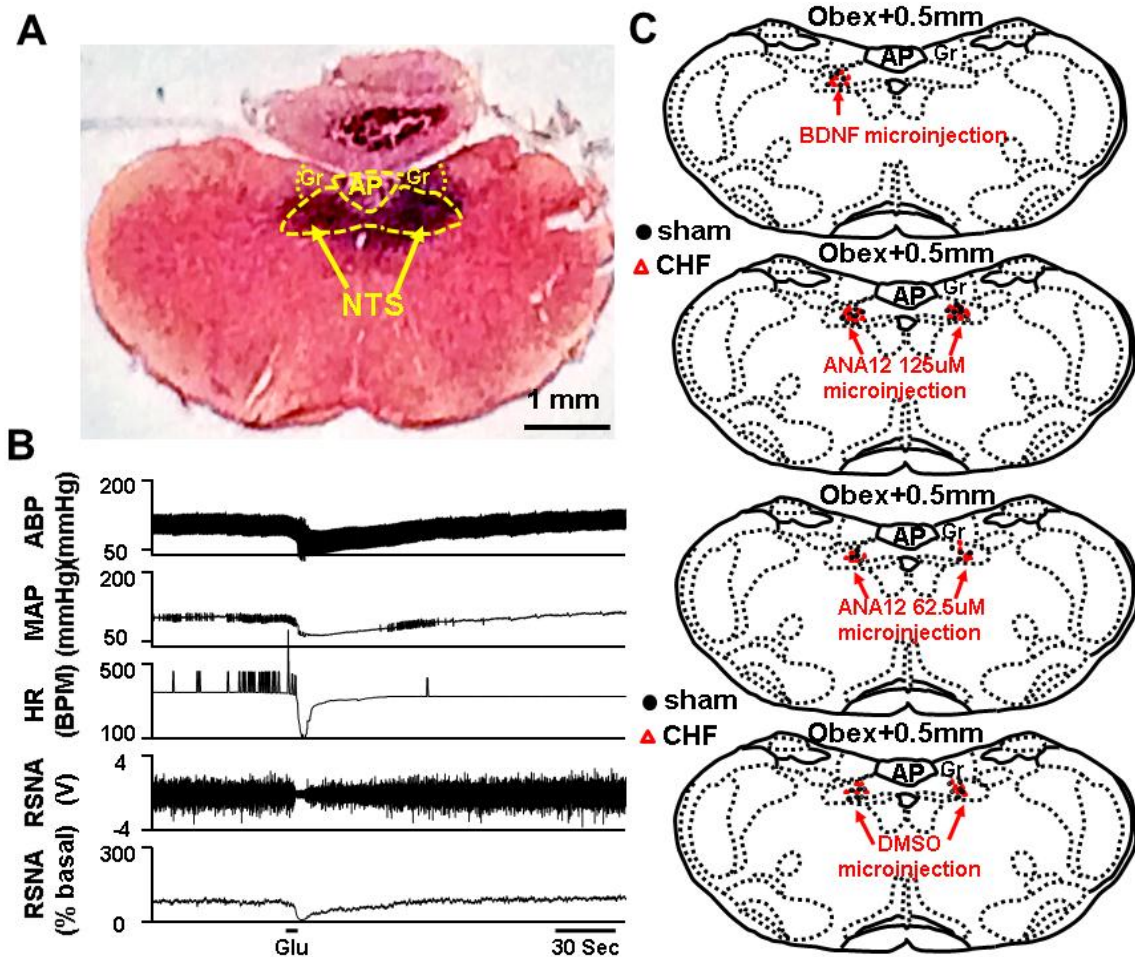


Figure 19. Histological analysis and functional identification of microinjection sites in the dorsal medial nucleus tractus solitarius (dmNTS)

A) original digital picture of the microinjection site filled with 2% Pontamine sky blue. AP, area postrema; Gr, gracile nucleus.

B) representative recording from one animal demonstrating the arterial blood pressure (ABP), mean blood pressure (MAP), heart rate (HR) and renal sympathetic nerve activity (RSNA) responses to unilateral microinjection of glutamate (50 nl; 10mM). The dmNTS region was identified by the presence of a depressor (>20 mmHg) and sympatho-inhibitory response to glutamate.

C) the distributions of the microinjection sites plotted on standard coronal sections according to the atlas of Paxinos and Watson (Paxinos & Watson, 1998). All microinjection sites in the current study were ~ 0.5mm rostral to obex (± 0.04 mm standard deviation).

Response to BDNF in the dmNTS in Sham and CHF Rats

After the stereotactic location of the dmNTS was confirmed by injection of glutamate with one barrel of a four-barrel micropipette, we injected 50 nL of either 10 pg or 100 pg BDNF or aCSF (vehicle) using one of the other barrels in randomized order. The time interval between injections was 15 minutes, which allowed cardiovascular parameters to recover to baseline. As shown in Figure 20-Figure 21, unilateral microinjection of BDNF into the dmNTS produced dose-dependent bradycardia, depressor and sympatho-inhibitory responses similar to that of glutamate in sham rats, indicating a robust activation of the barosensitive neurons in dmNTS in the normal state. Injections of 50 nL of 10 pg or 100 pg BDNF into the dmNTS of rats with CHF also produced the bradycardia, depressor, and sympatho-inhibitory responses. However, these effects were significantly blunted compared to those of sham rats (Figure 20-Figure 21). Microinjection of aCSF (vehicle) into the dmNTS failed to change basal MAP, HR and RSNA in sham and CHF rats.

Responses to ANA 12 into the dmNTS in Sham and CHF Rats

In separate groups of rats, we also investigated the effects of bilateral microinjection of the TrkB antagonist ANA 12 (65.2 μ M and 125 μ M) into the dmNTS on baseline MAP, HR and RSNA in sham and CHF rats. In contrast to the effects observed after BDNF, microinjection of ANA 12 into dmNTS resulted in tachycardia, an increase in MAP, and sympatho-excitatory responses in a dose-dependent manner in sham rats (Figure 20-Figure 21), indicating that the endogenous BDNF/TrkB signaling in dmNTS plays a tonic role in exciting barosensitive neurons in the NTS therefore suppressing blood pressure and sympathetic outflow in the normal state. The sympatho-excitatory effects of bilateral microinjection of ANA 12 into dmNTS on MAP, HR and RSNA were reduced in CHF rats compared to the sham rats. Microinjection of DMSO (vehicle) into the dmNTS failed to change basal MAP, HR and RSNA in both sham and CHF rats.

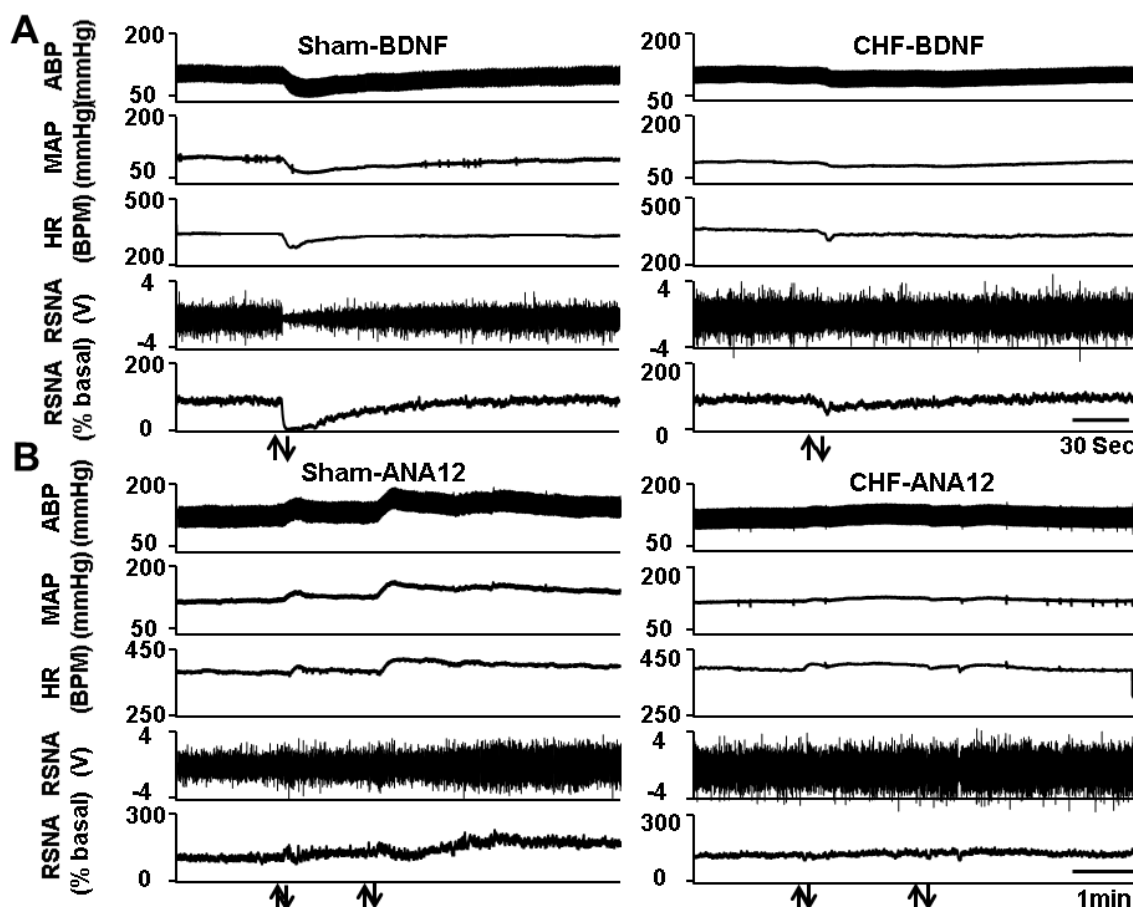


Figure 20 - Representative figures showing the effects of microinjection into the dmNTS

Effects of BDNF (100pg, 50nl) or ANA12 (125 μ M, 50nl) on arterial pressure, MAP, HR and RSNA in sham and CHF rats. Arrows indicate the start and end of the injection.

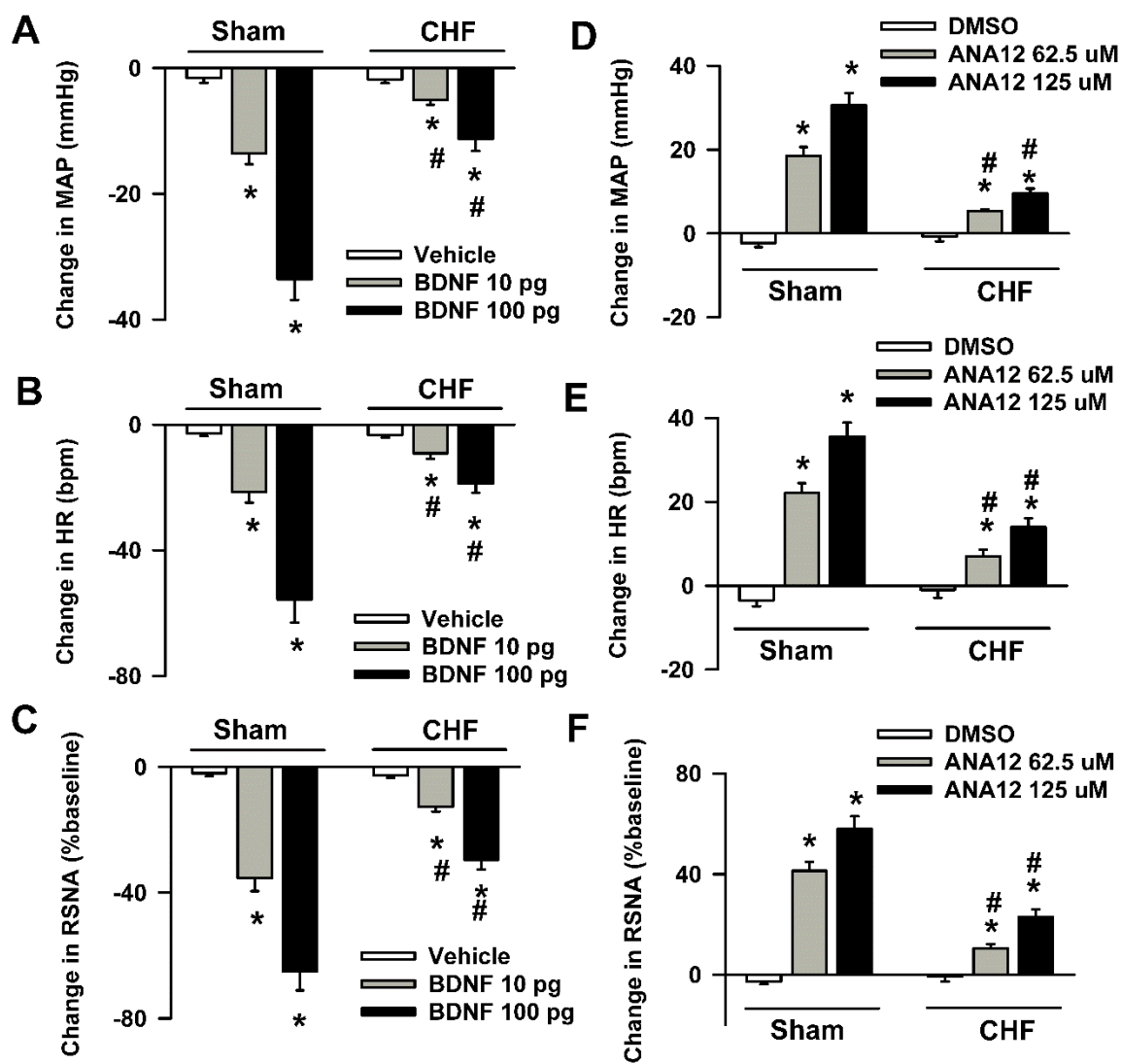


Figure 21 - Dose-dependent effects of microinjection of BDNF

Injections of (10 and 100pg, 50nl, A-C) and ANA12 (62.5 and 125uM, 50nl, D-F) into the dmNTS on AP, MAP, HR and RSNA in sham and CHF rats. DMSO and aCSF serve as the control for ANA12 and BDNF, respectively. Data are expressed as Mean \pm SEM. *, $P < 0.05$ vs. control, #, $P < 0.05$ vs. sham.

Effect of ANA 12 in the dmNTS on Baroreflex Sensitivity

To characterize the role of endogenous BDNF/TrkB signaling in the dmNTS in modulating BRS in the normal and CHF states, we performed baroreflex experiments before and after bilateral microinjections of 125 μ M ANA12 into the dmNTS in sham and CHF rats. Following TrkB inhibition by ANA-12, the HR response to increases in MAP was blunted for both range and maximal gain (Figure 22-Figure 24; Table 4) in sham rats. Similarly both the range and maximal gain of the RSNA response to increases in MAP were decreased following ANA-12 injections (Figure 22-Figure 24; Table 4). These data suggest that endogenous BDNF/TrkB signaling in the dmNTS plays an important role in modulating baroreflex function in the normal state.

Compared to sham rats, CHF rats exhibited significantly lower HR and RSNA responses to increases in MAP (Figure 22-Figure 24; Table 4). Bilateral injections of ANA-12 into the dmNTS did not result in any further decrease in range or maximal gain of the HR response to increased MAP (Figure 22-Figure 24; Table 4). Interestingly, although the RSNA response to increased MAP was already blunted in CHF rats, TrkB receptor inhibition by ANA-12 in the dmNTS further reduced both range and maximal gain of the RSNA response to increased MAP in CHF rats (Figure 22-Figure 24; Table 4).

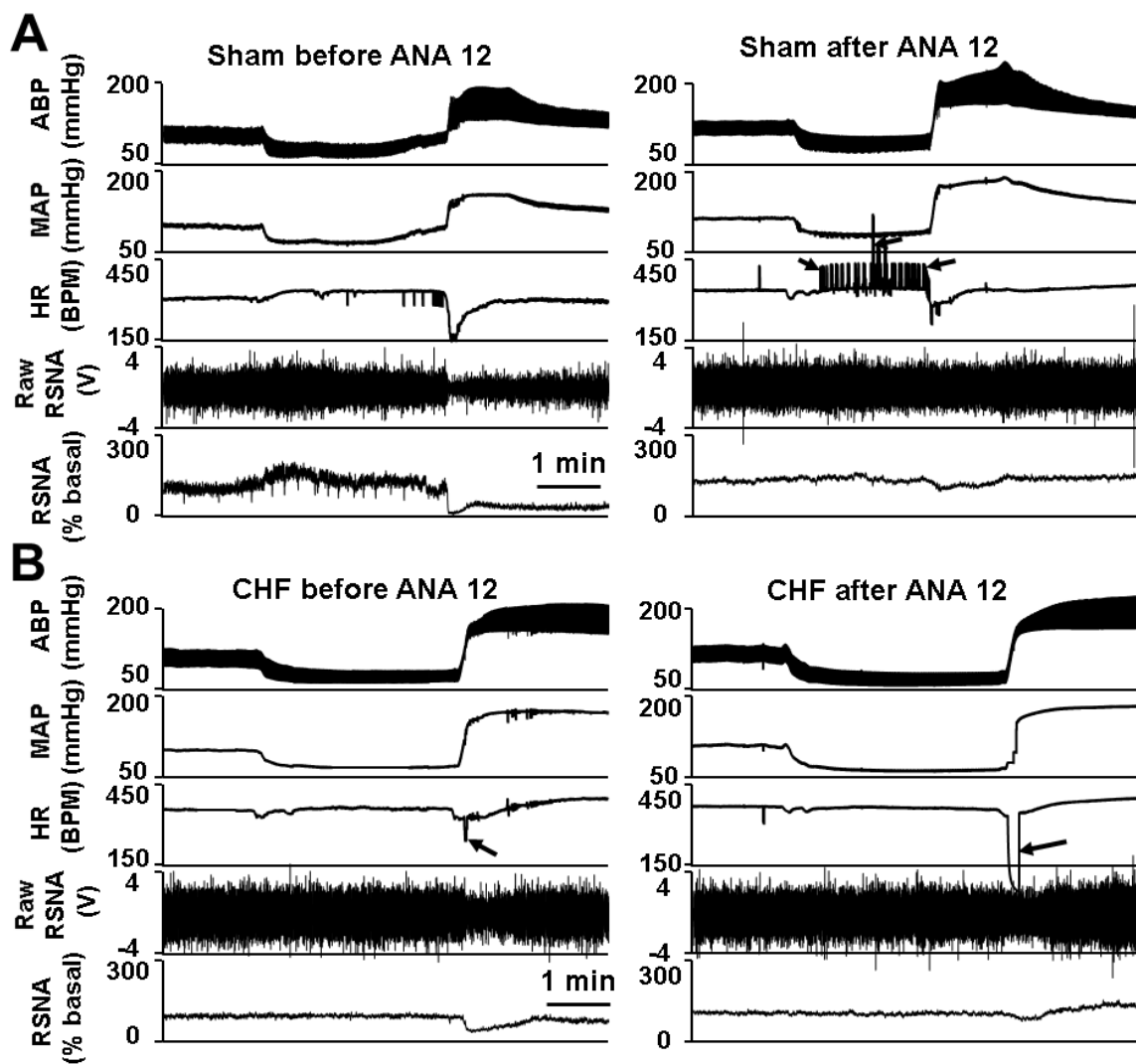


Figure 22 - Representative figures showing the effects of bilateral microinjection of ANA12 on BRS

Bilateral injections (125 μ M, 50 nl) into the dmNTS changes baroreflex-mediated MAP, HR and RSNA responses to intravenous administration of sodium nitroprusside (25 μ g) followed by phenylephrine (10 μ g) in sham and CHF rats. Arrows point to some artifacts of HR traces.

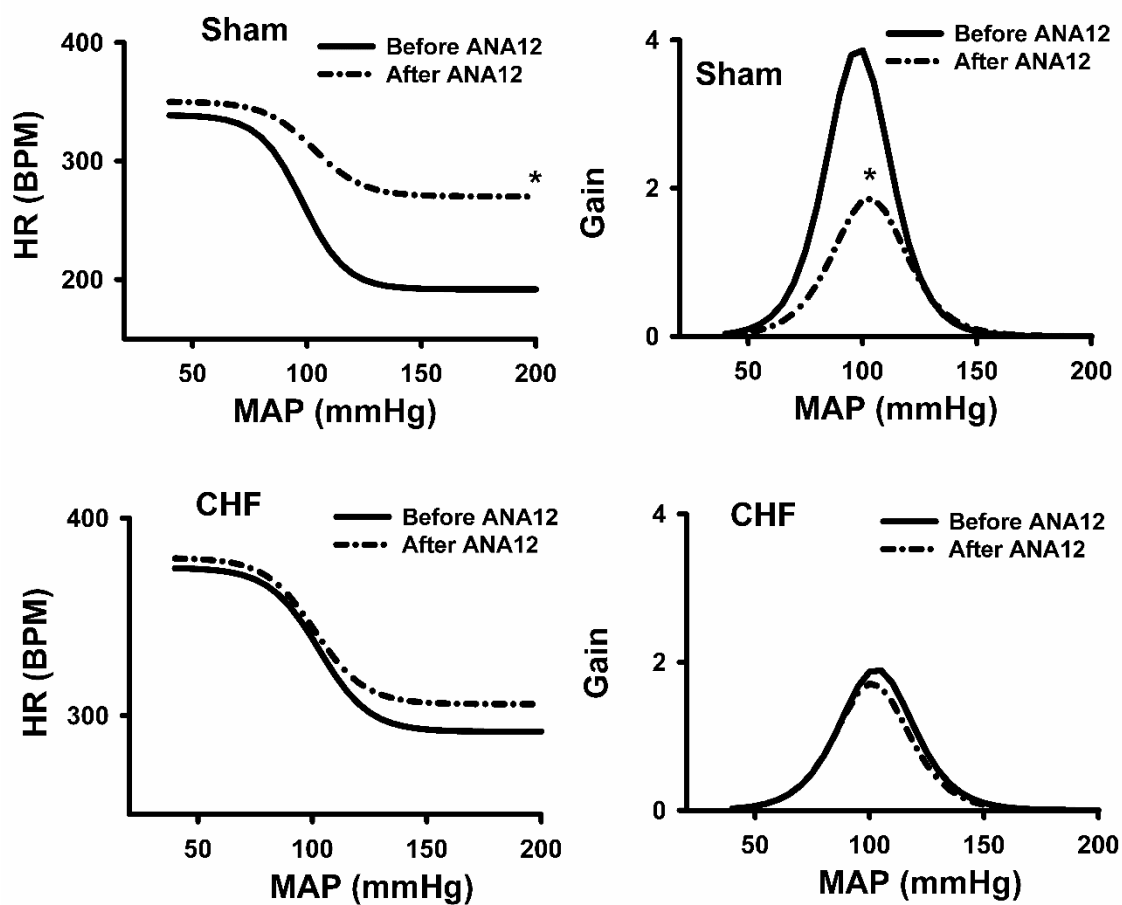


Figure 23 – Effects of ANA-12 on baroreflex control of HR

Mean data showing effects of bilateral microinjection of ANA12 (125 μ M, 50 nl) into the dmNTS on the baroreflex control of HR in sham and CHF rats. Data are expressed as Mean \pm SEM. n=8/each group. *, P<0.05 vs. before.

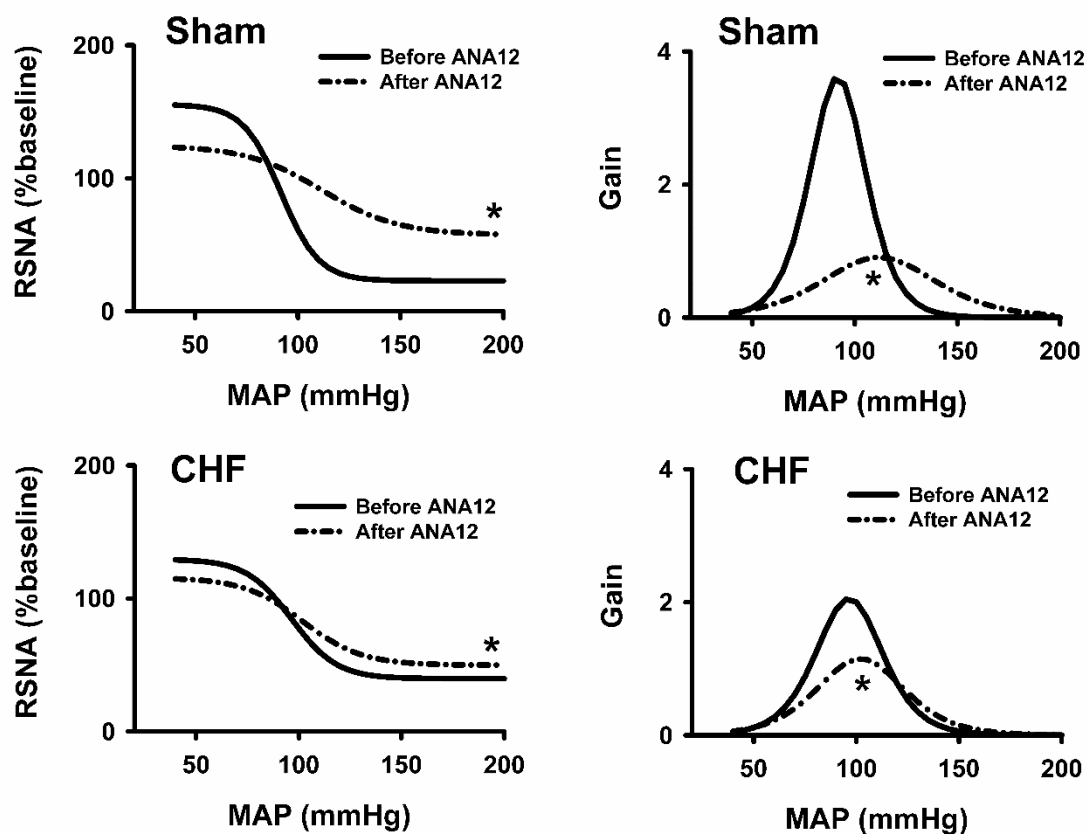


Figure 24 - Effects of ANA-12 on baroreflex control of sympathetic nerve activity

Mean data showing effects of bilateral microinjection of ANA12 (125 μ M, 50 nl) into the dmNTS on the baroreflex control of RSNA in sham and CHF rats. Data are expressed as Mean \pm SE. n=8/each group. *, P<0.05 vs. before.

Table 4 - Summary data for baroreflex function before and after microinjection of chemicals into the dmNTS in sham and CHF rats.

	a, range (% or bpm)	x0, BP50 (mmHg)	y0, min (% or bpm)	Gmax (% or bpm/mmHg)
MAP-RSNA				
Sham before DMSO	130.1 ± 5.0	93.2 ± 1.2	17.8 ± 2.3	3.73 ± 0.14
Sham after DMSO	126.1 ± 4.3	95.5 ± 1.0	17.3 ± 1.7	3.63 ± 0.10
CHF before DMSO	80.8 ± 3.5	98.3 ± 1.3	37.7 ± 3.5	1.88 ± 0.20
CHF after DMSO	77.6 ± 3.8	101.7 ± 0.8	37.0 ± 4.1	1.79 ± 0.21
Sham before ANA-12	132.6 ± 8.4	91.7 ± 3.7	22.9 ± 3.7	3.64 ± 0.18
Sham after ANA-12	67.5 ± 3.6*	111.7 ± 0.8*	57.3 ± 3.3*	0.91 ± 0.10*
CHF before ANA-12	89.8 ± 5.3	96.5 ± 2.6	39.7 ± 4.5	2.05 ± 0.10
CHF after ANA-12	65.9 ± 3.5*	102.0 ± 2.7	49.8 ± 3.1	1.15 ± 0.08*
MAP-HR				
Sham before DMSO	153.8 ± 4.9	98.7 ± 2.0	203.0 ± 8.0	4.08 ± 0.12
Sham after DMSO	144.9 ± 4.7	102.3 ± 2.9	204.6 ± 5.2	3.83 ± 0.08
CHF before DMSO	82.2 ± 4.3	101.8 ± 1.8	280.7 ± 7.8	1.77 ± 0.19
CHF after DMSO	77.3 ± 5.5	105.0 ± 2.3	282.1 ± 6.7	1.66 ± 0.20
Sham before ANA-12	147.1 ± 4.3	98.1 ± 4.4	191.7 ± 5.4	3.90 ± 0.11
Sham after ANA-12	80.1 ± 5.3*	103.0 ± 4.1*	270.0 ± 6.9*	1.88 ± 0.10*
CHF before ANA-12	83.0 ± 3.4	103.0 ± 5.2	291.9 ± 9.4	1.90 ± 0.11
CHF after ANA-12	74.0 ± 3.8	101.2 ± 5.1	305.8 ± 10.1	1.70 ± 0.12

Values are mean ± SEM. a is the RSNA or HR range, x0 is the pressure at the midpoint of the range (BP50), y0 is minimum RSNA or HR and Gmax is the maximum gain of baroreflex curve.

Expression of BDNF and TrkB in the dmNTS in Sham and CHF Rats

To further explore potential mechanisms for the impaired response to ANA-12 in the dmNTS of Sham and CHF animals, we performed western blot experiments to compare protein expression of BDNF and TrkB receptors in the dmNTS of Sham and CHF rats. The expression of TrkB protein in the dmNTS was significantly reduced in CHF rats compared to sham rats (Figure 25A). We failed to observe a significant difference in BDNF protein expression in the dmNTS between sham and CHF rats (Figure 25B).

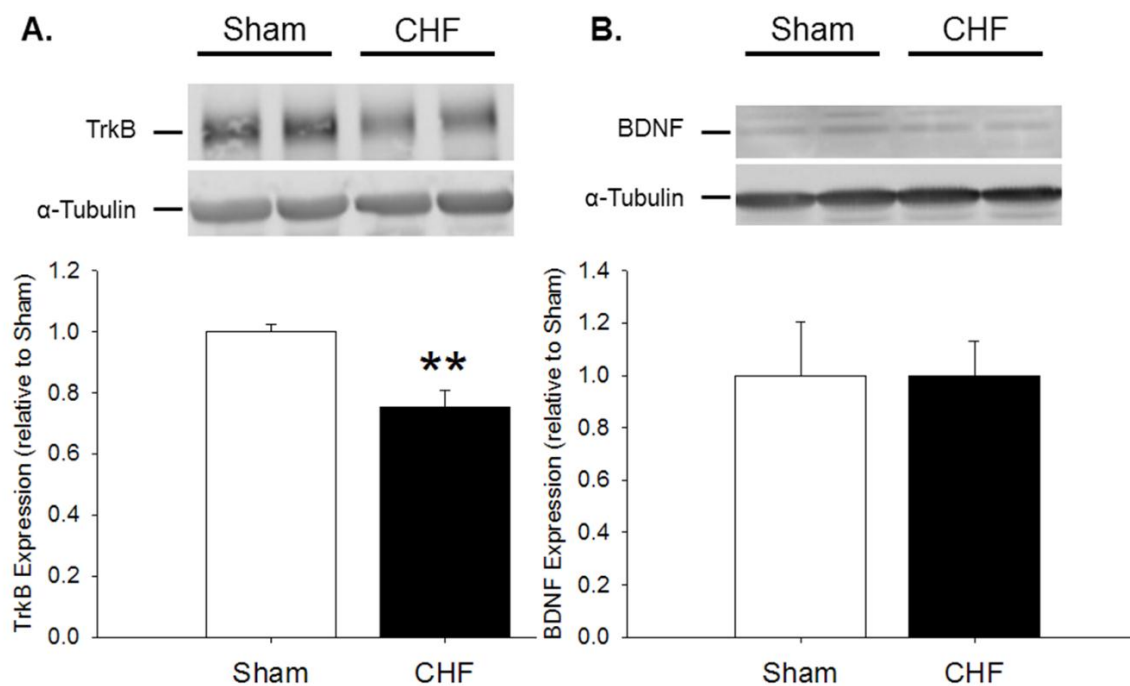


Figure 25 - Protein expression of BDNF and TrkB in dmNTS of sham and CHF rats

Mean \pm SEM. n=5/each group. *, P<0.05 vs. sham.

DISCUSSION

The primary objectives of this study were to investigate the role of BDNF/TrkB signaling in the dmNTS in regulating baroreflex control and to evaluate impaired BDNF/TrkB signaling as a potential mechanism for central desensitization of baroreflex control during CHF. Our results demonstrate a number of novel and important findings. First, our study provides evidence for tonic signaling of BDNF in the dmNTS in the normal state. Inhibition of endogenous BDNF signaling by selectively antagonizing the TrkB receptor with ANA-12 resulted in a sympatho-excitatory response in sham rats, suggesting a tonic sympatho-inhibitory role for BDNF neurotransmission in the dmNTS. Most importantly, BDNF/TrkB signaling in the dmNTS is integral for normal baroreflex function as evidenced by the blunting of BRS following antagonizing TrkB by ANA-12, which inhibited baroreflex gain and range. These observations together suggest a previously unknown role for BDNF neurotransmission in tonic sympatho-inhibition and baroreflex control. Second, the observation that this signaling pathway is impaired in the dmNTS during CHF provides a novel mechanism for understanding central alterations that contribute to baroreflex desensitization during CHF. Because both BDNF and ANA-12 had little effect on hemodynamic and RSNA parameters, the tonic sympatho-inhibition of BDNF may be withdrawn thus contributing to the increased sympathetic tone associated with CHF. Consistent with this finding, TrkB antagonism had little effect on the reduced BRS in CHF animals, which is likely due, in part, to decreased TrkB expression in the dmNTS during CHF. These results, taken together, implicate a reduction in BDNF/TrkB signaling in the dmNTS during CHF that contributes to sympatho-excitation and baroreflex desensitization.

The dmNTS has long been appreciated to be a primary site of baroreceptor afferent termination in the central nervous system (Seller & Illert, 1969; Jordan & Spyer, 1977), and early reports identified the role of dmNTS neurons in mediating the baroreflex (Crill & Reis, 1968; Palkovits *et al.*, 1977). Seminal work by Talman *et al.* provided indication for the role of glutamate

as the predominant neurotransmitter responsible for conducting the blood pressure information through the dmNTS (1980). Glutamatergic signaling within the dmNTS has been extensively examined and demonstrated to be integral to the function of normal baroreflex activation (Talman *et al.*, 1981; Dietrich *et al.*, 1982; Machado, 2001; Talman & Lin, 2013). A-fiber neuronal responses in the dmNTS were potentiated following stimulation of the aortic depressor nerve; an effect which increased baroreflex sensitivity. Interestingly, this was blocked by application of an NMDA antagonist, implicating the necessity of glutamatergic signaling in conducting and potentiating adaptation to baroreceptor input in the dmNTS (Tang & Dworkin, 2007b). Although glutamatergic signaling in the dmNTS is predominant, due to its complex neuronal composition, a variety of other neurotransmitters have also been demonstrated to be important in baroreflex arc conduction. Inhibitory potentials due to GABAergic signaling have been observed in rat dmNTS preparations (Glaum & Brooks, 1996). Furthermore, angiotensin II has also been demonstrated to elicit cardiovascular baroreflex responses in the dmNTS (Barnes *et al.*, 1993, 2003; Fow *et al.*, 1994).

Along with the well-known effects of neurotrophic factors on the developing nervous system, a large body of work has demonstrated the influence of neurotrophic factors on network patterning and long-term potentiation of synapses. The neurotrophins consist of a small family with varied tissue distribution and signaling mechanisms (Lewin & Barde, 1996; Minichiello, 2009). BDNF is highly expressed in the NTS (Conner *et al.*, 1997) and in baroreceptor afferents which project to the NTS (Martin *et al.*, 2009). BDNF signals primarily through TrkB and elicits several long-term neuromodulatory actions as well as immediate, rapid signaling affecting neuronal activity. BDNF rapidly enhances vesicular neurotransmitter release from excitatory neurons (Shinoda *et al.*, 2014) in the hippocampus. TrkB phosphorylation of NMDA receptors increases their open probability (Levine *et al.*, 1998), and BDNF/TrkB signaling results in rapid opening of TrpC channels (Li *et al.*, 1999), Nav1.9 channels (Blum *et al.*, 2002), and Ca²⁺ influx (Rose *et al.*, 2003).

Based on our observations that BDNF induces responses similar to that of glutamate in the dmNTS, we conclude that BDNF is excitatory to neurons in the dmNTS. This conclusion is further strengthened by the action of inhibiting TrkB thereby preventing endogenous BDNF signaling, which produced a neural inhibitory effect. Interestingly, a previous study (Clark *et al.*, 2011) demonstrated that microinjection of exogenous BDNF into the dmNTS evoked a sympatho-excitatory pressor response whereas administration of a non-specific TrkB antagonist K252a induced a depressor response in anesthetized rats, indicating that BDNF/TrkB signaling is inhibitory to NTS baroreceptor neurons in the normal state. The cause of the conflicting results by Clark *et al.* and our current findings is unclear. One possible explanation is that in the current study, we used a more specific TrkB receptor antagonist (ANA-12) (Cazorla *et al.*, 2011) instead of the non-specific, tyrosine kinase inhibitor, K252a, often used as a TrkB antagonist as in the previous study by Clark *et al.* However, this fails to explain the difference related to BDNF NTS microinjection experiments between these two studies (excitatory vs inhibitory). Importantly, our observation that BDNF is excitatory to NTS baroreceptor neurons has been supported by several other studies conducted in neuronal networks such as the hippocampus (Minichiello, 2009), amygdala (Scharfman, 2013), and cortical neurons (Kim *et al.*, 2012). Autonomic centers in the brainstem, such as the RVLM have also been shown to display neuronal excitation following injection of BDNF resulting in a pressor response (Wang & Zhou, 2002). Therefore, this is the first study to our knowledge to demonstrate that endogenous BDNF signaling in the dmNTS maintains tonic inhibition of sympathetic drive.

Furthermore, not only do our results suggest a tonic, background inhibition of sympathetic outflow by BDNF/TrkB in the dmNTS, but they also suggest the necessity of BDNF/TrkB signaling in mediating baroreflex function. Although previous studies have identified the presence of BDNF/TrkB signaling in the NTS, no study to our knowledge has investigated the implications of BDNF/TrkB signaling in the NTS on baroreflex function in both normal and diseases states. We found that inhibiting endogenous BDNF signaling in the dmNTS through bilateral injections of

ANA-12 blunted both the HR and RSNA responses to changes in MAP. This suggests that TrkB signaling is an integral and critical signaling component in the dmNTS for communicating baroreflex signals. A recent report investigating the actions of BDNF on synaptic vesicle release from cultured rat hippocampal neurons indicated that BDNF enhances transmitter release from excitatory synapses but not inhibitory synapses (Shinoda *et al.*, 2014). Furthermore, BDNF has been shown to decrease inhibitory GABA synaptic transmission and resultant IPSPs through its actions on the neuronal potassium chloride cotransporter 2 in Purkinje fibers (Huang *et al.*, 2012). Our results suggest that a similar, excitation-predominant, response also occurs in the dmNTS of rats. It is very likely that endogenous BDNF may modulate the NTS barosensitive neurons via interaction with glutamatergic or GABAergic systems or a combination thereof. This hypothesis needs to be confirmed in future studies.

Of particular interest in these observations is the potential that alterations in the BDNF/TrkB signaling in the dmNTS may play a role in the dysautonomia present during CHF. The diminished response to either BDNF or ANA-12 in the dmNTS of CHF rats suggests a preexisting suppression of this pathway during CHF, which is further strengthened by the observation that CHF rats had decreased TrkB expression in the dmNTS. Thus, withdrawal of BDNF/TrkB signaling in the dmNTS may be one explanation for the increased sympathetic tone associated with CHF (Zucker *et al.*, 2012).

Baroreflex function is decreased in many disease states such as CHF (Goldstein *et al.*, 1975; Wang *et al.*, 2004; Zucker *et al.*, 2009; Kar *et al.*, 2011) and correlates with increased rates of mortality (Schwartz *et al.*, 1988; La Rovere *et al.*, 1998). The progression of baroreflex desensitization is complex and consists of both peripheral alterations to baroreceptor afferent input and central neuronal network dysregulation (Gnecchi Ruscone *et al.*, 1987; Gao *et al.*, 2005a; Wang *et al.*, 2008). Many of the central mechanisms for baroreceptor desensitization remain unknown although evidence indicates a role for the renin-angiotensin system in mediating this dysfunction (Gao *et al.*, 2005a; Wang *et al.*, 2008; Zucker *et al.*, 2009). In our present study, we observed a

decrease in baroreflex sensitivity in CHF rats, and manipulation of dmNTS signaling by antagonism of endogenous BDNF/TrkB signaling evoked less changes in baroreflex sensitivity. The observation that there is a lack of further inhibition following ANA-12 in CHF rats provides a rationale for decreased central control of baroreflex function during CHF. In addition, this observation coupled with the decreased expression of TrkB in the dmNTS of CHF rats provides evidence that impaired BDNF/TrkB signaling in the dmNTS is a mechanism by which central alterations in BRS occur during CHF. This decrease in TrkB expression is consistent with the lack of response to both exogenous BDNF and ANA-12 because a decrease in receptor expression would limit the response of the system to both exogenous application of ligand and antagonism on the endogenous signaling pathway. Thus we propose that a decrease in BDNF/TrkB signaling is one factor contributing to the central mechanism by which baroreflex sensitivity is reduced during CHF.

Limitations

Although this study demonstrates impaired BDNF/TrkB signaling mechanisms in the dmNTS as a potential explanation for blunted baroreflex sensitivity during CHF, there are some limitations to consider. First, it is unclear from the present study what the initiating cause of altered BDNF/TrkB signaling is. One possibility is decreased afferent input from peripheral baroreceptors (Niebauer *et al.*, 1986) resulting in lower neuronal activity in the dmNTS. Because BDNF/TrkB signaling is highly regulated by neuronal activity (Zafra *et al.*, 1990), changes to peripheral afferents as seen in CHF may have a profound impact on the regulation of BDNF/TrkB signaling in central reflex arcs such as the dmNTS. Another potential interaction between BDNF/TrkB in the dmNTS and CHF is the role that angiotensin II may play centrally during the development of CHF. Previous work has shown that angiotensin II injections in the NTS can desensitize the reflex bradycardia and sympatho-inhibition in response to baroreflex activation (Polson *et al.*, 2007). It is possible that an interaction exists between the increased central renin-angiotensin system activity

in CHF (Wang *et al.*, 2007; Gao *et al.*, 2008; Zucker *et al.*, 2009) and BDNF/TrkB regulation in the dmNTS.

Another limitation of the current study is that all experiments were conducted under anesthesia. Although the baseline hemodynamic parameters and baroreflex sensitivity for our experiments were similar to those observed in the conscious state, we acknowledge that the impact of anesthetics could potentially play a role in confounding the results. However, given the inherent difficulty in conducting selective administration of reagents to the dmNTS in conscious animals, anesthetized preparations allow for the most selective and robust investigation into the signaling processes of the dmNTS.

Finally, although we observed a differential expression of TrkB protein in the dmNTS during CHF, we failed to observe any change in total BDNF protein expression in the dmNTS. Nevertheless, this does not definitively preclude the possibility that the amount of presynaptic BDNF release from the baroreceptor afferent terminals to dmNTS postsynaptic neurons may be altered due to the peripheral baroreflex afferent desensitization in the CHF state. This hypothesis can be further explored in the future by using the microdialysis technique.

Impairment of baroreflex function has been shown to be associated with progression of heart failure and a poor prognosis (Schwartz *et al.*, 1988; Mortara *et al.*, 1997; La Rovere *et al.*, 1998). The progression of baroreflex desensitization in CHF is at least, in part, due to central neuronal network dysregulation (Gnecchi Ruscone *et al.*, 1987; Gao *et al.*, 2005a; Wang *et al.*, 2008); however, the central mechanisms for baroreceptor desensitization remain largely unknown. Our data suggest a role for BDNF/TrkB signaling in the dmNTS in maintaining baroreflex control, and that BDNF/TrkB signaling is impaired during CHF. The specific mechanisms responsible for the BDNF/TrkB impairment during CHF remain to be investigated and possess a potential area for therapeutic intervention in sympatho-excitatory states such as CHF.

**CHAPTER IV: CONTRIBUTION OF BDNF/TRKB
SIGNALING TO SYMPATHO-EXCITATION
FOLLOWING ICV ANGTIOTENSIN II**

INTRODUCTION

Previously in this dissertation we have demonstrated the connection between Ang II and BDNF in modulation of potassium currents *in vitro* and that the suppression of BDNF signaling in the NTS contributes to baroreflex dysfunction in the CHF state. We have also demonstrated a reduction in Kv4.3 channels in the RVLM of rats during CHF, and that restoring levels of Kv4.3 in the RVLM attenuates the increased sympathetic tone associated with CHF. Therefore, the proposed cross-talk between central Ang II signaling and the actions of BDNF has been implicated but not directly investigated. Here we aim to demonstrate *in vivo* the connection between central Ang II signaling and BDNF in mediating sympatho-excitation.

A recent study in which BDNF was overexpressed in the PVN of rats showed an increase in MAP and an increased hemodynamic (pressor and tachycardia) response to acute stressors such as water and restraint stress (Erdos *et al.*, 2015) and demonstrated that BDNF overexpression augments Ang II signaling through the AT1R. However, the study did not investigate the relationship between Ang II and the BDNF/TrkB response which may be typical of cardiovascular disease states where central RAS activity may be elevated (Francis, 1985; Zucker *et al.*, 2012; Biancardi *et al.*, 2013).

Central Ang II evokes hypertension and increased SNA (Osborn & Camara, 1997; Camara & Osborn, 1998; Gao *et al.*, 2005b, 2014) and baroreflex dysfunction (Pan *et al.*, 2007; Gao *et al.*, 2008). Central Ang II has also been shown to modulate metabolic dysfunction through increased thirst (Fitzsimons, 1998) and promotion of cachexia, a catabolic state (Brink *et al.*, 1996, 2001; Yoshida *et al.*, 2012). Many of these effects are mediated by Ang II signaling through the AT1R in presympathetic areas of the brainstem and hypothalamus (Gao *et al.*, 2005b, 2008; Zucker *et al.*, 2009) and involve reactive oxygen signaling (Zimmerman *et al.*, 2004; Chan *et al.*, 2005; Sheh *et al.*, 2007; Yin *et al.*, 2010). However, little is understood about how AT1R activation by Ang II

induces long-term changes relating to neuronal excitability and synaptic plasticity of presympathetic centers, which ultimately results in sympatho-excitation.

As previously discussed in this dissertation, we propose BDNF/TrkB signaling as a potential mechanism by which Ang II causes long-term, robust changes to central neuronal activity promoting sympatho-excitation. As we have demonstrated *in vitro* Ang II treatment causes an increase in BDNF expression and results in perturbations to K⁺ currents, here **we hypothesize that central Ang II treatment will evoke a sympatho-excitatory state mediated through the actions of BDNF**. We investigated the effect of antagonizing TrkB with ANA-12 on the responses to ICV Ang II infusion.

METHODS

Animal Model

For these experiments male Sprague-Dawley rats with starting weights ranging between 300 and 350 g were used. The experimental protocols were approved by the Institutional Animal Care and Use Committee of the University of Nebraska Medical Center and were carried out under the guidelines of the National Institutes of Health *Guide for the Care and Use of Laboratory Animals*. An overview of the experimental paradigm and timeline is provided in Figure 26.

Animal Preparation and ICV Infusions

All rats were implanted with radiotelemetry devices as described in Chapter I. Immediately following telemetry implantation anesthetized rats were positioned in a stereotaxic apparatus. The skull was exposed and Bregma was identified. A small hole was bored in the skull at 0.8 mm caudal to Bregma and 1.75 mm lateral to the midline. An Alzet Brain Infusion Kit 2 cannula was inserted through the hole, and the tip of the cannula was positioned 4 mm deep to the surface of the skull into the right lateral ventricle. The cannula was fixed to the skull with dental acrylic with watch screws positioned both rostrally and caudally to the cannula for support. The cannula was attached to a catheter connected to a subcutaneous osmotic minipump (Alzet 2002; 0.5 μ l/h for 14 days) containing vehicle. The skin was closed over the skull, and the animal was allowed to recover.

Following one week of recovery, rats were placed in metabolic cages for 48 h to acclimate. Following acclimation, baseline metabolic and hemodynamic recordings were collected as described in Chapter II. Following one week of baseline recordings, rats were anesthetized with 2-4% isoflurane, a small incision was made close to the osmotic minipump, and pumps were removed and exchanged with a pump containing either Ang II, Ang II+ANA-12, ANA-12 alone, or vehicle.

Ang II and ANA-12 were purchased from Sigma-Aldrich. An effective ICV dose of 20 ng/min Ang II was used based on a survey of the literature (Camara & Osborn, 1998, 2001;

Fitzsimons, 1998; Clayton *et al.*, 2014) and through preliminary dose-response studies (Figure A3). ANA-12 was infused ICV at 50 ng/h alone or in combination with Ang II. All infusions were dissolved in vehicle composed of a 1:1 solution of aCSF to DMSO.

Conscious Parameters

Telemetry recordings were collected as described in detail in Chapter I for collection of MAP, HR, and HRV. The pulse wave recordings were exported to the freely available HemoLab Software (Iowa City, IA - <http://www.haraldstauss.com/HemoLab/HemoLab.html>) for processing of spontaneous baroreflex sensitivity (sBRS). Traces were filtered through a Butterworth low-pass filter with a corner frequency of 20 Hz and the baroreflex gain was determined by the sequence method of sBRS (Bertinieri *et al.*, 1985; Stauss *et al.*, 2006). In brief, baroreflex sequences were defined by a minimum of three consecutive beat to beat intervals of either increasing or decreasing systolic pressure associated with increasing or decreasing pulse interval, respectively. No time delay was applied between pressure and pulse interval changes, and no threshold for pressure changes was used. Only sequences with a correlation coefficient > 0.8 between pressure and pulse interval were used with the slope of the resultant linear correlation equation set as the baroreflex gain. Up sequences (pressure increases) and down sequences (pressure decreases) were differentiated and reported separately. Metabolic cage measurements were made once every 24 h at approximately 3 PM following completion of the day's telemetry recordings.

Acute Animal Preparation

For acute, terminal animal experiments, rats were prepared in the same manner as described in detail in Chapter I for recording of RSNA and baroreflex sensitivity.

Statistics

Daily MAP, HR, and metabolic data were analyzed using RM-ANOVA. All other group interactions were compared using a one or two-way ANOVA with a Tukey's post-hoc test. A P

value < 0.05 was considered statistically significant. All data was analyzed using SPSS or SigmaPlot software.

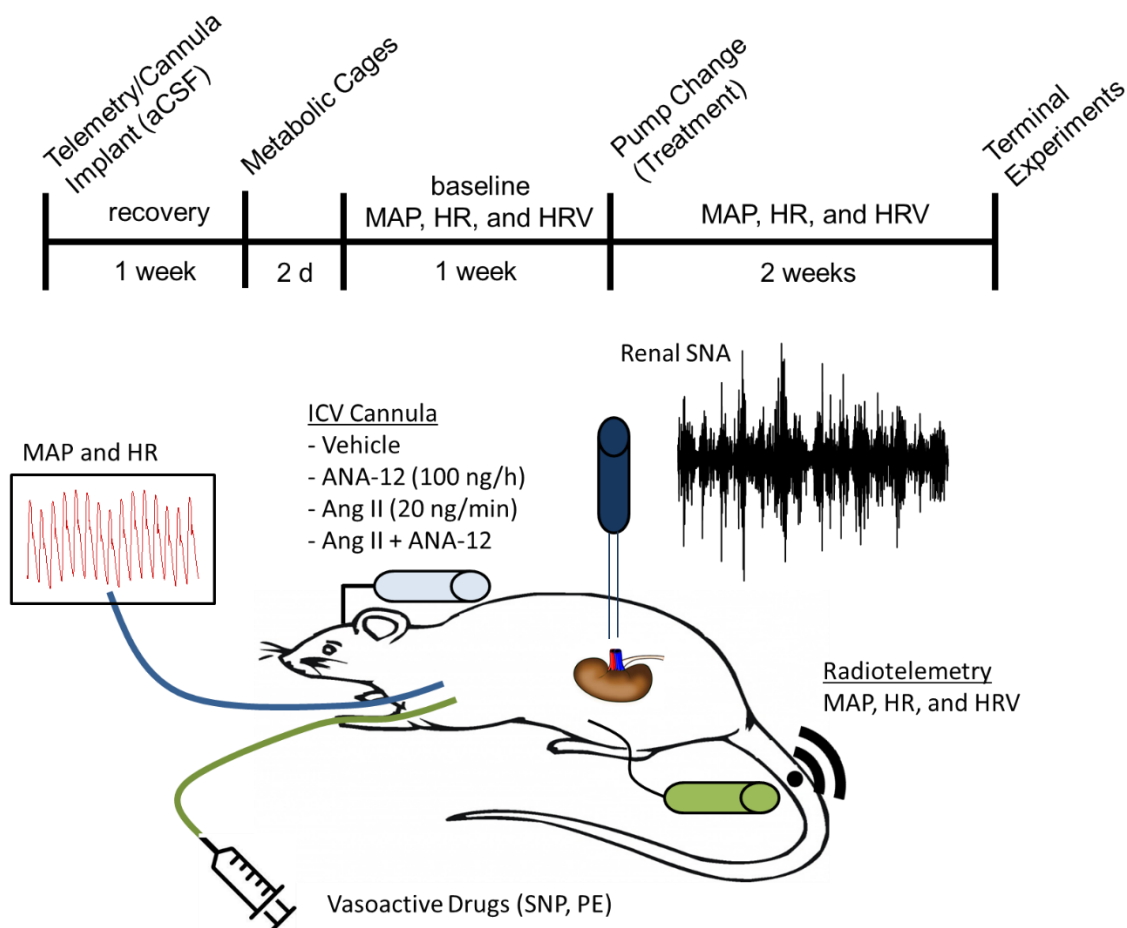


Figure 26 - Experimental timeline and schematic for ICV infusion of Ang II \pm ANA-12

RESULTS

Hemodynamic Responses to ICV Ang II

Rats administered 20 ng/min Ang II ICV demonstrated an immediate and sustained increase in MAP with a peak increase of approximately 50 mmHg (Figure 27B). Coinfusion of ANA-12 with Ang II also increased MAP relative to baseline with a peak increase of approximately 20 mmHg (Figure 27B); however this increase was attenuated as compared to Ang II alone (Figure 27A). Heart rate increased relative to baseline in ICV Ang II animals and in those coinfused with ANA-12. There was a peak increase in Ang II alone of 70 bpm at day 5 post infusion, and Ang II + ANA-12 delayed the increase in heart rate to the end of the infusion period and was increased approximately 40 bpm relative to baseline (Figure 28B). Vehicle and ANA-12 alone had no effect on blood pressure or heart rate.

Although no significant changes were observed relative to heart rate variability in terms of SDNN or RMSSD following ICV Ang II treatment (Figure 29), RMSSD trended toward a decrease in Ang II treated animals and was not affected by coinfusion of ANA-12. In the frequency domain, LF/HF ratio increased following Ang II (Figure 30), and similar to HRV this was not improved by coinfusion of ANA-12. There appeared to be a trend toward a blunted spontaneous baroreflex following ICV Ang II in both up and down sequences (Figure 31); however, neither of these parameters reached statistical significance.

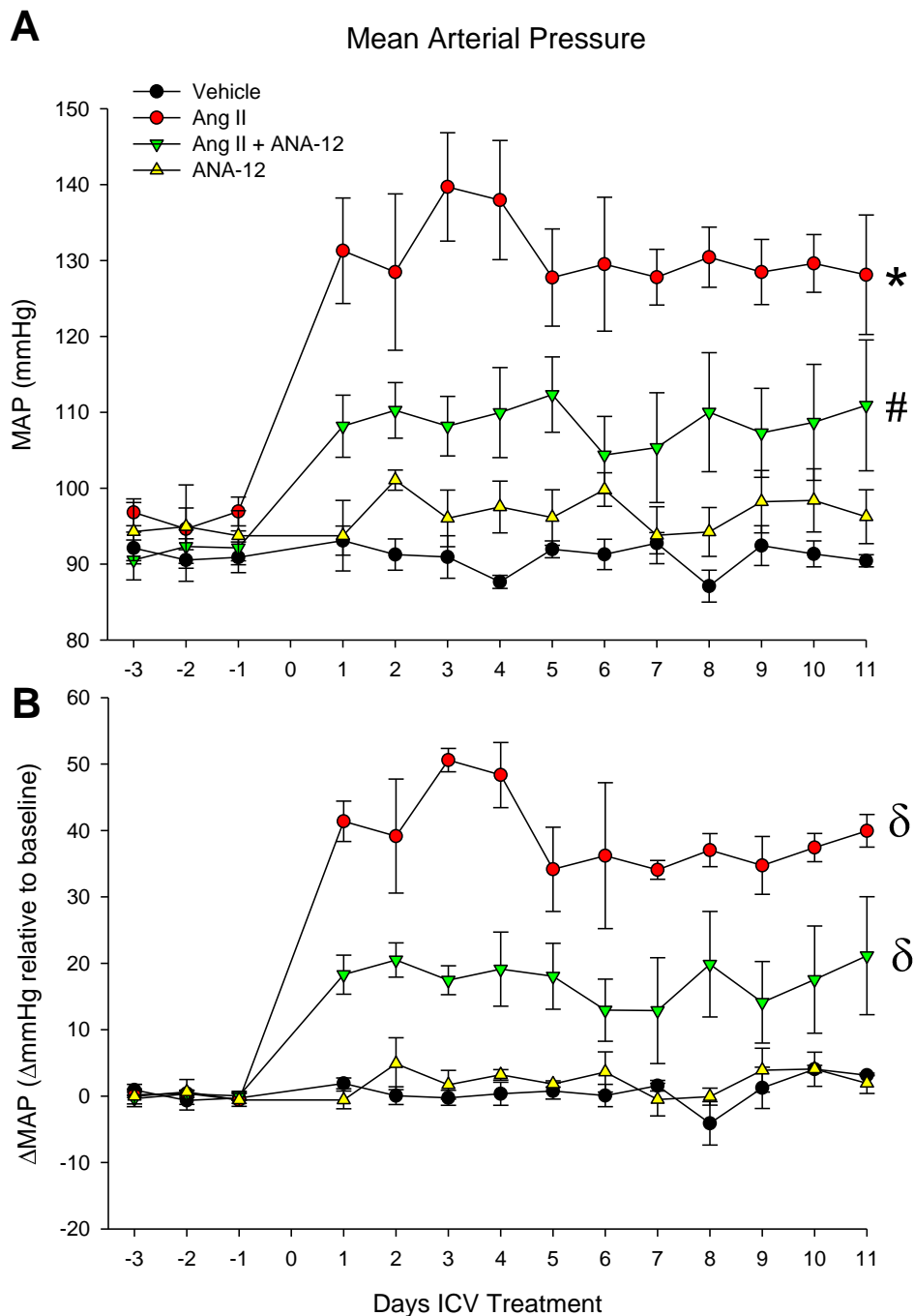


Figure 27 - Effect of ICV Ang II with or without ANA-12 on MAP

Mean daily MAP values for rats given ICV Ang II, Ang II + ANA-12, ANA-12 alone, or vehicle (A) and change in MAP relative to baseline measurements (B). RM-ANOVA was used to determine group interaction and change in pressure from baseline. * $P < 0.05$ vs. Vehicle; # $P < 0.05$ Ang II + ANA-12 vs. Ang II; $\delta P < 0.05$ vs. respective baseline; $n = 4/\text{group}$.

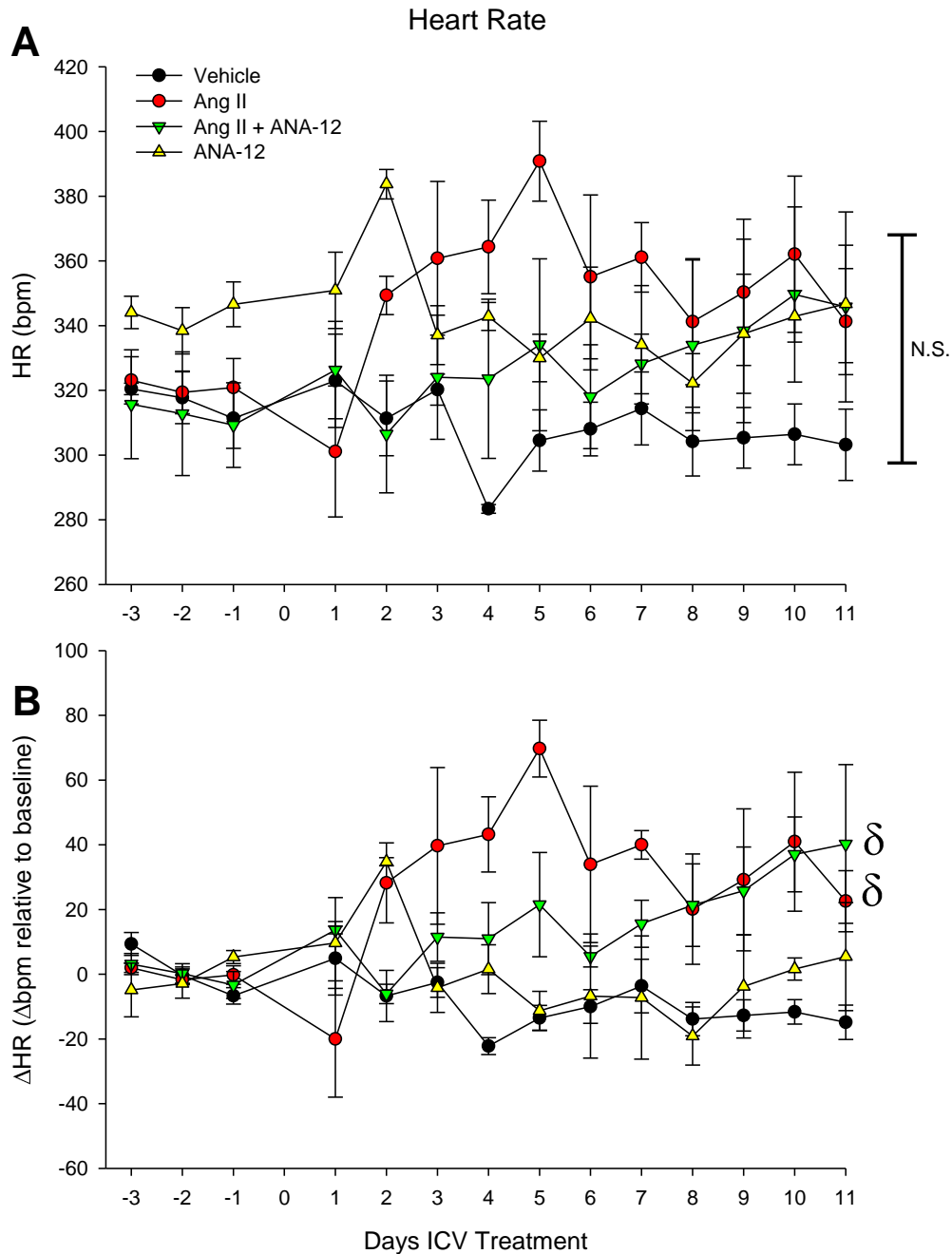


Figure 28 – Effect of ICV Ang II with or without ANA-12 on HR

Mean daily HR values for rats given ICV Ang II, Ang II + ANA-12, ANA-12 alone, or vehicle (A) and change in HR relative to baseline measurements (B). RM-ANOVA was used to determine group interaction and change in pressure from baseline. N.S. = not significant; δ , $P < 0.05$ vs. respective baseline; $n = 4/\text{group}$.

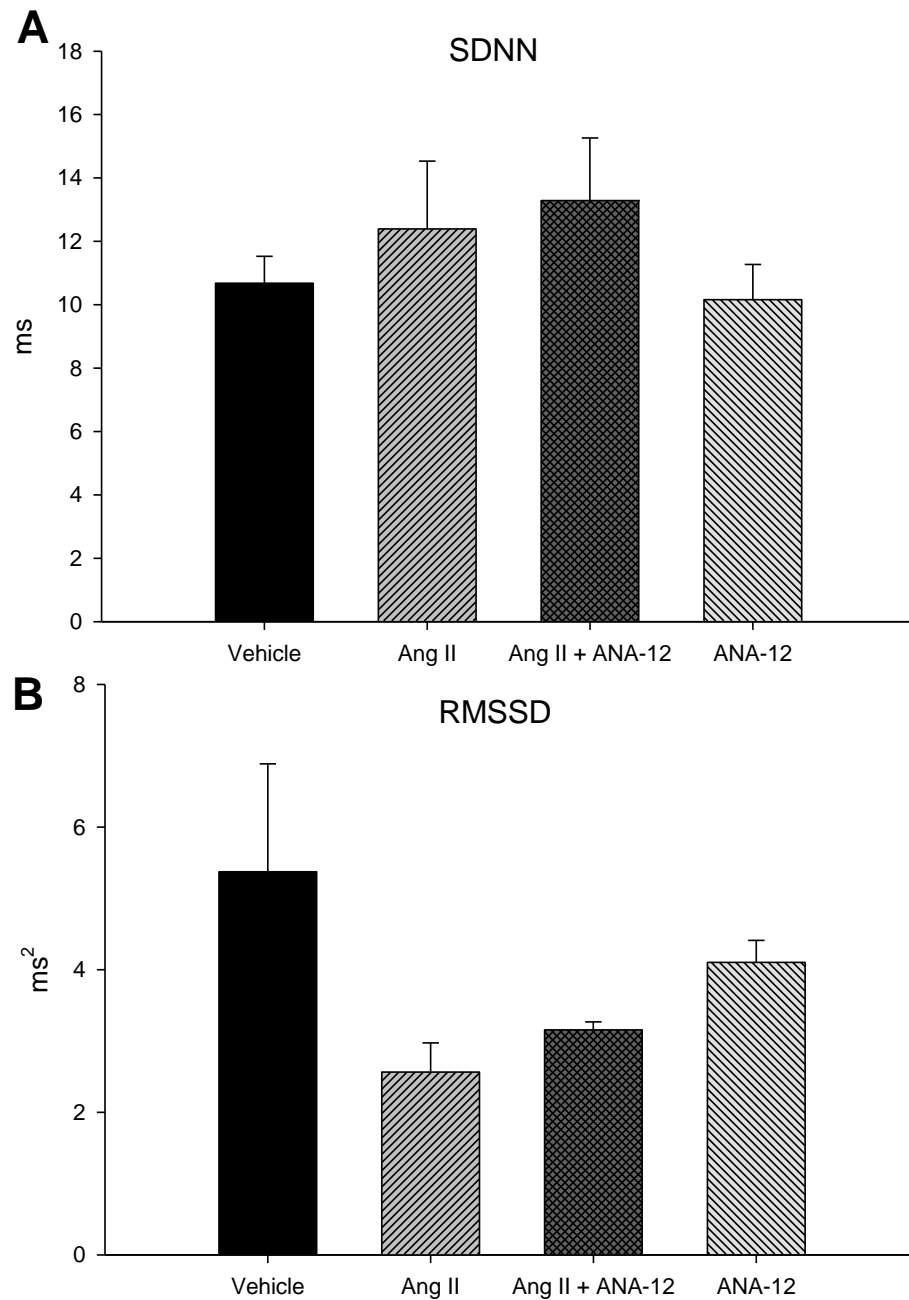


Figure 29 - Heart rate variability parameters following ICV Ang II

SDNN (A) and RMSSD (B) parameters following ICV infusion of Ang II with or without coinfusion of ANA-12. No significant differences were observed by one-way ANOVA. n = 4/group.

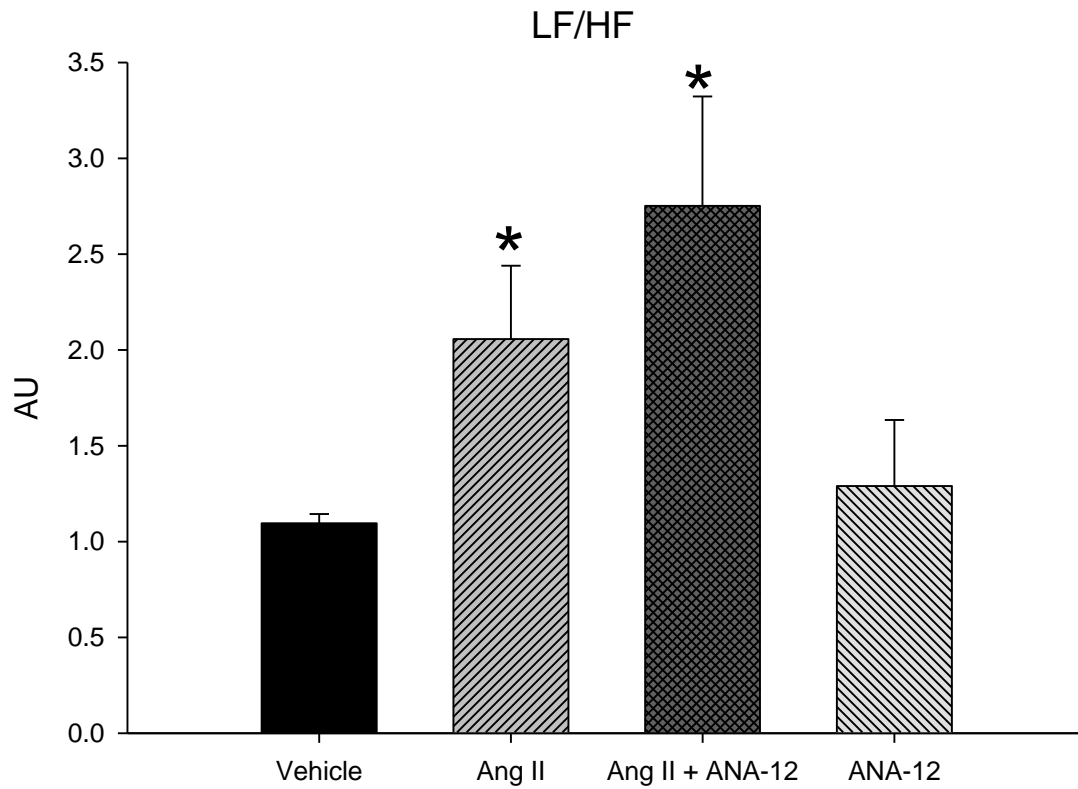


Figure 30 - Frequency domain analysis following IVC Ang II

Low frequency (0.06-0.7 Hz) / high frequency (0.7-3.0 Hz) ratio is elevated following Ang II infusion ICV. Coinfusion of ANA-12 has no effect on attenuating the LF/HF ratio. * $P < 0.05$ vs. Vehicle; $n = 4/\text{group}$.

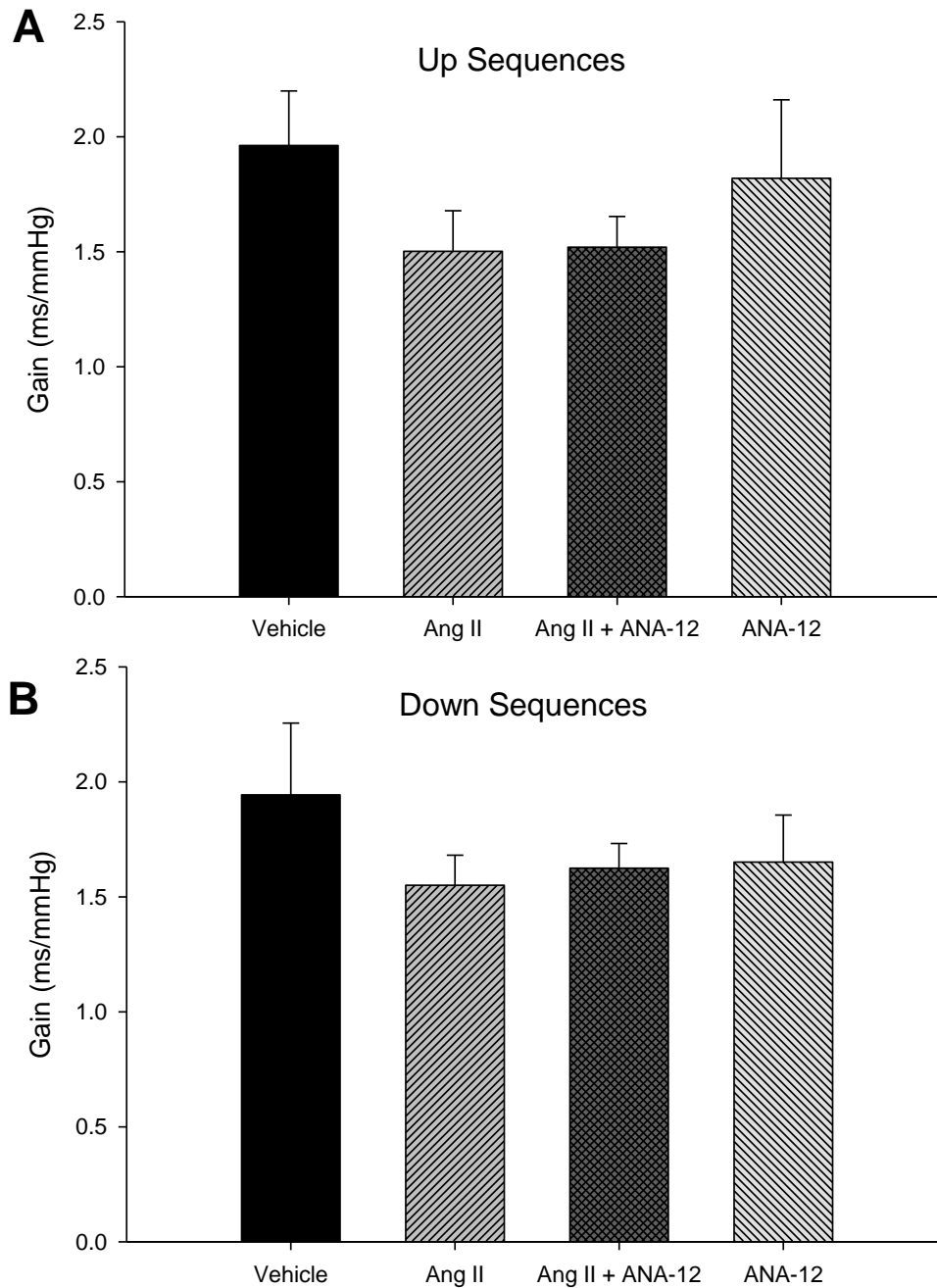


Figure 31 - Spontaneous baroreflex sensitivity following ICV Ang II.

No significant changes to either the up sequences (A) or down sequences (B) baroreflex gain following ICV Ang II with or without coinfusion of ANA-12. No group interaction as measured by one-way ANOVA; $n = 5/\text{group}$

ICV Ang II and ANA-12 Alter Metabolic Balance

Following ICV Ang II, daily water intake dramatically increased over the course of the two weeks of infusion to levels approximately 4-5 times the baseline daily intake by the end of the two-week infusion (Figure 32). Concurrent with the dipsogenic response, daily urine output also increased (Figure 32). Coinfusion of ANA-12 with Ang II augmented these responses in the early period of 2-8 days post infusion resulting in rats with 5 times the daily water intake by day 2 of infusion. Rats receiving ICV Ang II also demonstrated a lack of appetite with a decrease in daily food intake and fecal output (Figure 33). Coinfusion of ANA-12 with Ang II reversed the suppression of appetite as compared to IVC Ang II alone. ANA-12 alone or vehicle had no effect on water intake, urine output, food intake, or fecal output over the course of the ICV infusion.

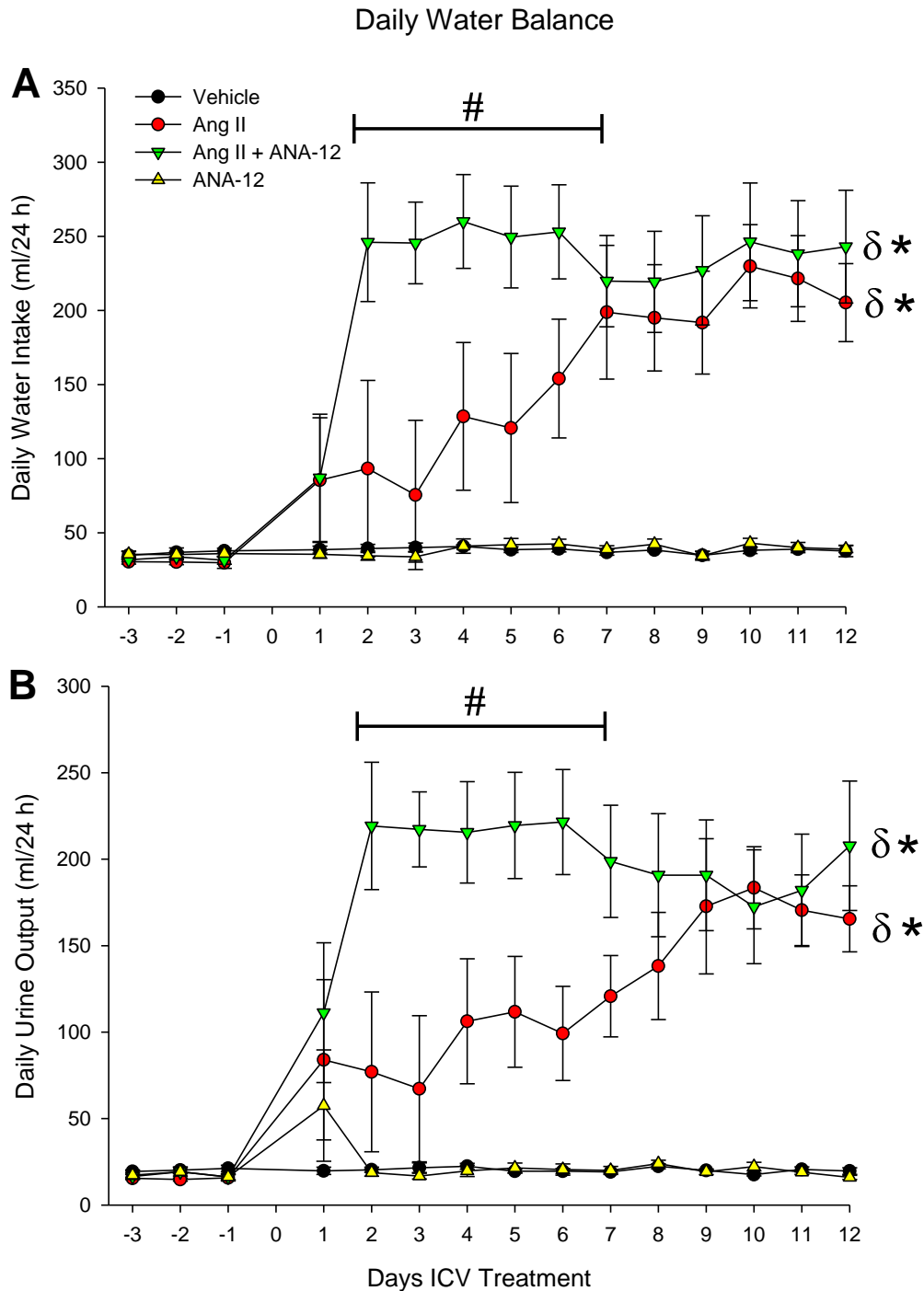


Figure 32 - Water balance following ICV Ang II.

ICV Ang II increased water intake (A) and urine output (B) and this effect was potentiated by coinfusion of ANA-12. RM-ANOVA; $\delta P < 0.05$ relative to respective baseline; $*P < 0.05$ vs. Vehicle; $\#P < 0.05$ vs. Ang II; $n = 4/\text{group}$.

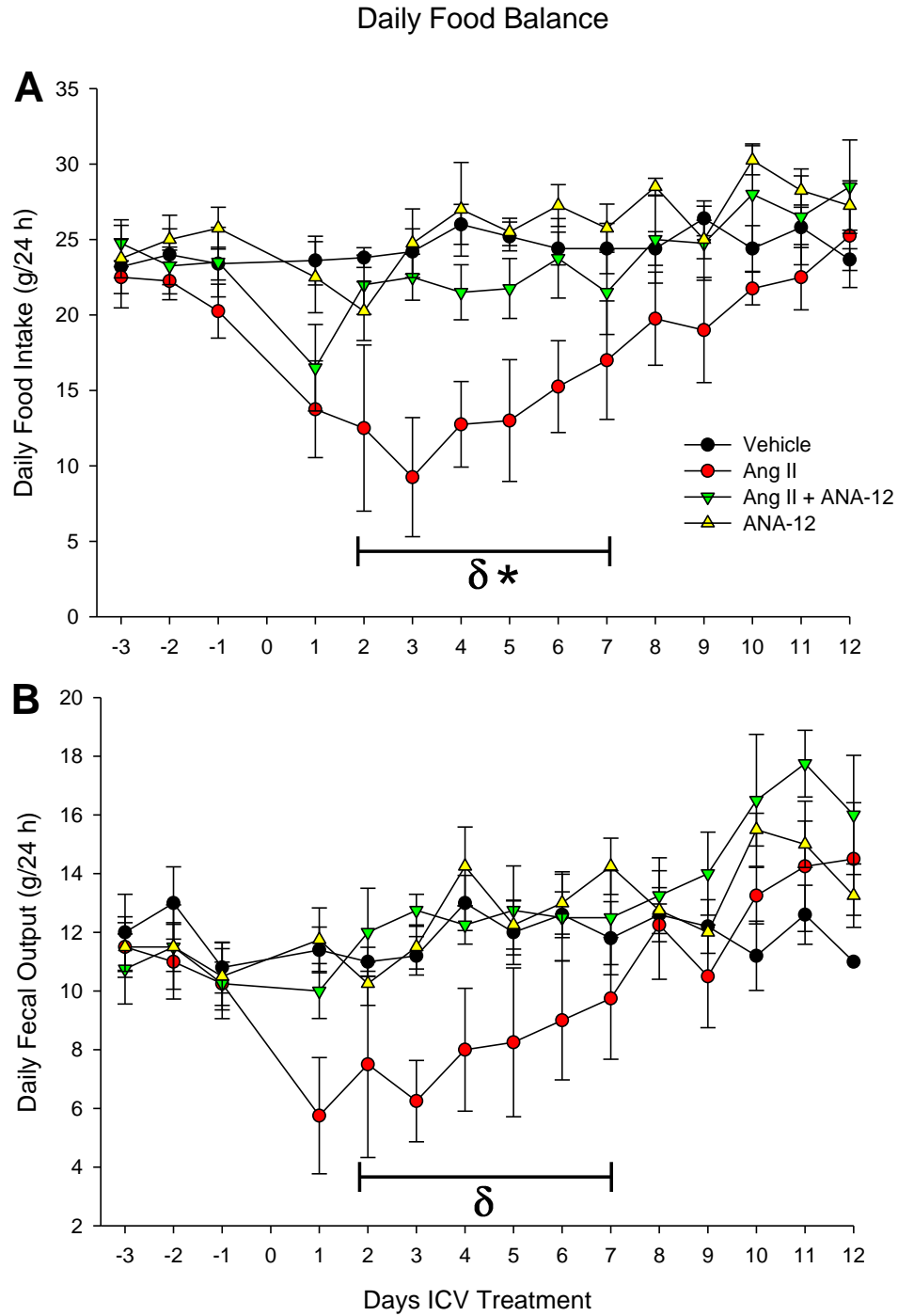


Figure 33 - Daily food balance following ICV Ang II.

ICV Ang II decreased food intake (A) and fecal output (B) and coinfusion of ANA-12 prevented this decreased appetite. RM-ANOVA; δ $P < 0.05$ Ang II relative to baseline; $n = 4/\text{group}$.

Acute Experiments Following ICV Ang II

Toward the end of the ICV infusion duration (day 12-13) rats were anesthetized and instrumented for measurement of baroreflex sensitivity and RSNA.

Rats given Ang II ICV exhibited baroreflex dysfunction with a blunted heart rate range compared to vehicle controls and max gain. Ang II + ANA-12 did not restore HR baroreflex range but improved max gain. ANA-12 alone had no effect on either parameter compared to vehicle (Figure 34 and Table 6). Baroreflex control of RSNA exhibited a trend toward a blunted range, and max gain was significantly blunted in Ang II treated animals compared to vehicle controls. Ang II + ANA-12 restored RSNA range and max gain compared to Ang II alone. ANA-12 alone had no effect compared to vehicle controls (Figure 35 and Table 6).

Resting RSNA levels were significantly elevated in ICV Ang II rats compared to vehicle controls. Coinfusion of ANA-12 with Ang II attenuated the increase in RSNA. ANA-12 alone had no effect on RSNA as compared to control (Figure 36-Figure 37).

Table 5 - Left Ventricular Hemodynamic Parameters

	Vehicle	Ang II	Ang II + ANA-12	ANA-12
n	3	4	4	3
Max Pressure (mmHg)	120.6 ± 7.6	144.3 ± 11.8	125.3 ± 11.4	126.3 ± 10.2
Min Pressure (mmHg)	1.3 ± 1.6	0.1 ± 0.9	2.7 ± 0.4	4.7 ± 1.0#
EDP (mmHg)	4.6 ± 1.6	5.9 ± 0.5	6.0 ± 0.4	8.7 ± 1.1
Mean Pressure (mmHg)	54.6 ± 3.7	54.7 ± 3.0	55.0 ± 4.7	62.1 ± 9.0
Max-Min Pressure (mmHg)	119.3 ± 8.2	144.2 ± 12.7	122.5 ± 11.3	121.6 ± 9.6
Systolic Duration (ms)	74.7 ± 1.9	72.5 ± 2.6	71.1 ± 3.7	77.0 ± 3.4
Diastolic Duration (ms)	71.1 ± 2.8	98.9 ± 6.1*	75.6 ± 5.0	71.3 ± 8.5#
Cycle Duration (ms)	145.8 ± 4.1	170.5 ± 2.8*	146.8 ± 6.4	148.1 ± 8.0#
Heart Rate (bpm)	413 ± 12	366 ± 3	414 ± 19	414 ± 23
Max dP/dT (mmHg/s)	7564 ± 1043	10449 ± 1599	8934 ± 1256	9514 ± 1746
Contractility Index (1/s)	91.6 ± 7.4	127.8 ± 14.0	136.3 ± 28.1	118.6 ± 16.6
Min dP/dT (mmHg/s)	-9460 ± 1396	-8338 ± 1292	-10718 ± 2126	-12021 ± 1670
IRP Average dP/dT (mmHg/s)	-3844 ± 381	-3745 ± 138	-4094 ± 657	-5206 ± 1172
Tau (ms)	10.9 ± 0.6	18.3 ± 3.9	12.0 ± 2.6	8.9 ± 1.4
Pressure Time Index (mmHg·s)	7.08 ± 0.30	7.78 ± 0.32	6.97 ± 0.38	7.97 ± 0.91

EDP = End diastolic pressure; IRP = isovolumetric relaxation period; *P < 0.05 vs. Vehicle, #P < 0.05 vs. Ang II

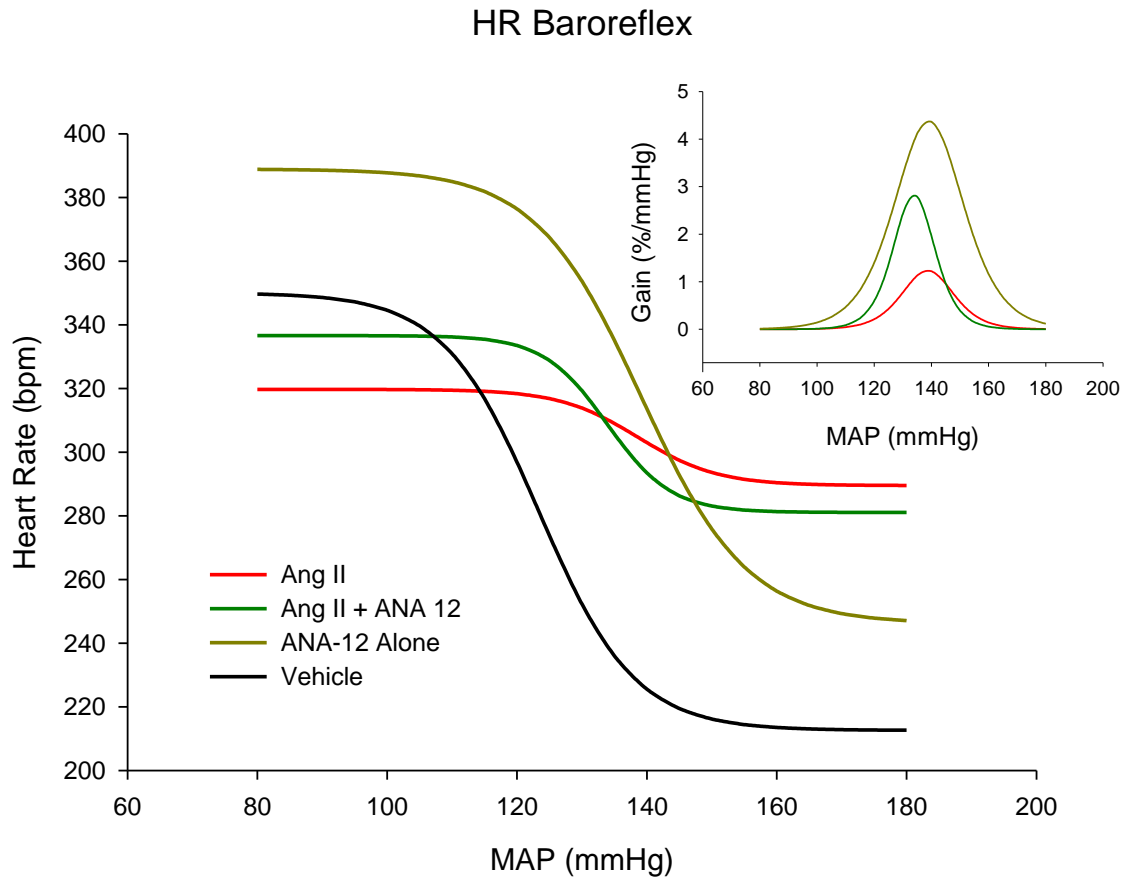


Figure 34 - Ang II blunts the HR baroreflex

Ang II blunted both the range and max gain of the HR response to changes in MAP. Coinfusion of ANA-12 improved the max gain, but failed to improve the range of the baroreflex response.

RSNA Baroreflex

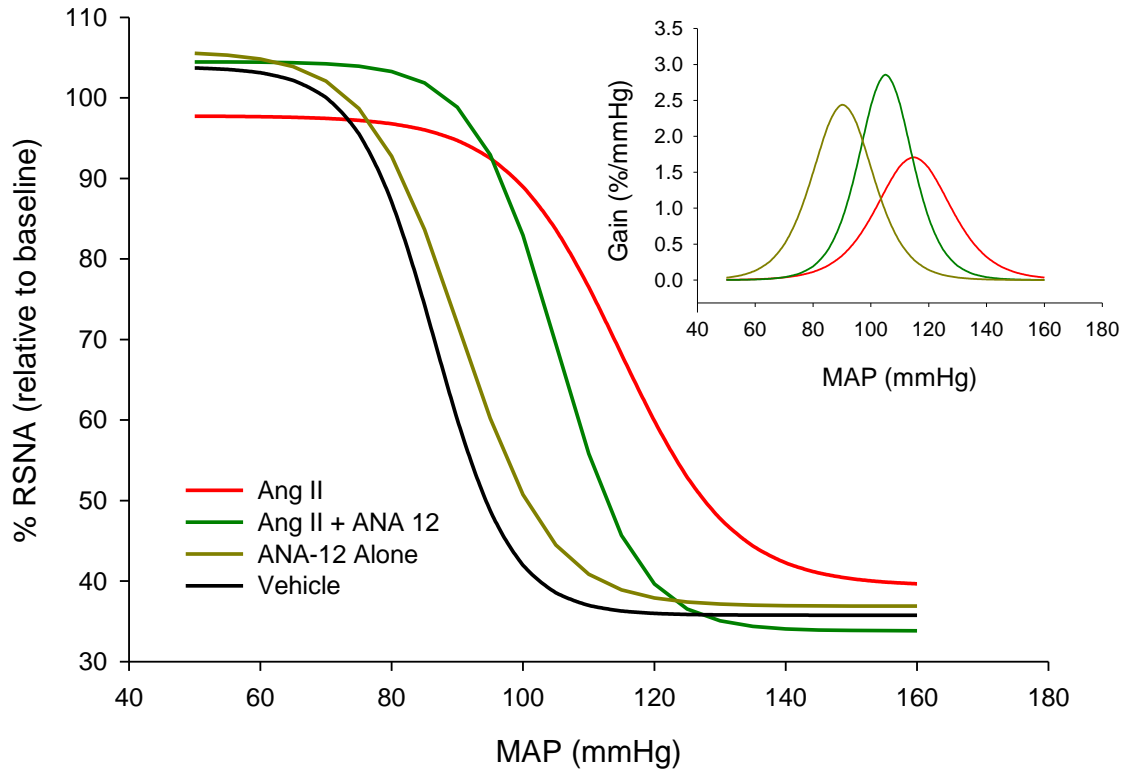


Figure 35 - Renal sympathetic nerve activity baroreflex following ICV Ang II

ICV Ang II caused a rightward shift and blunted max gain relative to vehicle. Coinfusion of ANA-12 improved the max gain of the RSNA response to changes in MAP and partially restored the shifted baroreflex.

Table 6 - Baroreflex parameters following ICV Ang ± ANA-12

	a, range (% or bpm)	x0, BP50 (mmHg)	y0, min (% or bpm)	Gmax (% or bpm/mmHg)
MAP-RSNA				
ICV Ang II	58.4 ± 10.7	114.7 ± 3.1*	39.4 ± 4.4	1.5 ± 0.2*
ICV Ang II + ANA-12	70.7 ± 13.5	105.1 ± 4.1	33.8 ± 8.0	2.8 ± 0.5†
ICV ANA-12	68.9 ± 2.9	90.3 ± 9.3	36.9 ± 4.4	2.4 ± 0.8
ICV Vehicle	68.1 ± 7.1	86.5 ± 7.3	35.8 ± 6.7	2.8 ± 0.2
MAP-HR				
ICV Ang II	30.2 ± 12.0*	138.7 ± 16.6	289.5 ± 19.0	1.0 ± 0.6*
ICV Ang II + ANA-12	55.6 ± 11.0	133.9 ± 4.2	281.0 ± 15.3	3.5 ± 1.5†
ICV ANA-12	142.8 ± 21.9	139.1 ± 7.0	246.1 ± 9.8	4.4 ± 1.0
ICV Vehicle	137.5 ± 21.7	123.4 ± 11.8	212.6 ± 18.5	4.2 ± 1.2

Values are mean ± SEM. a is the RSNA or HR range, x0 is the pressure at the midpoint of the range (BP50), y0 is minimum RSNA or HR and Gmax is the maximum gain of baroreflex curve. n = 4/group
 *, P < 0.05 relative to ICV Vehicle; †, P < 0.05 relative to ICV Ang II

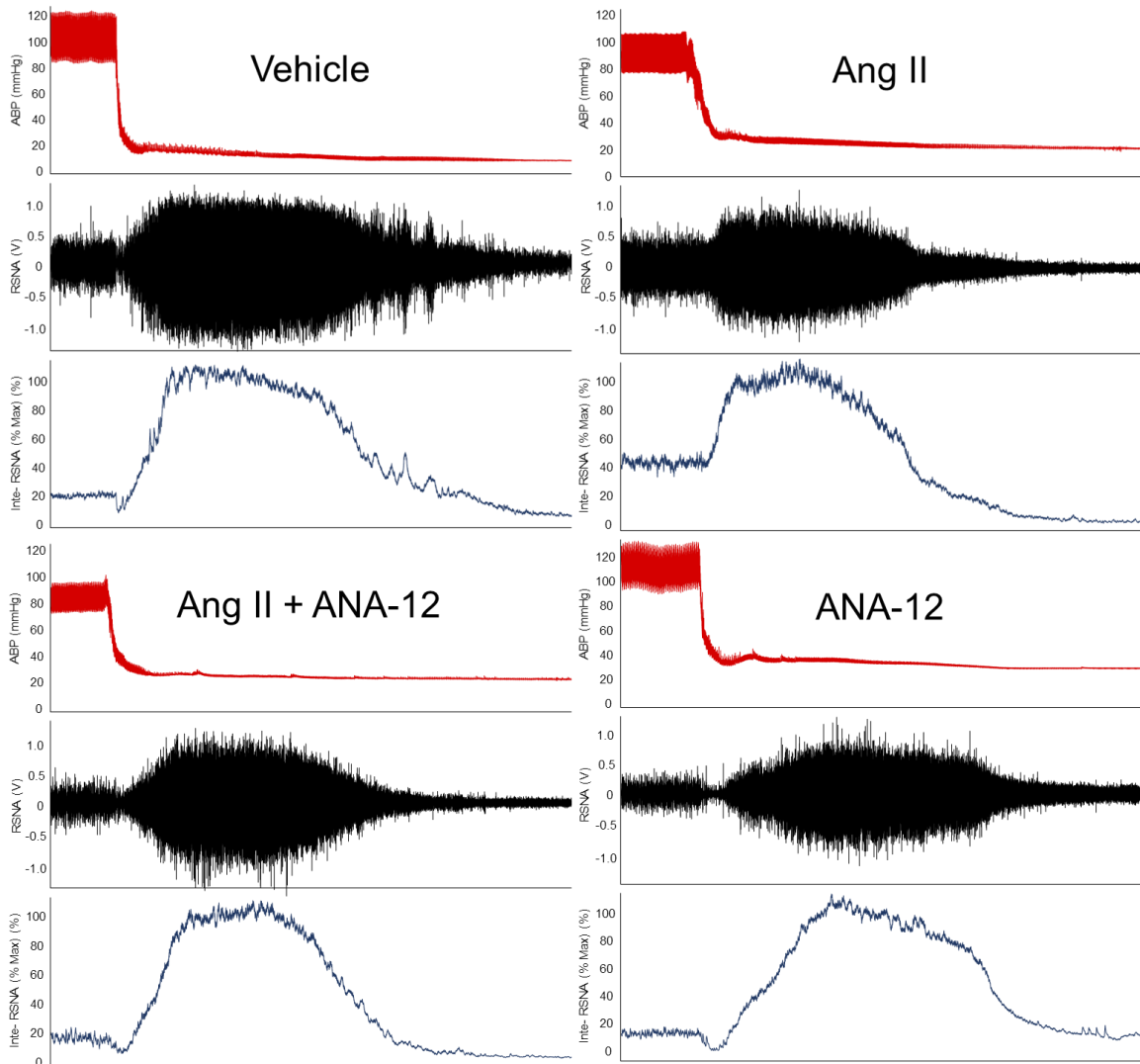


Figure 36 – Representative tracings of renal sympathetic nerve activity following Ang II or Ang II + ANA-12.

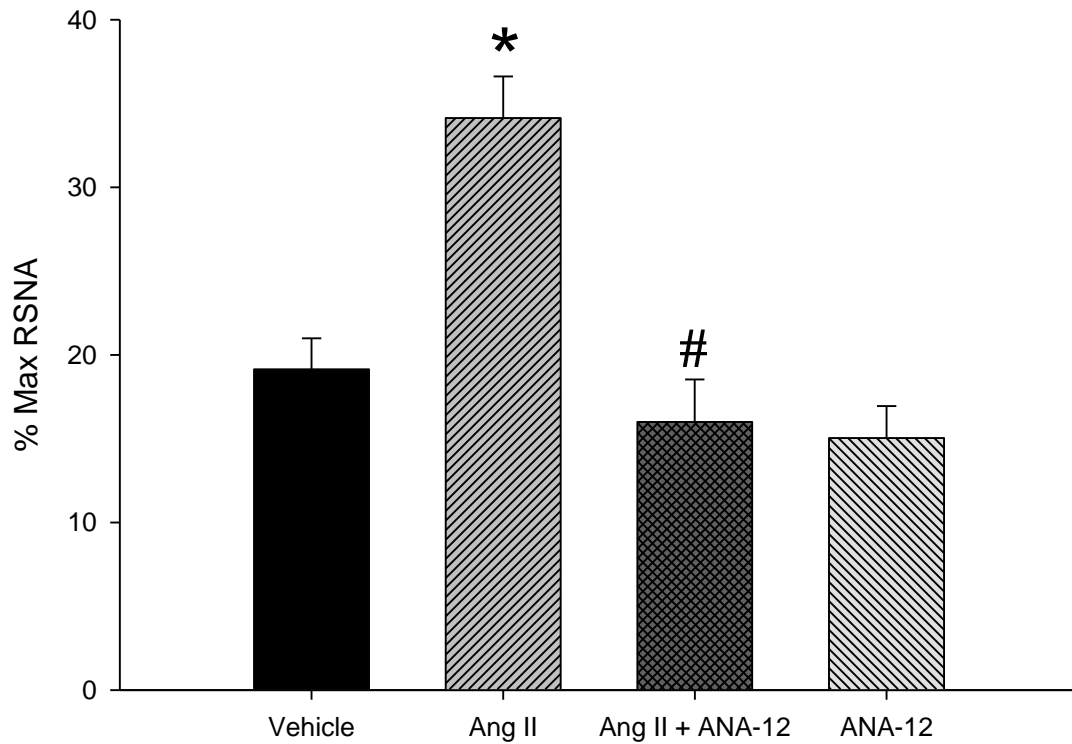


Figure 37 - Baseline renal sympathetic nerve activity following ICV Ang II

ICV Ang II increased RSNA as expressed as a % of maximum activity, and coinfusion of ANA-12 attenuated this increase. One-way ANOVA; *, $P < 0.05$ vs. Vehicle; #, $P < 0.05$ vs. Ang II. $n = 4/\text{group}$.

Body and Organ Weights Following ICV Ang II

Concomitant with the decrease in appetite as shown in Figure 33, rats receiving ICV Ang II had lower body weights as compared to vehicle controls (Table 7). Although ICV Ang II + ANA-12 animals did not exhibit an appreciable decrease in food intake, final body weight was significantly reduced compared to vehicle controls. Due to the drastic decrease in body weight of Ang II and Ang II+ANA-12 animals, many organs also were reduced in weight in terms of absolute weight or when normalized to tibia length. However, when organ weights were normalized relative to body weight, heart and wet lung weights trended toward an increase in Ang II treated animals, and both of these weight changes were attenuated by coinfusion of ANA-12. Interestingly, the spleen to body weight ratio dramatically decreased by approximately 30% relative to vehicle treated controls in Ang II rats and was not attenuated by coinfusion of ANA-12.

Table 7 - Final body and organ weights following ICV treatment

	Vehicle	Ang II	Ang II + ANA-12	ANA-12
n	4	4	4	4
Body weight (g)	480.0 ± 25.8	330.0 ± 28.5*	415.0 ± 11.5*#	502.5 ± 15.6#
Tibia (cm)	5.88 ± 0.03	5.80 ± 0.04	5.85 ± 0.03	5.85 ± 0.07
Heart weight (mg)	1571.7 ± 115.1	1257.0 ± 81.1	1361.5 ± 71.9	1555.5 ± 14.6
HW/BW	3.3 ± 0.2	3.8 ± 0.1	3.3 ± 0.1	3.1 ± 0.1#
HW/TL	267.0 ± 18.8	216.9 ± 14.7	232.7 ± 12.4	266.0 ± 2.0
Wet Lung (mg)	2089.4 ± 89.4	1730.0 ± 76.6*	1580.5 ± 47.4*	1776.0 ± 25.2*
WL/BW	4.5 ± 0.4	5.4 ± 0.5	3.8 ± 0.1#	3.6 ± 0.1#
WL/TL	355.6 ± 16.5	298.5 ± 14.2*	270.3 ± 9.0*	303.7 ± 4.8
Spleen (mg)	960.0 ± 46.9	435.1 ± 58.9*	471.4 ± 41.2*	800.4 ± 32.8
S/BW	1.9 ± 0.2	1.3 ± 0.1*	1.1 ± 0.1*	1.6 ± 0.1
S/TL	162.7 ± 8.0	75.2 ± 10.4*	80.6 ± 7.2*	137.0 ± 6.5
Liver (g)	17.7 ± 0.9	11.4 ± 1.2*	12.3 ± 1.1*	18.7 ± 0.8#†
L/BW	34.4 ± 1.2	35.2 ± 1.7	29.5 ± 2.0	37.2 ± 1.3†
L/TL	3.0 ± 0.2	2.1 ± 0.2*	2.1 ± 0.2*	3.2 ± 0.2#†
Left Kidney (mg)	1695.5 ± 17.0	1566.8 ± 97.8	1652.4 ± 118.8	2008.0 ± 63.7#
Right Kidney (mg)	1660.9 ± 24.0	1591.5 ± 99.4	1722.0 ± 105.3	2043.6 ± 72.9#

BW = body weight; HW = heart weight; TL = tibia length; S = spleen; L = liver; *P < 0.05 vs. Vehicle, #P < 0.05 vs.

Ang II; †P < 0.05 vs. Ang II + ANA-12 one-way ANOVA

DISCUSSION

The major findings of the current study are that TrkB antagonism by ANA-12 attenuated the increased MAP, RSNA, and baroreflex dysfunction caused by central Ang II signaling. Other important findings include a potentiated dipsogenic and polyuric response to ICV Ang II by coinjection of ANA-12 and decreased appetite and cachexia caused by central Ang II infusion. These *in vivo* observations implicate the importance of BDNF/TrkB signaling in Ang II-induced sympatho-excitation and suggest potentially disparate signaling mechanisms involved in sympathetic control vs. thirst/metabolic balance under central Ang II.

First, that BDNF/TrkB signaling is important in mediating the sympatho-excitation following ICV Ang II is in agreement with our *in vitro* observations of Ang II-induced increases in BDNF expression and the BDNF-mediated decrease of K⁺ currents (Becker *et al.*, 2015). Because antagonizing TrkB with ANA-12 attenuates the increased MAP (Figure 27) and completely prevents the increased RSNA (Figure 37) following Ang II, we conclude that BDNF/TrkB signaling is an important component in Ang II-mediated sympatho-excitation. A previous report has indicated that overexpression of BDNF in the PVN is sufficient to induce hypertension (Erdos *et al.*, 2015) implicating BDNF signaling in presympathetic centers of the brain as being hypertensive, and acute injections of BDNF into presympathetic areas such as the RVLM in anesthetized rat preparations increases MAP (Wang & Zhou, 2002). However, *in vivo* interactions between BDNF and Ang II in promotion of sympathetic nerve activity are lacking. Here we extend these previous reports suggesting a sympatho-excitatory effect of BDNF and integrate BDNF/TrkB signaling with centrally mediated Ang II-induced sympathetic activity, which itself has long been appreciated (Zimmerman *et al.*, 2004; Patel & Zheng, 2011; Zucker *et al.*, 2012; Xiao *et al.*, 2013; Biancardi *et al.*, 2013).

ANA-12 was able to completely prevent the increase in RSNA caused by central Ang II; however, ANA-12 only partially attenuated the hypertensive response to Ang II and had no

measurable impact on LF/HF ratio or HR. One potential explanation for this disparity is the nature of the experimental preparation for each parameter. RSNA was measured in anesthetized animals at the very end of the infusion period whereas LF/HF ratio and HR were measured in conscious animals over the course of the infusion time. The effect of ANA-12 could be washed out by the involvement of higher centers' influence on these conscious parameters. The effect of Ang II may also be disparate across different sympathetic nerve beds. The renal sympathetic bed may be more directly influenced by an Ang II-BDNF interaction than the cardiac sympathetic bed, which would result in an observable difference in RSNA, but not HR or markers of HRV. Vasomotor sympathetic tone may be under mixed influence from BDNF-dependent and BDNF-independent presympathetic centers thus antagonism of TrkB may only partially prevent an Ang II-induced hypertensive response. We are unable to directly elucidate the answers to these questions from the current study, and future work will be important in exploring the particular autonomic centers impacted by an Ang II-BDNF signaling mechanism. In a salt-loaded model, previous studies have found that renal denervation blunts the hypertensive response of ICV Ang II (Osborn & Camara, 1997). Thus the renal nerves may play a predominant role in mediating central Ang II-induced hypertension, and RSNA may be preferentially activated relative to other sympathetic nerve beds.

Central administration of Ang II is well known to evoke a potent and immediate drinking response (as comprehensively reviewed by Fitzsimons, 1998). This response is a primary, neurogenic dipsogenic response as adrenalectomized, hypophysectomized (Avrith *et al.*, 1980) or bilaterally nephrectomized rats (Avrith & Fitzsimons, 1980) still respond to bolus central injections of Ang II. Interestingly, in rats receiving 6 $\mu\text{g/h}$ (100 ng/min) in the lateral cerebral ventricle for 7 days, there was only a transient dipsogenic response that the authors speculated was due to thirst inhibition by the sustained increase in MAP (Dinicolantonio *et al.*, 1982). The dose used in the present study is lower than used by Di Nicolantonio *et al.* and displays a less drastic hypertensive response, which could explain the lack of a complete pressor-mediated suppression of Ang II-induced thirst. Furthermore, in animals receiving coinfusion of ANA-12, there is a more robust and

immediate increase in daily water intake following Ang II, suggesting a potential uncoupling of the inhibitory feedback control of Ang II-induced thirst. Previous studies investigating the influence of arterial pressure and baroreflex input on the dipsogenic response of central Ang II found a reciprocal relationship between MAP and central Ang II-induced thirst that was not affected by sino-aortic denervation indicating the relationship is baroreflex independent (Thunhorst & Johnson, 1993). Due to the observation that coinfusion of ANA-12 blunted the hypertensive response to central Ang II, this lower pressure would have reduced negative feedback on Ang II-induced thirst. Hence, it is likely that ANA-12 is predominately attenuating the increase in sympathetic tone following central Ang II and the potentiating effect on thirst is a secondary response to attenuated MAP. Although there was an initial potentiation of thirst by coinfusion of ANA-12 with Ang II, both groups exhibited similar drinking behavior by the end of the 12 day infusion protocol. To our knowledge few studies have investigated this relationship for longer infusion periods as most studies are acute or conclude by day 7 of ICV infusion. The convergence of drinking behavior at the later stages of infusion suggests a withdrawal of the pressure-mediated inhibition of drinking and provides observations warranting further study in long-term, chronically instrumented animals.

We observed baroreflex dysfunction in both the Ang II and Ang II + ANA-12 groups. Previous work has implicated central Ang II signaling in baroreflex dysfunction (Gao *et al.*, 2005b, 2014; Pan *et al.*, 2007) particularly through its action on the AT1R and promotion of sympatho-excitation in presympathetic areas such as the PVN and RVLM. Here we also observed baroreflex dysfunction following central Ang II, and coinfusion of ANA-12 had modest improvements on a number of baroreflex parameters. It is unclear however, if ANA-12 itself had an effect on mediating baroreflex sensitivity or if improvements to the baroreflex were secondary to improvements in sympathetic tone and MAP. As hypertension itself promotes baroreflex dysfunction through resetting and shifting response curves to higher pressures (Gao *et al.*, 2005b; Pan *et al.*, 2007; Yamamoto *et al.*, 2013) and blunting sensitivity, the baroreflex dysfunction observed in our hands in the current study could be explained as a secondary result of the increased MAP and sympathetic

outflow. Accordingly, the reduction in sympathetic tone and MAP by coinfusion of ANA-12 also attenuated the rightward shift of the baroreflex.

The direct effects of ANA-12 on modulating the baroreflex through its actions on central autonomic neurons cannot be excluded. As we demonstrated in the previous chapter, ANA-12 in the dmNTS inhibits baroreflex function, a finding that appears in conflict with the results presented here. An important distinction between these two studies is the route of ANA-12 delivery. In the preceding chapter, ANA-12 was directly microinjected into the dmNTS thereby isolating its effects to a specific, sympatho-inhibitory autonomic center. Conversely, in the present study, ANA-12 was infused ICV and would likely affect multiple autonomic centers and particularly the presympathetic areas of the SFO and PVN, which are sensitive to factors circulating in the CSF (Buggy *et al.*; Mangiapane & Simpson, 1980; Fitzsimons, 1998). These sites also contain a high concentration of AT1R making them likely targets for the action of ICV Ang II (Song *et al.*, 1992; Lenkei *et al.*, 1997; Allen *et al.*, 2000). Therefore the predominant actions of ICV infusion of Ang II and ANA-12 are on control of neuronal activity of these presympathetic sites, and less likely through actions on areas such as the NTS. Furthermore, the SFO, PVN, and RVLM are autonomic integration sites that provide excitatory neuronal output toward the sympathetic nervous system, with the PVN and RVLM possessing direct neuronal projections to the IML. Thus even if central Ang II and ANA-12 have an effect on NTS or other higher order neurons, the effect may be buffered by the direct effects on these autonomic centers with direct outflow to the peripheral sympathetic nervous system. The effects of ANA-12 on baroreflex function are therefore mostly due to sympathetic withdrawal from direct actions on sites such as the SFO, PVN, and RVLM and less likely due to effects on higher order neurons such as the NTS.

Another observation from this study is the marked cachexia and appetite suppression following ICV Ang II. Peripheral Ang II signaling results in cachexia through direct actions on skeletal muscle and activation of neurohumoral factors (Brink *et al.*, 1996, 2001). The central actions of Ang II on metabolic state, appetite, and muscle wasting are less known; however,

previous work with ICV Ang II infusion also demonstrated a decrease in appetite and severe fat and muscle tissue wasting concurrent with a decrease in orexigenic peptides such as neuropeptide Y and orexin in the hypothalamus (Yoshida *et al.*, 2012). The present study demonstrates a similar finding with a robust decrease in body mass and food intake following ICV infusion of Ang II. Interestingly, coinfusion with ANA-12 prevented the depressed appetite of Ang II and attenuated the decrease in body mass relative to Ang II alone, but did not normalize body mass to that of vehicle controls. This indicates that BDNF/TrkB signaling may be involved in the appetite suppressant actions of central Ang II, but may only be partially effective in reducing the sympathetic-driven cachexia (Hryniewicz *et al.*, 2003; Laviano *et al.*, 2008).

Consistent with a decrease in total body mass, most organ masses were reduced following ICV Ang II or Ang II + ANA-12 (Table 7). When normalized to body mass, most organ masses were similar across groups with the noticeable exception of spleen mass. Spleen to body mass ratio was decreased in both Ang II and Ang II + ANA-12 rats. In the salt-Ang II model of neurogenic hypertension, splanchnic sympathetic nervous system activity is thought to invoke a robust constriction of splanchnic veins and arteries, decreasing splanchnic and vascular capacitance promoting hypertension (King *et al.*, 2007; Osborn *et al.*, 2011). Splanchnic sympathetic tone is robustly increased following Ang II and may explain the decreased spleen weight observed here. ANA-12 did not attenuate this decrease in spleen size, further suggesting that there is differential control between Ang II and BDNF/TrkB centrally in mediating different vascular and organ bed sympathetic activity. Further work will be required to elucidate the specific sites of action.

In conclusion, antagonizing BDNF/TrkB signaling with ANA-12 attenuated parameters of sympatho-excitation and hypertension following ICV Ang II infusion further implicating the necessity of BDNF/TrkB in mediating the neuronal effects of Ang II. ANA-12 however did not prevent all effects of ICV Ang II such as slight cachexia, decrease in spleen weight, and water balance, suggesting differential control of the Ang II – BDNF/TrkB axis in mediating various organ bed sympathetic tone, thirst, and metabolism.

DISCUSSION

Major Findings of the Dissertation

The major findings of the dissertation are:

1. That Kv4.3 overexpression in the RVLM is sympatho-inhibitory (Chapter I).
2. That BDNF is a necessary component of the mechanism by which Ang II reduces K⁺ currents (Chapter II)
3. That BDNF is an important component in modulation of baroreflex function in normal physiological states (Chapter III).
4. That BDNF/TrkB signaling is reduced in the NTS in the CHF state resulting in central baroreflex dysfunction (Chapter III).
5. That BDNF/TrkB signaling is a necessary component in maintaining central Ang II-mediated hypertensive and sympatho-excitatory responses (Chapter IV).

In addition to these major findings, we have provided evidence supporting the previously observed reductions in Kv4.3 channel protein in the RVLM post-MI (Chapter I) (Gao *et al.*, 2010). We have also demonstrated that BDNF signaling is downstream of Ang II in mediating reductions in I_A, and requires p38 MAPK (Chapter II), that a reduction in TrkB expression in the dmNTS likely mediates blunted baroreflex sensitivity during CHF (Chapter III), and that in addition to the hemodynamic protection of antagonizing TrkB during central Ang II, ANA-12 blunts the depressed appetite and cachexia due to ICV Ang II.

Taken together, these findings indicate that **BDNF/TrkB signaling is important for the effects of Ang II on neuronal function in autonomic control centers of the brain in cardiovascular disease states such as CHF and hypertension**. Figure 38 presents an overview of the major findings and a proposed mechanism of Ang II/BDNF interaction in promoting sympatho-excitation.

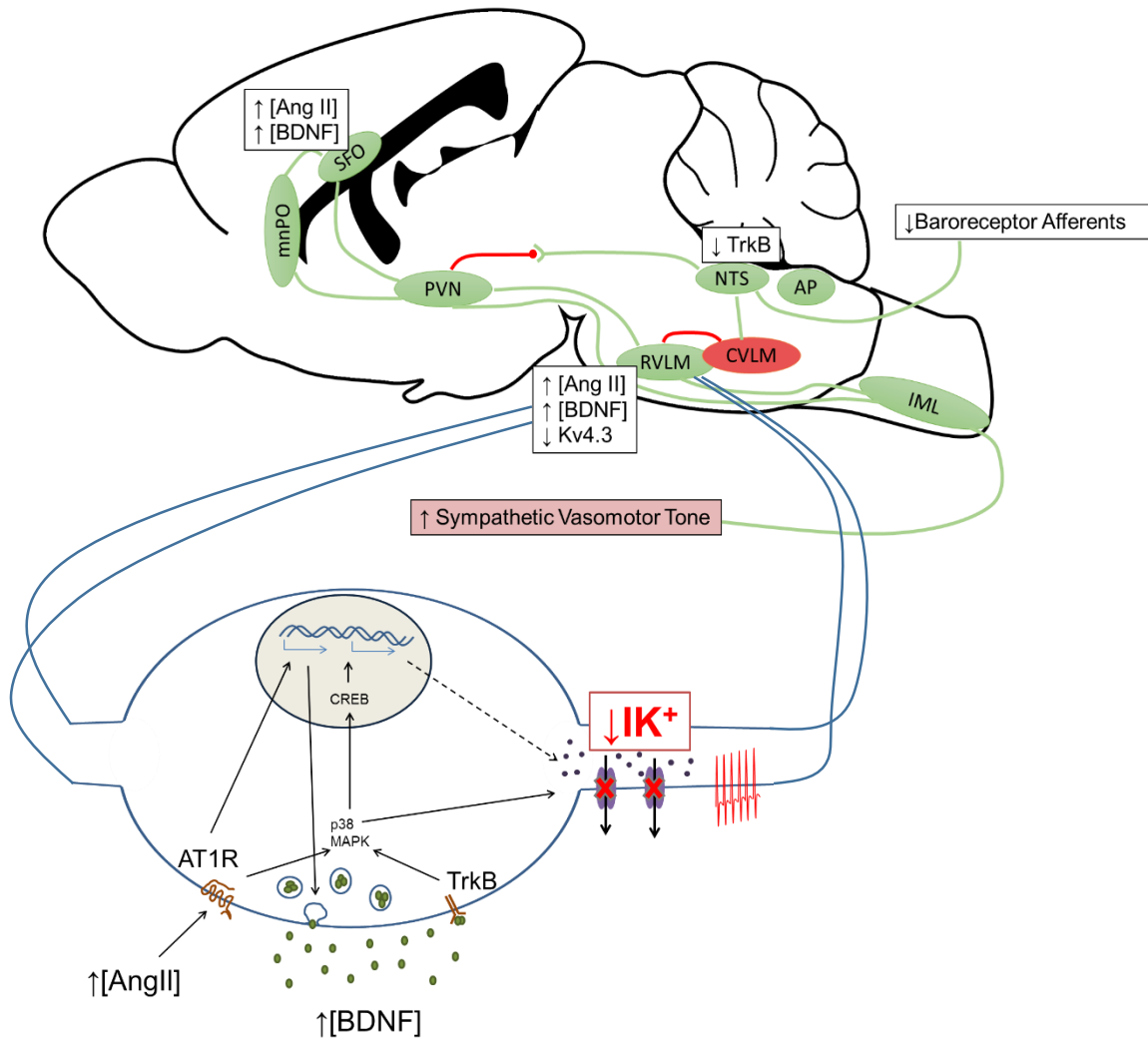


Figure 38 - Representative Diagram of the Major Findings of the Dissertation

(see text for details)

Objectives 1-2: BDNF and Potassium Currents

Similar to a previous study from this laboratory (Gao *et al.*, 2010) we have observed a decreased expression of Kv4.3 in the RVLM of rats post-MI (Figure 5). As Kv4.3 mediates I_A , it is likely that the decreased expression of this channel protein contributes to the sympatho-excitation in cardiovascular diseases such as CHF and hypertension. We demonstrated that overexpression of Kv4.3 in the RVLM attenuates the sympatho-excitation following MI (Figure 12), lending further support to the hypothesis that I_A is an important negative regulator of neuronal activity in presympathetic neurons of the central nervous system. However, these results are based on the use of moderately-infarcted groups of rats, and may not be representative of CHF. Further work will be necessary to confirm the beneficial effects of Kv4.3 expression in the RVLM by use of confirmed and well-defined CHF models.

The effects of BDNF in the hippocampus and other tissues have been well studied including the ability of BDNF to modulate K^+ currents (Chao, 2003; Benarroch, 2015). BDNF/TrkB and Ang II/AT1R signaling share many secondary messengers including PKA, MAPK/ERK (York *et al.*, 1998; Chan *et al.*, 2005, 2007; Park & Poo, 2012; Xiao *et al.*, 2013), CAMKs (Sun *et al.*, 2003; Caldeira *et al.*, 2007; Minichiello, 2009), suggesting a potential for convergent signaling of both Ang II and BDNF. Furthermore, MAPK/ERK directly phosphorylates Kv4.2 (Adams *et al.*, 2000), and the CamKII-MAPK pathway destabilizes Kv4.3 mRNA (Zhou *et al.*, 2012) suggesting that these points of convergence are important in modulating I_A .

Here, we demonstrate, for the first time to our knowledge, that BDNF is an important mediator of the effects of Ang II on reducing I_A (Figure 16) thus linking the BDNF and Ang II pathways in modulation of neuronal K^+ currents. This connection appears to be unidirectional in that Ang II signaling increases BDNF expression as blocking the action of BDNF attenuated the Ang II-induced reductions in K^+ currents, but AT1R blockade had no effect on the ability of BDNF to suppress K^+ currents (Figure 17). Our experiments would then suggest that BDNF expression

and activity is a result of Ang II signaling and that the effects of BDNF are independent of Ang II. Interestingly, *in vivo* work done recently by Erdos et al. (2015) suggests that BDNF signaling in the PVN increases local RAS activity. A potential explanation is the inherent difference in experimental design. We investigated the effects of BDNF and Ang II on K⁺ currents in an *in vitro* cell culture line, whereas Erdos et al. overexpressed BDNF in a presympathetic nucleus in an intact animal. Although there are scattered reports of spontaneous APs firing from CATH.a cells (Du *et al.*, 2004), in our hands we have not been able to observe either spontaneous or current infused APs from CATH.a cells. This limits our ability to draw conclusions about the activity-dependent modulation of signaling processes. One potential explanation for the observation of Erdos et al. that BDNF potentiated AT1R signaling could be that increased neuronal activity (i.e. increased AP frequency) mediated by BDNF caused differential expression of the local RAS. The expression of BDNF is under potent activity-based control (Nagappan & Lu, 2005; Rothman & Mattson, 2012), and it would be an exciting observation that the RAS may likewise be modulated by changes to neuronal activity. Our cell culture model is limited in this regard; however, this limitation itself provides an opportunity for conclusions to be made about the regulation of BDNF expression. Devoid of observable changes to neuronal activity, we still observed an increased BDNF expression following Ang II treatment indicating that BDNF expression may be under control of Ang II signaling. The potential of the neuronal RAS to be under activity-dependent control and the particular transcriptional regulation of Ang II-induced BDNF expression warrant future study and will be exciting avenues for further understanding the role Ang II and BDNF play in mediating presympathetic neuronal activity.

Future work will be important in continuing the initial observations made in this dissertation. As we have shown that BDNF is a component of the Ang II-mediated decrease in K⁺ currents, that Kv4.3 is important in limiting the sympatho-excitation following MI, and that antagonizing TrkB blunts the effects of ICV Ang II (Chapter IV), it will be important for future work to specifically target presympathetic areas such as the RVLM, manipulate the activity of

BDNF and the RAS *in vivo*, and measure its effects on I_A . Such work could include studies overexpressing dominant-negative TrkB mutants in the RVLM of rats with CHF and evaluating changes to the hemodynamic state and sympathetic nervous system. We have demonstrated that p38 MAPK is needed to mediate the effects of BDNF on K^+ currents (Figure 18), but future work is needed to investigate other areas of BDNF and AT1R convergence such as CaMK, or to determine if reactive oxygen species play a role in mediating BDNF expression or BDNF-mediated reductions in I_A . We have demonstrated the effects of Ang II and BDNF on cultured neuron-like cells; however, future work using brain slice or acutely dissociated central neurons will be instrumental in better understanding of the role of Ang II-BDNF interactions in primary neurons.

Objective 3: BDNF in Baroreflex Control

Because baroreflex dysfunction is a common observation during CHF, we explored the hypothesis that BDNF/TrkB signaling is involved in mediating the central desensitization of baroreflex function in a rat model of CHF. The implications of this study are two-fold. First, we observed a previously undescribed role for BDNF in the dmNTS mediating the baroreflex in normal (sham CHF) physiological conditions. Of particular interest was the observation that ANA-12 evoked a pressor and sympatho-excitatory response in sham animals, suggesting that endogenous BDNF signaling in the dmNTS exerts a tonic, sympatho-inhibitory role. Antagonizing TrkB in the dmNTS also blunted baroreflex-mediated decreases in HR and RSNA following increased pressure. The role of BDNF in the dmNTS mediating sympathetic nerve activity and baroreflex control has not previously been observed and provides a novel area for future research. Future experiments will be required to elucidate the precise actions of BDNF in the dmNTS such as whether it plays a role in mediating glutamatergic or GABAergic signaling, if the effects are mediated by projections to the CVLM, PVN, or other autonomic control centers, and if the effects of BDNF are due to acute changes to NMDA receptors, Na^+ channels, or other receptors and ion

channels. Future imaging studies and pharmacological manipulation will be instrumental in exploring these questions.

Second, these studies uncovered BDNF/TrkB dysfunction in the dmNTS in CHF and provide a novel explanation for baroreflex desensitization in the CHF state. Through a reduction in TrkB expression, both the effects of exogenous BDNF microinjection and ANA-12 inhibition of endogenous BDNF signaling were blunted in CHF rats. Similarly, as these rats already possessed blunted baroreflex responses, ANA-12 had little effect on further desensitization. This indicates that a reduction in BDNF/TrkB signaling in the dmNTS may be a causative factor for blunted baroreflex sensitivity in CHF. Similar to the future studies proposed above, in-depth analysis of the particular neuronal pathways involved and location of TrkB expression will be instrumental in further understanding of the mechanisms by which TrkB is reduced in CHF.

Objective 4: Central Ang II-induced Sympatho-excitation and BDNF

The first three objectives of this dissertation established a relationship between K⁺ channel dysfunction, Ang II, and BDNF. The goal of the final study was to incorporate Ang II and BDNF signaling in an *in vivo* approach. We found that antagonizing TrkB with ANA-12 attenuated many of the hemodynamic and sympatho-excitatory responses of ICV Ang II. This extends the findings of Chapter II into the animal model and demonstrates the involvement of BDNF in mediating many of the neuronal effects of Ang II.

Unexpected results of this study included a differential role for BDNF/TrkB signaling between the hemodynamic/sympatho-excitatory responses and the metabolic interaction with Ang II. Although ANA-12 attenuated the sympathetic nerve activity response to Ang II, it potentiated the dipsogenic and polyuric responses. As discussed in detail in Chapter IV, this may be due to the removal of pressure-mediated negative feedback on drinking, but the possibility of a differential signaling mechanism between presympathetic centers of the brain and osmosensitive areas cannot be excluded. Future work will be important in evaluating what nuclei are important in mediating

these effects. Overexpression and knockdown studies will be useful in determining the interaction between Ang II and BDNF/TrkB in specific nuclei such as the RVLM.

At present, we cannot conclude that the protective effects of ANA-12 on ICV Ang II are due to preserving K⁺ channels in the central nervous system. Molecular analysis is currently being carried out where we are examining Kv4.3 expression, phosphorylated-TrkB, and total TrkB in brain areas such as the RVLM, PVN, NTS, and OVLT. These results will further expand our understanding of the interaction between Ang II and BDNF in modulating sympathetic nerve activity.

ICV Ang II resulted in impaired baroreflex function as measured in the acute anesthetized preparation. Although ANA-12 seemed to have a tendency toward attenuating this dysfunction it was still significantly impaired. In light of the work presented in Chapter III, ANA-12 given ICV may not restore baroreflex dysfunction as blocking TrkB in the dmNTS itself blunts baroreflex sensitivity. Some of the improvement may be due to withdrawal of activity from presympathetic areas such as the RVLM, but confounding interactions due to actions at the dmNTS may prevent robust improvements in baroreflex function.

Conclusions and Perspectives

The overall conclusions of the work presented in this dissertation are that BDNF is an important component in the Ang II-mediated effects on K⁺ currents, sympathetic nerve activity, and baroreflex function. The Ang II-induced expression of BDNF observed in cultured CATH.a cells, and the resulting effects of BDNF in suppressing K⁺ currents provide a pathway by which K⁺ current suppression may occur in presympathetic neurons increasing sensitivity and AP frequency. Consistent with this notion, ICV Ang II increased MAP and sympathetic nerve activity, which were attenuated by TrkB antagonism. The effects of ICV Ang II and ANA-12 on K⁺ channels has yet to be established.

Along with its sympatho-excitatory effects, BDNF plays a role mediating sympatho-inhibition and baroreflex function in the dmNTS. These disparate effects of BDNF may appear to be conflicting. How can BDNF/TrkB signaling be both sympatho-excitatory and sympatho-inhibitory at the same time? The answer likely comes by examining the nature and function of the particular neuronal pathway in question. When acting predominately through sympatho-excitatory areas as is likely in ICV infusion, BDNF sensitization of neurons and neuronal pathways results in a sympatho-excitatory physiological response. However, when acting through sympatho-inhibitory areas such as the dmNTS, BDNF sensitization of neurons results in an overall sympatho-inhibitory physiological response. The effects of BDNF/TrkB on the particular neuron are the same (excitation) but the resulting integrative physiological outcome is quite different.

Broader speculation over this point could suggest BDNF is simply serving a similar purpose in autonomic networks as it has long been appreciated to play in hippocampal networks associated with LTP and memory formation (Yamada *et al.*, 2002; Lynch *et al.*, 2004; Bramham & Messaoudi, 2005). Although instead of forming cognitive memories through LTP of synaptic pathways in the hippocampus, here it serves to promote a “sympatho-excitatory memory” through potentiation of presympathetic neuronal pathways. Neuronal pathways sensitive to Ang II signaling either through direct Ang II-mediated transcriptional increases in BDNF expression, Ang II-mediated increases in neuronal activity (such as reactive oxygen species signaling acute alterations of ion currents), or a combination thereof would thus increase their “sympatho-excitatory memory.” The effects of this could be multifaceted. It would lead to initial increases in sympatho-excitation through direct activation of sympathetic pathways, but the formation of the “sympatho-excitatory memory” would result in a long-term, sensitized sympathetic pathway. Although broadly speculative, this idea has some experimental support. Recent work from Johnson and co-workers has shown a sensitized Ang II response following a so-call “sub-pressor” dose of Ang II or aldosterone. Subsequent infusions of Ang II were exaggerated in animals that received the prior doses suggesting a sensitization of sympathetic pathways (Xue *et al.*, 2012a, 2012b; Clayton *et al.*,

2014). Furthermore, the most recent of these studies observed an increase in the expression of pro-BDNF and BDNF in lamina terminalis, implicating its involvement in the sensitization pathway, or “sympatho-excitatory memory” (Clayton *et al.*, 2014).

Because baroreceptor afferent discharge is reduced during CHF (Niebauer & Zucker, 1985; Niebauer *et al.*, 1986; Wang *et al.*, 1991), NTS neurological input would be reduced. This reduction in activity would lead to a decrease in the baroreflex arc “memory” consistent with our observations of decreased expression of TrkB and decreased ability of BDNF or ANA-12 to evoke a physiological response. This would account for the disparate effects and roles of BDNF across separate autonomic pathways. Not only would BDNF potentiate the “sympatho-excitatory memory” but reductions in activity through sympatho-inhibitory pathways such as the NTS during CHF would reduce the “sympatho-inhibitory memory.”

Taken together these two pathways would explain both the increased sympatho-excitatory effects of BDNF following Ang II and the withdrawal of BDNF signaling from the sympatho-inhibitory center of the dmNTS during CHF. Although more work is needed to fully define the nature of potentiating a “sympatho-excitatory memory” pathway, the work presented in this dissertation provides evidence in favor of the synergistic connection between Ang II signaling and BDNF in mediating sympatho-excitation and baroreflex dysfunction in cardiovascular disease states.

REFERENCES

- Adams JP, Anderson a E, Varga a W, Dineley KT, Cook RG, Pfaffinger PJ & Sweatt JD (2000). The A-type potassium channel Kv4.2 is a substrate for the mitogen-activated protein kinase ERK. *J Neurochem* **75**, 2277–2287.
- Adams Kirkwood F J et al. (2005). Characteristics and outcomes of patients hospitalized for heart failure in the United States: rationale, design, and preliminary observations from the first 100,000 cases in the Acute Decompensated Heart Failure National Registry ({ADHERE}). *Am Hear J* **149**, 209–216.
- Alhusban A, Kozak A, Ergul A & Fagan SC (2013). AT1 Receptor Antagonism Is Proangiogenic in the Brain: BDNF a Novel Mediator. *J Pharmacol Exp Ther* **344**, 348–359.
- Allen AM, Zhuo J & Mendelsohn F a O (2000). Localization and Function of Angiotensin AT 1 Receptors. **7061**, 31–38.
- Andresen MC & Yang M (1995). Dynamics of sensory afferent synaptic transmission in aortic baroreceptor regions on nucleus tractus solitarius. *J Neurophysiol* **74**, 1518–1528.
- Avrith DB & Fitzsimons JT (1980). Increased sodium appetite in the rat induced by intracranial administration of components of the renin-angiotensin system. *J Physiol* **301**, 349–364.
- Avrith DB, Wiselka MJ & Fitzsimons JT (1980). Increased sodium appetite in adrenalectomized or hypophysectomized rats after intracranial injections of renin or angiotensin II. *J Endocrinol* **87**, 109–112.
- Barnes KL, Deweese DM, Andresen MC, Karen L & Andresen C (2003). Angiotensin potentiates excitatory sensory synaptic transmission to medial solitary tract nucleus neurons. **44195**, 1340–1353.
- Barnes KL, McQueeney a J & Ferrario CM (1993). Receptor subtype that mediates the neuronal effects of angiotensin II in the rat dorsal medulla. *Brain Res Bull* **31**, 195–200.
- Becker BK, Wang H, Tian C & Zucker IH (2015). BDNF contributes to angiotensin II-mediated reductions in peak voltage-gated K + current in cultured CATH.a cells. *Physiol Rep* **3**, 1–8.
- Benarroch EE (2015). Brain-derived neurotrophic factor: Regulation, effects, and potential clinical relevance. *Neurology* **84**, 1693–1704.
- Bertinieri G, di Rienzo M, Cavallazzi A, Ferrari AU, Pedotti A & Mancia G (1985). A new approach to analysis of the arterial baroreflex. *J Hypertens Suppl* **3**, S79–S81.
- Bhatia V, Rarick KR & Stauss HM (2010). Effect of the data sampling rate on accuracy of indices for heart rate and blood pressure variability and baroreflex function in resting rats and mice. *Physiol Meas* **31**, 1185–1201.
- Biancardi VC, Son SJ, Ahmadi S, Filosa JA & Stern JE (2013). Circulating Angiotensin II Gains Access to the Hypothalamus and Brain Stem During Hypertension via Breakdown of the Blood-Brain Barrier. *Hypertension*; DOI: 10.1161/HYPERTENSIONAHA.113.01743.

- Birnbaum SG, Varga AW, Yuan L-L, Anderson AE, Sweatt JD & Schrader L a (2004). Structure and function of Kv4-family transient potassium channels. *Physiol Rev* **84**, 803–833.
- Blum R, Kafitz KW & Konnerth A (2002). Neurotrophin-evoked depolarization requires the sodium channel Na(V)1.9. *Nature* **419**, 687–693.
- Blum R & Konnerth A (2005). Neurotrophin-mediated rapid signaling in the central nervous system: mechanisms and functions. *Physiology (Bethesda)* **20**, 70–78.
- Bramham CR & Messaoudi E (2005). BDNF function in adult synaptic plasticity: the synaptic consolidation hypothesis. *Prog Neurobiol* **76**, 99–125.
- Brink M, Price SR, Chrast J, Bailey JL, Anwar a, Mitch WE & Delafontaine P (2001). Angiotensin II induces skeletal muscle wasting through enhanced protein degradation and down-regulates autocrine insulin-like growth factor I. *Endocrinology* **142**, 1489–1496.
- Brink M, Wellen J & Delafontaine P (1996). Angiotensin II causes weight loss and decreases circulating insulin-like growth factor I in rats through a pressor-independent mechanism. *J Clin Invest* **97**, 2509–2516.
- Buggy J, Fink GD, Haywood JR, Johnson AK & Brody MJ. Interruption of the maintenance phase of established hypertension by ablation of the anteroventral third ventricle (AV3V) in rats. *Clin Exp Hypertens* **1**, 337–353.
- Caldeira M V, Melo C V, Pereira DB, Carvalho R, Correia SS, Backos DS, Carvalho a L, Esteban J a & Duarte CB (2007). Brain-derived neurotrophic factor regulates the expression and synaptic delivery of alpha-amino-3-hydroxy-5-methyl-4-isoxazole propionic acid receptor subunits in hippocampal neurons. *J Biol Chem* **282**, 12619–12628.
- Camara a K & Osborn J (2001). Central AT1 and AT2 receptors mediate chronic intracerebroventricular angiotensin II-induced drinking in rats fed high sodium chloride diet from weaning. *Acta Physiol Scand* **171**, 195–201.
- Camara a K & Osborn JL (1998). AT1 receptors mediate chronic central nervous system AII hypertension in rats fed high sodium chloride diet from weaning. *J Auton Nerv Syst* **72**, 16–23.
- Cao X-H, Byun H-S, Chen S-R, Cai Y-Q & Pan H-L (2010). Reduction in voltage-gated K⁺ channel activity in primary sensory neurons in painful diabetic neuropathy: role of brain-derived neurotrophic factor. *J Neurochem* **114**, 1460–1475.
- Cao X-H, Chen S-R, Li L & Pan H-L (2012). Nerve injury increases brain-derived neurotrophic factor levels to suppress BK channel activity in primary sensory neurons. *J Neurochem* **121**, 944–953.
- Carrasquillo Y, Burkhalter A & Nerbonne JM (2012). A-type K⁺ channels encoded by Kv4.2, Kv4.3 and Kv1.4 differentially regulate intrinsic excitability of cortical pyramidal neurons. *J Physiol* **590**, 3877–3890.

- Cazorla M, Prémont J, Mann A, Girard N, Kellendonk C & Rognan D (2011). Identification of a low-molecular weight TrkB antagonist with anxiolytic and antidepressant activity in mice. *J Clin Invest* **121**, 1846–1857.
- Ceccatelli S, Ernfors P, Villar MJ, Persson H & Hökfelt T (1991). Expanded distribution of mRNA for nerve growth factor, brain-derived neurotrophic factor, and neurotrophin 3 in the rat brain after colchicine treatment. *Proc Natl Acad Sci U S A* **88**, 10352–10356.
- Chan SHH, Hsu K, Huang C, Wang L, Chan JYH & Ou C-C (2005). NADPH oxidase-derived superoxide anion mediates angiotensin II-induced pressor effect via activation of p38 mitogen-activated protein kinase in the rostral ventrolateral medulla. *Circ Res* **97**, 772–780.
- Chan SHH, Wang L-L, Tseng H-L & Chan JYH (2007). Upregulation of AT1 receptor gene on activation of protein kinase Cbeta/nicotinamide adenine dinucleotide diphosphate oxidase/ERK1/2/c-fos signaling cascade mediates long-term pressor effect of angiotensin II in rostral ventrolateral medulla. *J Hypertens* **25**, 1845–1861.
- Chan SHH, Wu C-WJ, Chang AYW, Hsu K-S & Chan JYH (2010). Transcriptional upregulation of brain-derived neurotrophic factor in rostral ventrolateral medulla by angiotensin II: significance in superoxide homeostasis and neural regulation of arterial pressure. *Circ Res* **107**, 1127–1139.
- Chao M V. (2003). Neurotrophins and their receptors: A convergence point for many signalling pathways. *Nat Rev Neurosci* **4**, 299–309.
- Chen X, Yuan L-L, Zhao C, Birnbaum SG, Frick a., Jung WE, Schwarz TL, Sweatt JD & Johnston D (2006). Deletion of Kv4.2 Gene Eliminates Dendritic A-Type K⁺ Current and Enhances Induction of Long-Term Potentiation in Hippocampal CA1 Pyramidal Neurons. *J Neurosci* **26**, 12143–12151.
- Chien L-Y, Cheng J-K, Chu D, Cheng C-F & Tsaor M-L (2007). Reduced Expression of A-Type Potassium Channels in Primary Sensory Neurons Induces Mechanical Hypersensitivity. *J Neurosci* **27**, 9855–9865.
- Clark CG, Hasser EM, Kunze DL, Katz DM & Kline DD (2011). Endogenous brain-derived neurotrophic factor in the nucleus tractus solitarius tonically regulates synaptic and autonomic function. *J Neurosci* **31**, 12318–12329.
- Clayton SC, Zhang Z, Beltz T, Xue B & Johnson AK (2014). CNS neuroplasticity and salt-sensitive hypertension induced by prior treatment with subpressor doses of ANG II or aldosterone. *Am J Physiol Regul Integr Comp Physiol* **306**, R908–R917.
- Cohen S & Levi-Montalcini R (1960). Purification and Properties of a Nerve Growth-promoting Factor Isolated from Mouse Sarcoma 180 *. *Proc Natl Acad Sci USA* **46**, 302–311.
- Conner JM, Lauterborn JC, Yan Q, Gall CM & Varon S (1997). Distribution of Brain-Derived Neurotrophic Factor (BDNF) Protein and mRNA in the Normal Adult Rat CNS : Evidence for Anterograde Axonal Transport. **17**, 2295–2313.

- Connor J a & Stevens CF (1971). Voltage clamp studies of a transient outward membrane current in gastropod neural somata. *J Physiol* **213**, 21–30.
- Crill WE & Reis DJ (1968). Distribution of carotid sinus and depressor nerves in cat brain stem. *Am J Physiol* **214**, 269–276.
- Davies MK, Gibbs CR & Lip GY (2000). ABC of heart failure. *BMJ* **320**, 297–300.
- DeGiorgio CM, Miller P, Meymandi S, Chin A, Epps J, Gordon S, Gornbein J & Harper RM (2011). RMSSD, a Measure of Heart Rate Variability, Is Associated With Risk Factors For SUDEP: The SUDEP-7 Inventory. *Epilepsy Behav* **19**, 78–81.
- Dietrich WD, Lowry OH & Loewy a. D (1982). The distribution of glutamate, GABA and aspartate in the nucleus tractus solitarius of the cat. *Brain Res* **237**, 254–260.
- Dinicolantonio R, Mendelsohn F a O, Hutchinson JS, Takata Y & Doyle a E (1982). Dissociation of Dipsogenic and Pressor-Responses to Chronic Central Angiotensin-II in Rats. *Am J Physiol* **242**, R498–R504.
- Du J-Q, Sun C-W & Tang J-S (2004). Effect of angiotensin II type 1 receptor on delayed rectifier potassium current in catecholaminergic CATH.a cells. *Acta Pharmacol Sin* **25**, 1145–1150.
- Erdos B, Backes I, McCowan ML, Hayward LF & Scheuer D a (2015). Brain-derived neurotrophic factor modulates angiotensin signaling in the hypothalamus to increase blood pressure in rats. *Am J Physiol - Hear Circ Physiol* **00776**.2014.
- Faraco G & Iadecola C (2013). Hypertension: A harbinger of stroke and dementia. *Hypertension* **62**, 810–817.
- Farsang C (2011). Indications for and utilization of angiotensin receptor II blockers in patients at high cardiovascular risk. *Vasc Health Risk Manag* **7**, 605–622.
- Ferguson A V (2009). Angiotensinergic regulation of autonomic and neuroendocrine outputs: critical roles for the subfornical organ and paraventricular nucleus. *Neuroendocrinology* **89**, 370–376.
- Ferguson DW, Berg WJ & Sanders JS (1990). Clinical and hemodynamic correlates of sympathetic nerve activity in normal humans and patients with heart failure: evidence from direct microneurographic recordings. *J Am Coll Cardiol* **16**, 1125–1134.
- Fishbein MC, Maclean D & Maroko PR (1978). Experimental myocardial infarction in the rat: qualitative and quantitative changes during pathologic evolution. *Am J Pathol* **90**, 57–70.
- Fitzsimons JT (1998). Angiotensin, thirst, and sodium appetite. *Physiol Rev* **78**, 583–686.
- Fow JE, Averill DB & Barnes KL (1994). Mechanisms of angiotensin-induced hypotension and bradycardia in the medial solitary tract nucleus. *Am J Physiol* **267**, H259–H266.

- Francis GS (1985). Neurohumoral mechanisms involved in congestive heart failure. *Am J Cardiol* **55**, 15A – 21A.
- Fransén E & Tigerholm J (2010). Role of A-type potassium currents in excitability, network synchronicity, and epilepsy. *Hippocampus* **20**, 877–887.
- Franzosi M & Santoro E (1998). Indications for ACE inhibitors in the early treatment of acute myocardial infarction: systematic overview of individual data from 100,000 patients in randomized trials. ACE Inhibitor Myocardial Infarction Collaborative Group. *Circulation* **97**, 2202–2212.
- Gaiddon C, Loeffler JP & Larmet Y (1996). Brain-Derived Neurotrophic Factor Stimulates AP-1 and Cyclic AMP-Responsive Element Dependent Transcriptional Activity in Central Nervous System Neurons.
- Gao J, Zucker IH & Gao L (2014). Activation of central Angiotensin type 2 receptors by compound 21 improves arterial baroreflex sensitivity in rats with heart failure. *Am J Hypertens* **27**, 1248–1256.
- Gao L, Li Y, Schultz HD, Wang W-Z, Wang W, Finch M, Smith LM & Zucker IH (2010). Downregulated Kv4.3 expression in the RVLM as a potential mechanism for sympathoexcitation in rats with chronic heart failure. *Am J Physiol Heart Circ Physiol* **298**, H945–H955.
- Gao L, Schultz HD, Patel KP, Zucker IH & Wang W (2005a). Augmented input from cardiac sympathetic afferents inhibits baroreflex in rats with heart failure. *Hypertension* **45**, 1173–1181.
- Gao L, Wang W, Li Y-L, Schultz HD, Liu D, Cornish KG & Zucker IH (2004). Superoxide mediates sympathoexcitation in heart failure: roles of angiotensin II and NAD(P)H oxidase. *Circ Res* **95**, 937–944.
- Gao L, Wang W, Li Y-L, Schultz HD, Liu D, Cornish KG & Zucker IH (2005b). Sympathoexcitation by central ANG II: roles for AT1 receptor upregulation and NAD(P)H oxidase in RVLM. *Am J Physiol Heart Circ Physiol* **288**, H2271–H2279.
- Gao L, Wang W-Z, Wang W-Z & Zucker IH (2008). Imbalance of angiotensin type 1 receptor and angiotensin II type 2 receptor in the rostral ventrolateral medulla: potential mechanism for sympathetic overactivity in heart failure. *Hypertension* **52**, 708–714.
- Geraldes V, Goncalves-Rosa N, Liu B, Paton JFR & Rocha I (2014). Essential role of RVL medullary neuronal activity in the long term maintenance of hypertension in conscious SHR. *Auton Neurosci* **186**, 22–31.
- Ginty DD, Bonni a & Greenberg ME (1994). Nerve growth factor activates a Ras-dependent protein kinase that stimulates c-fos transcription via phosphorylation of CREB. *Cell* **77**, 713–725.

- Glaum SR & Brooks P a (1996). Tetanus-induced sustained potentiation of monosynaptic inhibitory transmission in the rat medulla: evidence for a presynaptic locus. *J Neurophysiol* **76**, 30–38.
- Gnecchi Ruscone T, Lombardi F, Malfatto G & Malliani A (1987). Attenuation of baroreceptive mechanisms by cardiovascular sympathetic afferent fibers. *Am J Physiol* **253**, H787–H791.
- Go a. S et al. (2013). *Heart Disease and Stroke Statistics--2014 Update: A Report From the American Heart Association*. Available at: <http://circ.ahajournals.org/cgi/doi/10.1161/01.cir.0000441139.02102.80> [Accessed December 19, 2013].
- Goldstein RE, Beiser GD, Stampfer M & Epstein SE (1975). Impairment of autonomically mediated heart rate control in patients with cardiac dysfunction. *Circ Res* **36**, 571–578.
- Grobe JL, Xu D & Sigmund CD (2008). An intracellular renin-angiotensin system in neurons: fact, hypothesis, or fantasy. *Physiology (Bethesda)* **23**, 187–193.
- Guyenet PG (2006). The sympathetic control of blood pressure. *Nat Rev Neurosci* **7**, 335–346.
- Haack KK V, Engler CW, Papoutsi E, Pipinos II, Patel KP & Zucker IH (2012). Parallel changes in neuronal AT1R and GRK5 expression following exercise training in heart failure. *Hypertension* **60**, 354–361.
- Hagiwara S, Kusano K & Saito N (1961). Membrane changes of Onchidium nerve cell in potassium-rich media. *J Physiol* **155**, 470–489.
- Hall JE (2011). *Guyton and Hall textbook of medical physiology*, 12th edn.ed. Hall JE. Saunders, Philadelphia.
- Hryniewicz K, Androne AS, Hudaihed A & Katz SD (2003). Partial reversal of cachexia by beta-adrenergic receptor blocker therapy in patients with chronic heart failure. *J Card Fail* **9**, 464–468.
- Huang EJ & Reichardt LF (2003). Trk receptors: roles in neuronal signal transduction. *Annu Rev Biochem* **72**, 609–642.
- Huang Y, Ko H, Cheung ZH, Yung KKL, Yao T, Wang J-J, Morozov A, Ke Y, Ip NY & Yung W-H (2012). Dual actions of brain-derived neurotrophic factor on GABAergic transmission in cerebellar Purkinje neurons. *Exp Neurol* **233**, 791–798.
- Jordan D & Spyer KM (1977). Studies on the termination of sinus nerve afferents. *Pflugers Arch* **369**, 65–73.
- Jung S-C, Kim J & Hoffman D a (2008). Rapid, bidirectional remodeling of synaptic NMDA receptor subunit composition by A-type K⁺ channel activity in hippocampal CA1 pyramidal neurons. *Neuron* **60**, 657–671.

- Kang J, Summers C & Posner P (1992). Modulation of net outward current in cultured neurons by angiotensin II: involvement of AT1 and AT2 receptors. *Brain Res* **580**, 317–324.
- Kang J, Summers C & Posner P (1993). Angiotensin II type 2 receptor-modulated changes in potassium currents in cultured neurons. *AmJPhysiol* **265**, C607–C616.
- Kar S, Gao L, Belatti DA, Curry PL & Zucker IH (2011). Central angiotensin (1-7) enhances baroreflex gain in conscious rabbits with heart failure. *Hypertension* **58**, 627–634.
- Katoh-Semba R, Kaneko R, Kitajima S, Tsuzuki M, Ichisaka S, Hata Y, Yamada H, Miyazaki N, Takahashi Y & Kato K (2009). Activation of p38 mitogen-activated protein kinase is required for in vivo brain-derived neurotrophic factor production in the rat hippocampus. *Neuroscience* **163**, 352–361.
- Kearney PM, Whelton M, Reynolds K, Muntner P, Whelton PK & Jiang H (2005). Global burden of hypertension--analysis of worldwide data. *Lancet* **365**, 217–223.
- Kent BB, Drane JW, Blumenstein B & Manning JW (1972). A mathematical model to assess changes in the baroreceptor reflex. *Cardiology* **57**, 295–310.
- Kim E & Hoffman D a (2012). Dynamic regulation of synaptic maturation state by voltage-gated A-type K⁺ channels in CA1 hippocampal pyramidal neurons. *J Neurosci* **32**, 14427–14432.
- Kim J & Hoffman D a. (2007). Potassium Channels: Newly Found Players in Synaptic Plasticity. *Neurosci* **14**, 276–286.
- Kim J, Jung S-C, Clemens AM, Petralia RS & Hoffman D a (2007). Regulation of dendritic excitability by activity-dependent trafficking of the A-type K⁺ channel subunit Kv4.2 in hippocampal neurons. *Neuron* **54**, 933–947.
- Kim J, Wei D-S & Hoffman D a (2005). Kv4 potassium channel subunits control action potential repolarization and frequency-dependent broadening in rat hippocampal CA1 pyramidal neurons. *J Physiol* **569**, 41–57.
- Kim JH, Roberts DS, Hu Y, Lau GC, Brooks-Kayal AR, Farb DH & Russek SJ (2012). Brain-derived neurotrophic factor uses CREB and Egr3 to regulate NMDA receptor levels in cortical neurons. *J Neurochem* **120**, 210–219.
- King AJ, Osborn JW & Fink GD (2007). Splanchnic circulation is a critical neural target in angiotensin II salt hypertension in rats. *Hypertension* **50**, 547–556.
- Latchford KJ, Ferguson A V, Kevin J & Angiotensin AVF (2005). Angiotensin depolarizes parvocellular neurons in paraventricular nucleus through modulation of putative nonselective cationic and potassium conductances. **6**, 52–58.
- Laviano A, Inui A, Marks DL, Meguid MM, Pichard C, Fanelli FR & Seelaender M (2008). Neural control of the anorexia-cachexia syndrome. 1000–1008.

- Lenkei Z, Palkovits M, Corvol P & Llorens-Cortès C (1997). Expression of angiotensin type-1 (AT1) and type-2 (AT2) receptor mRNAs in the adult rat brain: a functional neuroanatomical review. *Front Neuroendocrinol* **18**, 383–439.
- Lerche H, Shah M, Beck H, Noebels J, Johnston D & Vincent A (2013). Ion channels in genetic and acquired forms of epilepsy. *J Physiol* **591**, 753–764.
- Levi-Montalcini R & Calissano P (1979). The nerve-growth factor. *Sci Am* **240**, 68–77.
- Levi-Montalcini R, Meyer H & Hamburger V (1954). In Vitro Experiments on the Effects of Mouse Sarcomas 180 and 37 on the Spinal and Sympathetic Ganglia of the Chick Embryo. *Cancer Res* **14**, 49–57.
- Levine ES, Crozier R a, Black IB & Plummer MR (1998). Brain-derived neurotrophic factor modulates hippocampal synaptic transmission by increasing N-methyl-D-aspartic acid receptor activity. *Proc Natl Acad Sci U S A* **95**, 10235–10239.
- Lewin GR & Barde YA (1996). Physiology of the neurotrophins. *Annu Rev Neurosci* **19**, 289–317.
- Li HS, Xu XZS & Montell C (1999). Activation of a trpc3-dependent cation current through the neurotrophin bdnf. *Neuron* **24**, 261–273.
- Lynch MA, Introduction I, Erk B, Potentiation L, Age D & Cognition E (2004). Long-Term Potentiation and Memory. 87–136.
- Machado BH (2001). Neurotransmission of the cardiovascular reflexes in the nucleus tractus solitarii of awake rats. *Ann N Y Acad Sci* **940**, 179–196.
- Maisonpierre PC, Friedman B, Alderson RF, Wiegand J, Furth E, Lindsay M, Yancopoulos D, Belluscio L, Friedman B, Alderson RF, Wiegand SJ, Furth ME, Lindsay RM & Yancopoulos GD (1990). NT-3 , BDNF , and NGF in the Developing Rat Nervous System : Parallel as well as - - Reciprocal Patterns of Expression factors. *Neuron* **5**, 501–509.
- Mangiapane ML & Simpson JB (1980). Subfornical organ: forebrain site of pressor and dipsogenic action of angiotensin II. *AmJPhysiol* **239**, R382–R389.
- Martin JL, Jenkins VK, Hsieh H & Balkowiec A (2009). Brain-derived neurotrophic factor in arterial baroreceptor pathways: implications for activity-dependent plasticity at baroafferent synapses. *J Neurochem* **108**, 450–464.
- Martin KJ, Shpiro N, Traynor R, Elliott M & Arthur JSC (n.d.). Comparison of the specificity of Trk inhibitors in recombinant and neuronal assays. *Neuropharmacology* **61**, 148–155.
- Mattson MP & Wan R (2008). Neurotrophic factors in autonomic nervous system plasticity and dysfunction. *Neuromolecular Med* **10**, 157–168.
- Minichiello L (2009). TrkB signalling pathways in LTP and learning. *Nat Rev Neurosci* **10**, 850–860.

- Mitra AK, Gao L & Zucker IH (2010). Angiotensin II-induced upregulation of AT(1) receptor expression: sequential activation of NF-kappaB and Elk-1 in neurons. *Am J Physiol Cell Physiol* **299**, C561–C569.
- Mortara A, La Rovere MT, Pinna GD, Prpa A, Maestri R, Febo O, Pozzoli M, Opasich C & Tavazzi L (1997). Arterial Baroreflex Modulation of Heart Rate in Chronic Heart Failure : Clinical and Hemodynamic Correlates and Prognostic Implications. *Circulation* **96**, 3450–3458.
- Nagappan G & Lu B (2005). Activity-dependent modulation of the BDNF receptor TrkB: mechanisms and implications. *Trends Neurosci* **28**, 464–471.
- Nerbonne JM, Gerber BR, Norris A & Burkhalter A (2008). Electrical remodelling maintains firing properties in cortical pyramidal neurons lacking KCND2-encoded A-type K+ currents. *J Physiol* **586**, 1565–1579.
- Niebauer M & Zucker IH (1985). Static and dynamic responses of carotid sinus baroreceptors in dogs with chronic volume overload. *J Physiol* **369**, 295–310.
- Niebauer MJ, Holmberg MJ & Zucker IH (1986). Aortic baroreceptor characteristics in dogs with chronic high output failure. *Basic Res Cardiol* **81**, 111–122.
- Osborn JL & Camara AKS (1997). Renal Neurogenic Mediation of Intracerebroventricular Angiotensin II Hypertension in Rats Raised on High Sodium Chloride Diet. *Hypertension* **30**, 331–336.
- Osborn JW, Fink GD & Kuroki MT (2011). Neural mechanisms of angiotensin II-salt hypertension: implications for therapies targeting neural control of the splanchnic circulation. *Curr Hypertens Rep* **13**, 221–228.
- Oshima N, McMullan S, Goodchild AK & Pilowsky PM (2006). A monosynaptic connection between baroinhibited neurons in the RVLM and IML in Sprague-Dawley rats. *Brain Res* **1089**, 153–161.
- Oz M & Renaud LP (2002). Angiotensin AT(1)-receptors depolarize neonatal spinal motoneurons and other ventral horn neurons via two different conductances. *J Neurophysiol* **88**, 2857–2863.
- Palkovits M BM (1983). *Brain Microdissection Techniques*. John Wiley & Sons, Chichester.
- Palkovits M, Dejong W, Zandberg P, Versteeg DH, Vandergugten J & Léránth C (1977). Central hypertension and nucleus tractus solitarii catecholamines after surgical lesions in the medulla oblongata of the rat. *Brain Res* **127**, 307–312.
- Pan Y-X, Gao L, Wang W-Z, Zheng H, Liu D, Patel KP, Zucker IH & Wang W (2007). Exercise training prevents arterial baroreflex dysfunction in rats treated with central angiotensin II. *Hypertension* **49**, 519–527.

- Park H & Poo M (2012). Neurotrophin regulation of neural circuit development and function. *Nat Rev Neurosci* **14**, 7–23.
- Park H, Popescu A & Poo M (2014). Article Essential Role of Presynaptic NMDA Receptors in Activity-Dependent BDNF Secretion and Corticostriatal LTP. *Neuron* **84**, 1009–1022.
- Patel KP & Zheng H (2011). Central Neural Control of Sympathetic Nerve Activity in Heart Failure Following Exercise Training. *Am J Physiol Heart Circ Physiol* **302**, H527–H537.
- Paxinos G & Watson C (1998). *The Rat Brain in Stereotaxic Coordinates*, 3rd edn. Academic Press, New York.
- Pellegrino PR, Schiller a. M & Zucker IH (2014). Validation of pulse rate variability as a surrogate for heart rate variability in chronically instrumented rabbits. *AJP Hear Circ Physiol* **307**, H97–H109.
- Pfeffer M a, Pfeffer JM, Fishbein MC, Fletcher PJ, Spadaro J, Kloner R a & Braunwald E (1979). Myocardial infarct size and ventricular function in rats. *Circ Res* **44**, 503–512.
- Polson JW, Dampney R a L, Boscan P, Pickering a E & Paton JFR (2007). Differential baroreflex control of sympathetic drive by angiotensin II in the nucleus tractus solitarii. *Am J Physiol Regul Integr Comp Physiol* **293**, R1954–R1960.
- Qi Y, Wang JK, McMillian M & Chikaraishi DM (1997). Characterization of a CNS cell line, CAD, in which morphological differentiation is initiated by serum deprivation. *J Neurosci* **17**, 1217–1225.
- Rose CR, Blum R, Kafitz KW, Kovalchuk Y & Konnerth A (2004). From modulator to mediator: rapid effects of BDNF on ion channels. *Bioessays* **26**, 1185–1194.
- Rose CR, Blum R, Pichler B, Lepier A, Kafitz KW & Konnerth A (2003). Truncated TrkB-T1 mediates neurotrophin-evoked calcium signalling in glia cells. *Nature* **426**, 74–78.
- Rosendorff C, Lackland DT, Allison M, Aronow WS, Black HR, Blumenthal RS, Cannon CP, de Lemos J a., Elliott WJ, Findeiss L, Gersh BJ, Gore JM, Levy D, Long JB, O'Connor CM, O'Gara PT, Ogedegbe G, Oparil S & White WB (2015). *Treatment of Hypertension in Patients With Coronary Artery Disease: A Scientific Statement From the American Heart Association, American College of Cardiology, and American Society of Hypertension*. Available at: <http://circ.ahajournals.org/cgi/doi/10.1161/CIR.0000000000000207>.
- Rothman SM & Mattson MP (2012). Activity-dependent, stress-responsive BDNF signaling and the quest for optimal brain health and resilience throughout the lifespan. *Neuroscience*; DOI: 10.1016/j.neuroscience.2012.10.014.
- La Rovere MT, Bigger JT, Marcus FI, Mortara A & Schwartz PJ (1998). Baroreflex sensitivity and heart-rate variability in prediction of total cardiac mortality after myocardial infarction. ATRAMI. *Lancet* **351**, 478–484.

- Salim S, Asghar M, Taneja M, Hovatta I, Chugh G, Vollert C & Vu A (2011). Potential contribution of oxidative stress and inflammation to anxiety and hypertension. *Brain Res* **1404**, 63–71.
- Scharfman HE (2013). Hyperexcitability in Combined Entorhinal / Hippocampal Slices of Adult Rat After Exposure to Brain-Derived Neurotrophic Factor Hyperexcitability in Combined Entorhinal / Hippocampal Slices of Adult Rat After Exposure to Brain-Derived Neurotrophic Factor. 1082–1095.
- Schreihöfer AM, Stornetta RL & Guyenet PG (2000). Regulation of sympathetic tone and arterial pressure by rostral ventrolateral medulla after depletion of C1 cells in rat. *J Physiol* **529**, 221–236.
- Schwartz PJ, Vanoli E, Stramba-Badiale M, De Ferrari GM, Billman GE & Foreman RD (1988). Autonomic mechanisms and sudden death. New insights from analysis of baroreceptor reflexes in conscious dogs with and without a myocardial infarction. *Circulation* **78**, 969–979.
- Seller H & Illert M (1969). The localization of the first synapse in the carotid sinus baroreceptor reflex pathway and its alteration of the afferent input. *Pflugers Arch* **306**, 1–19.
- Serôdio P & Rudy B (1998). Differential expression of Kv4 K⁺ channel subunits mediating subthreshold transient K⁺ (A-type) currents in rat brain. *J Neurophysiol* **79**, 1081–1091.
- Sheh Y-L, Hsu C, Chan SHH & Chan JYH (2007). NADPH oxidase- and mitochondrion-derived superoxide at rostral ventrolateral medulla in endotoxin-induced cardiovascular depression. *Free Radic Biol Med* **42**, 1610–1623.
- Shelton DL & Reichardt LF (1986). Studies on the expression of the beta nerve growth factor (NGF) gene in the central nervous system: level and regional distribution of NGF mRNA suggest that NGF functions as a trophic factor for several distinct populations of neurons. *Proc Natl Acad Sci U S A* **83**, 2714–2718.
- Shinoda Y, Ahmed S, Ramachandran B, Bharat V, Brockelt D, Altas B & Dean C (2014). BDNF enhances spontaneous and activity-dependent neurotransmitter release at excitatory terminals but not at inhibitory terminals in hippocampal neurons. *Front Synaptic Neurosci* **6**, 27.
- Song K, Allen AM, Paxinos G & Mendelsohn FA (1992). Mapping of angiotensin II receptor subtype heterogeneity in rat brain. *J Comp Neurol* **316**, 467–484.
- Sonner PM, Filosa J a & Stern JE (2008). Diminished A-type potassium current and altered firing properties in presympathetic PVN neurones in renovascular hypertensive rats. *J Physiol* **586**, 1605–1622.
- Sonner PM & Stern JE (2007). Functional role of A-type potassium currents in rat presympathetic PVN neurones. *J Physiol* **582**, 1219–1238.

- Stauss HM, Moffitt J a, Chapleau MW, Abboud FM & Johnson AK (2006). Baroreceptor reflex sensitivity estimated by the sequence technique is reliable in rats. *Am J Physiol Heart Circ Physiol* **291**, H482–H483.
- Stein PK, Bosner MS, Kleiger RE & Conger BM (1994). Heart rate variability: A measure of cardiac autonomic tone. *Am Heart J* **127**, 1376–1381.
- Stevens G (2009). Global Health Risks: Mortality and burden of disease attributable to selected major risks. *Bull World Health Organ* **87**, 646–646.
- Sun C, Du J, Sumners C & Raizada MK (2003). PI3-kinase inhibitors abolish the enhanced chronotropic effects of angiotensin II in spontaneously hypertensive rat brain neurons. *J Neurophysiol* **90**, 3155–3160.
- Suri C, Fung BP, Tischler a S & Chikaraishi DM (1993). Catecholaminergic cell lines from the brain and adrenal glands of tyrosine hydroxylase-SV40 T antigen transgenic mice. *J Neurosci* **13**, 1280–1291.
- Szekeres M, Nádasy GL, Turu G, Süpeki K, Szidonya L, Buday L, Chaplin T, Clark AJL & Hunyady L (2010). Angiotensin II-induced expression of brain-derived neurotrophic factor in human and rat adrenocortical cells. *Endocrinology* **151**, 1695–1703.
- Talman WT & Lin L-H (2013). Sudden death following selective neuronal lesions in the rat nucleus tractus solitarii. *Auton Neurosci* **175**, 9–16.
- Talman WT, Perrone MH & Reis DJ (1980). Evidence for L-glutamate as the neurotransmitter of baroreceptor afferent nerve fibers. *Science* **209**, 813–815.
- Talman WT, Perrone MH & Reis DJ (1981). Acute hypertension after the local injection of kainic acid into the nucleus tractus solitarii of rats. *Circ Res* **48**, 292–298.
- Tang X & Dworkin BR (2007a). Baroreflexes of the rat. IV. ADN-evoked responses at the NTS. *Am J Physiol Regul Integr Comp Physiol* **293**, R2243–R2253.
- Tang X & Dworkin BR (2007b). Baroreflexes of the rat. V. Tetanus-induced potentiation of ADN A-fiber responses at the NTS. *Am J Physiol Regul Integr Comp Physiol* **293**, R2254–R2259.
- Tang X & Dworkin BR (2009). The dmNTS is not the source of increased blood pressure variability in baroreflex denervated rats. *Auton Neurosci* **148**, 21–27.
- Thunhorst RL & Johnson a K (1993). Effects of arterial pressure on drinking and urinary responses to intracerebroventricular angiotensin II. *Am J Physiol* **264**, R211–R217.
- Timmusk T, Belluardo N, Metsis M & Persson H (1993). Widespread and developmentally regulated expression of neurotrophin-4 mRNA in rat brain and peripheral tissues. *Eur J Neurosci* **5**, 605–613.

- Unger T, Steckelings UM & dos Santos RAS (2015). *The Protective Arm of the Renin Angiotensin System (RAS)*, 1st edn.ed. Unger T, Steckelings UM & dos Santos RAS. Academic Press, London.
- Wang D, Sumners C, Posner P & Gelband CH (1997). A-Type K⁺ Current in Neurons Cultured From Neonatal Rat Hypothalamus and Brain Stem : Modulation by Angiotensin II A-Type K⁺ Current in Neurons Cultured From Neonatal Rat Hypothalamus and Brain Stem : Modulation by Angiotensin II. 1021–1029.
- Wang H & Zhou X-F (2002). Injection of brain-derived neurotrophic factor in the rostral ventrolateral medulla increases arterial blood pressure in anaesthetized rats. *Neuroscience* **112**, 967–975.
- Wang H-J, Li Y-L, Gao L, Zucker IH & Wang W (2010a). Alteration in skeletal muscle afferents in rats with chronic heart failure. *J Physiol* **588**, 5033–5047.
- Wang H-J, Pan Y-X, Wang W-Z, Gao L, Zimmerman MC, Zucker IH & Wang W (2010b). Exercise training prevents the exaggerated exercise pressor reflex in rats with chronic heart failure. *J Appl Physiol* **108**, 1365–1375.
- Wang H-J, Wang W, Cornish KG, Rozanski GJ & Zucker IH (2014). Cardiac sympathetic afferent denervation attenuates cardiac remodeling and improves cardiovascular dysfunction in rats with heart failure. *Hypertension* **64**, 745–755.
- Wang W, Chen JS & Zucker IH (1991). Postexcitatory depression of baroreceptors in dogs with experimental heart failure. *Am J Physiol* **260**, H1160–H1165.
- Wang W, Zhu G-Q, Gao L, Tan W & Qian Z-M (2004). Baroreceptor reflex in heart failure. *Sheng Li Xue Bao* **56**, 269–281.
- Wang W-Z, Gao L, Pan Y-X, Zucker IH & Wang W (2007). AT1 receptors in the nucleus tractus solitarii mediate the interaction between the baroreflex and the cardiac sympathetic afferent reflex in anesthetized rats. *Am J Physiol Regul Integr Comp Physiol* **292**, R1137–R1145.
- Wang W-Z, Gao L, Wang H-J, Zucker IH & Wang W (2008). Interaction between cardiac sympathetic afferent reflex and chemoreflex is mediated by the NTS AT1 receptors in heart failure. *Am J Physiol Heart Circ Physiol* **295**, H1216–H1226.
- Wu KLH, Chan SHH & Chan JYH (2012). Neuroinflammation and oxidative stress in rostral ventrolateral medulla contribute to neurogenic hypertension induced by systemic inflammation. *J Neuroinflammation* **7317123**, 212.
- Xiao L, Gao L, Lazartigues E & Zucker IH (2011). Brain-selective overexpression of angiotensin-converting enzyme 2 attenuates sympathetic nerve activity and enhances baroreflex function in chronic heart failure. *Hypertension* **58**, 1057–1065.
- Xiao L, Haack KK & Zucker IH (2013). Angiotensin II regulates ACE and ACE2 in neurons through p38 mitogen-activated protein kinase and extracellular signal-regulated kinase 1/2 signaling. *Am J Physiol Cell Physiol* **304**, C1073–C1079.

- Xue B, Zhang Z, Johnson RF & Johnson AK (2012a). Sensitization of slow pressor angiotensin II (Ang II)-initiated hypertension: Induction of sensitization by prior Ang II treatment. *Hypertension* **59**, 459–466.
- Xue B, Zhang Z, Roncari CF, Guo F & Johnson AK (2012b). Aldosterone Acting Through the Central Nervous System Sensitizes Angiotensin II-Induced Hypertension. *Hypertension* **60**, 1023–1030.
- Yamada K, Mizuno M & Nabeshima T (2002). Role for brain-derived neurotrophic factor in learning and memory. *Life Sci* **70**, 735–744.
- Yamamoto K, Eubank W, Franzke M & Mifflin S (2013). Resetting of the sympathetic baroreflex is associated with the onset of hypertension during chronic intermittent hypoxia. *Auton Neurosci* **173**, 22–27.
- Yang R-F, Yin J-X, Li Y-L, Zimmerman MC & Schultz HD (2011). Angiotensin-(1-7) increases neuronal potassium current via a nitric oxide-dependent mechanism. *Am J Physiol Cell Physiol* **300**, C58–C64.
- Yin J-X, Yang R-F, Li S, Renshaw AO, Li Y-L, Schultz HD & Zimmerman MC (2010). Mitochondria-produced superoxide mediates angiotensin II-induced inhibition of neuronal potassium current. *Am J Physiol Cell Physiol* **298**, C857–C865.
- York RD, Yao H, Dillon T, Ellig CL, Eckert SP, McCleskey EW & Stork PJ (1998). Rap1 mediates sustained MAP kinase activation induced by nerve growth factor. *Nature* **392**, 622–626.
- Yoshida T, Semprun-Prieto L, Wainford RD, Sukhanov S, Kapusta DR & Delafontaine P (2012). Angiotensin II reduces food intake by altering orexigenic neuropeptide expression in the mouse hypothalamus. *Endocrinology* **153**, 1411–1420.
- Young CN & Davisson RL (2015). Angiotensin-II, the Brain, and Hypertension: Figure. *Hypertension* **66**, 920–926.
- Young D, Waitches G, Birchmeier C, Fasano O & Wigler M (1986). Isolation and characterization of a new cellular oncogene encoding a protein with multiple potential transmembrane domains. *Cell* **45**, 711–719.
- Youssoufian M & Walmsley B (2007). Brain-derived neurotrophic factor modulates cell excitability in the mouse medial nucleus of the trapezoid body. *Eur J Neurosci* **25**, 1647–1652.
- Yue C, Feng L & Huang Q (2014). RVLM-IML pathway may implicate controlling peripheral airways by melanocortinergic-sympathetic signaling : a transneuronal labeling study using pseudorabies virus. **7**, 7962–7966.
- Zafra F, Hengerer B, Leibrock J, Thoenen H & Lindholm D (1990). Activity dependent regulation of BDNF and NGF mRNAs in the rat hippocampus is mediated by non-NMDA glutamate receptors. *EMBO J* **9**, 3545–3550.

- Zaika O, Lara LS, Gamper N, Hilgemann DW, Jaffe DB & Shapiro MS (2006). Angiotensin II regulates neuronal excitability via phosphatidylinositol 4,5-bisphosphate-dependent modulation of Kv7 (M-type) K⁺ channels. *J Physiol* **575**, 49–67.
- Zhou C, Cavolo SL & Levitan ES (2012). Delayed endosome-dependent CamKII and p38 kinase signaling in cardiomyocytes destabilizes Kv4.3 mRNA. *J Mol Cell Cardiol* **52**, 1–7.
- Zimmerman MC (2002). Superoxide Mediates the Actions of Angiotensin II in the Central Nervous System. *Circ Res* **91**, 1038–1045.
- Zimmerman MC, Lazartigues E, Sharma R V & Davisson RL (2004). Hypertension caused by angiotensin II infusion involves increased superoxide production in the central nervous system. *Circ Res* **95**, 210–216.
- Zucker IH, Patel KP & Schultz HD (2012). Neurohumoral stimulation. *Heart Fail Clin* **8**, 87–99.
- Zucker IH, Schultz HD, Patel KP, Wang W & Gao L (2009). Regulation of central angiotensin type 1 receptors and sympathetic outflow in heart failure. *Am J Physiol Heart Circ Physiol* **297**, H1557–H1566.

APPENDIX

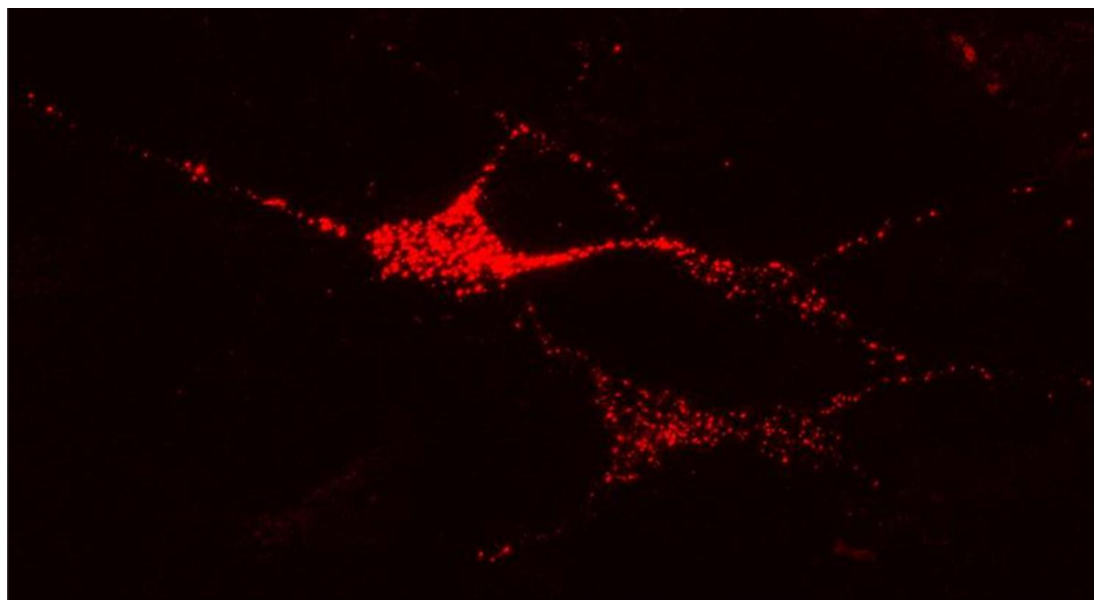
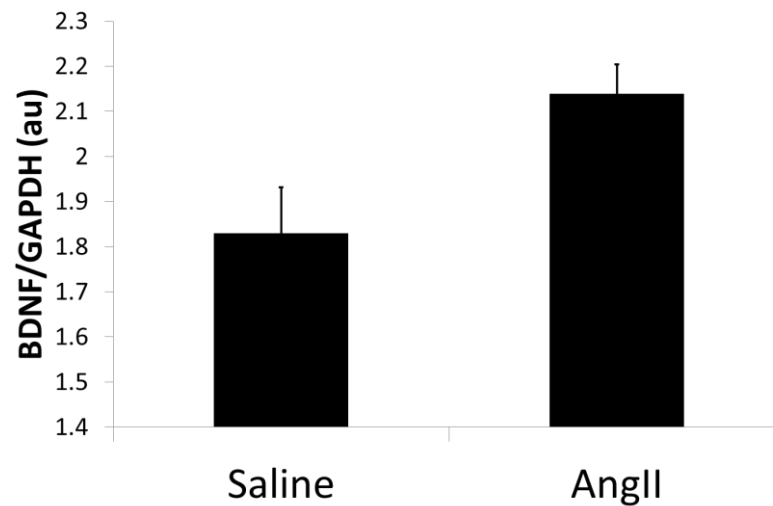


Figure A1 – Representative confocal image of labeled RVLM neurons following IML injection of rhodamine beads.

RVLM neurons are labeled by retrograde translocation of rhodamine beads injected into the IML at level T3-T5 3 days post-injection demonstrating direct projection of RVLM neurons to the sympathetic outflow tract of the spinal cord.

A. Mouse Brainstem



B. PVN - BDNF Expression

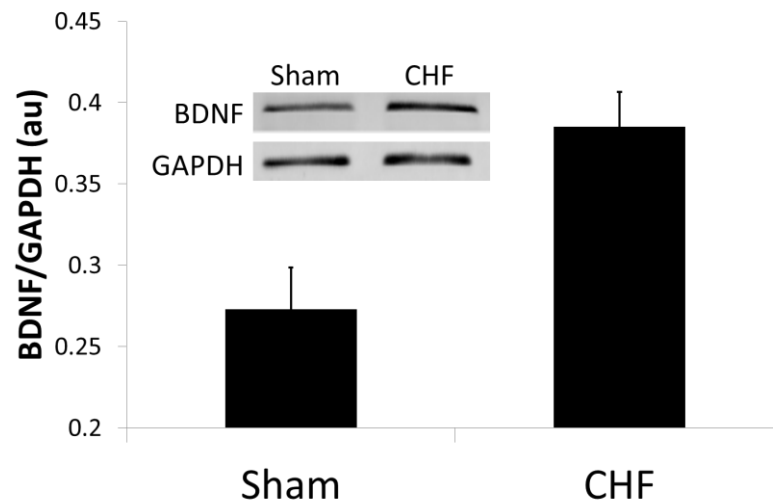


Figure A2 – Increased expression of BDNF in whole brainstem of mice following Ang II and PVN of rats with CHF.

Preliminary evidence indicating increased expression of BDNF in whole brainstem homogenates from C57/B6 mice receiving 600ng/kg/min of subcutaneous Ang II for 14 days (A) and increased expression of BDNF in punches taken from the PVN of rats with CHF (B). n = 2-3/group

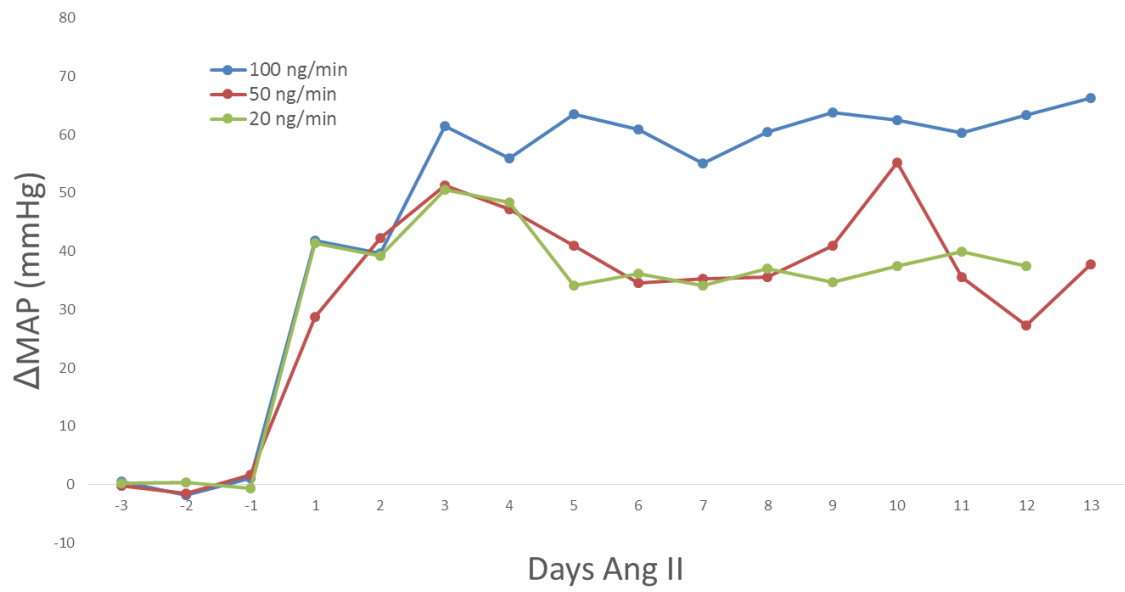


Figure A3 – Preliminary results exploring dose-response of ICV Ang II

Change in mean arterial blood pressure following 100 ng/min, 50 ng/min, or 20 ng/min ICV Ang II. n = 2/group